



# Gravitational Solitons in Anti-de Sitter Spacetimes

by

© **Turkuler Durgut**

A thesis submitted to the School of Graduate Studies in  
partial fulfillment of the requirements for the degree of  
Doctor of Philosophy.

Interdisciplinary Program of Theoretical Physics  
Memorial University

August 2023

St. John's, Newfoundland and Labrador, Canada

# Abstract

A gravitational soliton is a geodesically complete, globally stationary (and horizon-free) non-trivial solution of the Einstein equations, with prescribed asymptotic geometry. It is a classic theorem of Lichnerowicz [1] that in the standard four-dimensional Einstein-Maxwell theory, asymptotically flat solitons do not exist, and that the only non-trivial electrovacuum solutions must contain black holes. However, in dimensions greater than four, many explicit asymptotically flat examples are now known. This thesis is concerned with gravitational solitons that are asymptotic to (locally) anti-de Sitter (AdS) spacetime. AdS is the maximally symmetric solution of the Einstein equations with negative cosmological constant. Asymptotically AdS geometries have attracted a great deal of interest in theoretical physics over the past two decades.

In Chapter 2, we construct supersymmetric, asymptotically AdS<sub>5</sub> gravitational soliton solutions of five-dimensional gauged supergravity. We show that the solitons contain evanescent ergosurfaces and give an argument that these solitons should be nonlinearly unstable. In Chapter 3, we revisit a well-known example of a gravitational soliton in AdS, the Eguchi-Hanson-AdS<sub>5</sub> solution, and investigate a number of its geometric and thermodynamic properties. In particular we show that the linear scalar (Klein-Gordon) wave equation admits normal mode solutions, just like pure AdS. In Chapter 4, we then construct supersymmetric gravitational soliton solutions that are complete, globally stationary, 1/4-BPS and are asymptotically locally AdS<sub>5</sub>. Finally, in Chapter 5, we discuss some future directions and ongoing research.

to my grandmother Dudu Koc...

*I mean, it's not that you can't pass  
ten or fifteen years inside  
and more-  
you can,  
as long as the jewel  
on the left side of your chest doesn't lose its luster!*

*Nazim Hikmet*

# Lay summary

Black holes are one of the most fascinating and interesting objects in the theory of General Relativity. They can be described as a region where the gravity is so strong that not even light can escape them. This “no-escape” boundary, called the event horizon, divides spacetime into two regions, and it plays a significant role in determining the properties of black holes. Considering the importance of the existence of an event horizon, the natural question to ask would be, “*What happens if we had objects that behave like black holes but do not have an event horizon?*”

Many physical systems that are governed by nonlinear equations admit soliton solutions. These are localized ‘packets’ of energy that are smooth and maintain their shape as they move. By analogy, a *gravitational soliton* is a non-trivial solution of Einstein field equations that is asymptotically flat, globally stationary, and geodesically complete. Unlike black holes, gravitational solitons do not have event horizons. More interestingly, those asymptotically flat and electrovacuum solutions do not exist in four-dimensional spacetimes. But, they do, indeed, exist in greater than four dimensions.

In this thesis, we have looked at certain types of gravitational solitons in asymptotically negatively-curved spacetimes, i.e., anti de-Sitter spacetimes. We construct the solutions, analyze their geometric structure, calculate their physical properties and investigate their stability by solving the wave equation on fixed soliton backgrounds.

# Acknowledgements

I first would like to express my deepest appreciation to my Ph.D. supervisor Dr. Hari K. Kunduri. During my graduate studies, there has not been any moment when I did not feel fully supported, both academically and personally. Dr. Kunduri has not only taught me the beauty of general relativity and introduced me to the mysterious nature of gravitational solitons but also set the example of being an open-minded, independent researcher. I could not have imagined having a better mentor and advisor for my academic journey.

I am also extremely grateful to have Dr. Ivan Booth as my departmental chair. As a graduate student, being mentored by such a student-oriented and progressive academician has been a privilege. I have always been inspired by his efforts to make the academic environment more diverse and equitable. Dōmo arigatō, Sensei!

I could not have reached this point without the support of Dr. Robie A. Hennigar. His advice and general wisdom have helped me greatly during the more challenging times. He has been an amazing source of motivation and academic recommendation while also often providing emotional support.

I would also like to acknowledge my deepest gratitude to Dr. Robert B. Mann for asking me one question at a conference, ultimately leading to a collaboration. It has been very educational to observe his experience.

Moreover, I would like to recognize the good people at the Department of Mathematics and Statistics of Memorial University. In particular, I would like to thank Dr. Graham Cox for sharing his mathematical expertise, Dr. JC Loredó-Osti for giving me the opportunity to teach, Dr. Danny Dyer for supporting first-time instructors, and my supervisory committee members, Dr. Eduardo Martínez-Pedroza and Dr. Tom Baird,

for their generous support during my degree. I would also be remiss in not mentioning the hard work and the amazing attitude toward students of the staff members; Tara Stuckless, Dawn Harvey, Melissa Strong, Carolyn Evans, and Leigh Herman.

Lastly, I thank my grandmother for teaching me fortitude, resilience, and courage. Without her teachings, I would not be who I am today.

# Statement of contribution

This Ph.D. thesis is supervised by Dr. Hari K. Kunduri. The other collaborators are Dr. Robert B. Mann and Dr. Robie A. Hennigar.

The thesis is written in the *manuscript style* as follows:

Chapter 2: “Supersymmetric multicharge solitons in AdS<sub>5</sub>”

Authors: Turkuler Durgut and Hari K. Kunduri

Published: Phys. Rev. D 105, 064068 (2022) [2].

Contribution of the student: practical aspects of research and manuscripts preparation.

Chapter 3: “Phase Transitions and Stability of Eguchi-Hanson-AdS Solitons”

Authors: Turkuler Durgut, Robie A. Hennigar, Hari K. Kunduri and Robert B. Mann

Published: JHEP 114 (2023) [3].

Contribution of the student: practical aspects of research and manuscripts preparation.

Chapter 4: “Supersymmetric asymptotically locally AdS<sub>5</sub> gravitational solitons”

Authors: Turkuler Durgut and Hari K. Kunduri

Accepted: Annals of Physics 457 (169435) in October 2023.

Contribution of the student: practical aspects of research.

# Contents

Title page	i
Abstract	ii
Lay summary	iv
Acknowledgements	v
Statement of contribution	vii
Contents	viii
List of Tables	xi
List of Figures	xii
List of symbols	xiii
List of abbreviations	xiv
<b>1 Introduction</b>	<b>1</b>
1.1 Supplementary Material . . . . .	14
<b>2 Supersymmetric Multicharge Solitons in AdS<sub>5</sub></b>	<b>17</b>
2.1 Abstract . . . . .	17

2.2	Introduction . . . . .	17
2.3	Supersymmetric AdS <sub>5</sub> solitons . . . . .	20
2.3.1	Supersymmetric solutions to gauged supergravity . . . . .	20
2.3.2	The local solution . . . . .	23
2.3.3	Global analysis and conserved charges . . . . .	28
2.3.4	The $U(1)^3$ supergravity theory . . . . .	31
2.4	Evanescent ergosurface and stable trapping . . . . .	35
<b>3</b>	<b>Phase Transitions and Stability of Eguchi-Hanson-AdS Solitons</b>	<b>39</b>
3.1	Abstract . . . . .	39
3.2	Introduction . . . . .	40
3.3	Metric and Structure . . . . .	43
3.3.1	The Large $p$ Limit of the Metric: AdS Soliton . . . . .	44
3.4	Soliton Mechanics . . . . .	45
3.4.1	Smarr Relation & First Law . . . . .	45
3.4.2	Euclidean action . . . . .	49
3.5	Geodesics . . . . .	51
3.5.1	Time-like Geodesics: Negative Mass Repulsion . . . . .	54
3.5.2	Null Geodesics: Absence of Stable Trapping . . . . .	56
3.5.3	Null Geodesics: Light-Crossing Time . . . . .	59
3.6	Wave Equation on Eguchi-Hanson Solitons . . . . .	61
3.6.1	Approximate Solution: WKB Analysis . . . . .	62
3.6.2	Numerical Solution: Boundary Conditions & Regularity . . . . .	65
3.6.3	Numerical Solution: Normal Modes . . . . .	67
3.7	Conclusions . . . . .	78
3.8	Appendix A: Comparison of Komar Mass with Holographic Renormalization . . . . .	80

3.9	Appendix B: Solution of the Radial Equation via the Shooting Method	82
3.10	Appendix C: Radial Equation at Large $p$ : Extracting the Slope of the Eigenvalues	86
3.10.1	Subleading Terms in a Large $p$ Expansion	87
3.11	Appendix D: Eguchi-Hanson Solitons as $p \rightarrow 2$	89
3.11.1	Solution of the Radial Equation as $p \rightarrow 2$	90
3.12	Appendix E: Tabulated Normal Mode Frequencies	92
<b>4</b>	<b>Supersymmetric Asymptotically Locally AdS<sub>5</sub> Gravitational Solitons</b>	<b>97</b>
4.1	Abstract	97
4.2	Introduction	98
4.3	Asymptotically locally AdS <sub>5</sub> supersymmetric solitons	101
4.3.1	Supersymmetric solutions to gauged supergravity	101
4.3.2	Derivation of the local solution	105
4.3.3	Global analysis and conserved charges	111
4.4	Discussion	123
<b>5</b>	<b>Conclusion and Future Work</b>	<b>125</b>
5.1	Conclusion	125
5.2	Future Work	126
5.2.1	Asymptotically locally AdS <sub>5</sub> solutions	126
5.2.2	Conserved charges	128
5.2.3	Euclidean Action	129
5.2.4	Klein-Gordon Equation	132
	<b>Bibliography</b>	<b>135</b>

# List of Tables

3.1	A selection of numerical values for the fundamental frequency for a few values of $p$ . . . . .	65
3.2	A selection of numerically obtained $\alpha_{N,n}$ values computed using the pseudospectral method to show accuracy . . . . .	88
3.3	A selection of normal modes and their overtones for $p = 3$ . . . . .	94
3.4	A selection of normal modes and their overtones for $p = 4$ . . . . .	95
3.5	A selection of normal modes and their overtones for $p = 5$ . . . . .	96

# List of Figures

1.1	Penrose diagram for AdS spacetime . . . . .	10
3.1	Figure 3.1: A plot of the light-crossing time $T_p$ as a function of $p$ . . . . .	60
3.2	Figure 3.2: A plot of a comparison of the WKB approximate results for $n = k = 0$ with the numerically computed eigenvalues for $p = 3, 4, 5, 6$ . . . . .	69
3.3	Figure 3.3: A plot showing the error in the WKB approximation as a function of overtone number for $p = 3, 4, 5, 6$ . . . . .	70
3.4	Figure 3.4: A plot showing the difference between the overtone spacing for the numerically computed frequencies $\Delta\omega_{\text{Num}} = \omega_{N+1} - \omega_N$ and the fundamental frequency $\omega_{\text{fun}}$ on a logarithmic scale . . . . .	70
3.5	Figure 3.5: Four plots comparing the approximate form of fundamental mode against the numerically determined spectra . . . . .	73
3.6	Figure 3.6: Four plots of the frequencies versus $p$ for different $k$ values . . . . .	74
3.7	Figure 3.7: Three plots of the fundamental mode for different $k$ values . . . . .	76
3.8	Figure 3.8: Three plots of the logarithmic derivative of the numerical solutions . . . . .	83
3.9	Figure 3.9: Plots of the integrated (reciprocal) residual for different $n$ values . . . . .	85
3.10	Figure 3.10: Four plots showing the dependency of of the number of points $\mathcal{N}$ used in the Chebychev discretization . . . . .	92
3.11	Figure 3.11: Two plots of the frequency as a function of $p$ for different $n$ values . . . . .	93

# List of symbols

$\mathbb{Z}$  integers

$\mathbb{R}$  real numbers

# List of abbreviations

BPS	Bogomol'nyi–Prasad–Sommerfield.
GR	General relativity
LIGO	Laser Interferometer Gravitational-Wave Observatory
AdS	Anti-de Sitter spacetime
CFT	Conformal field theory

# Chapter 1

## Introduction

The theory of general relativity (GR) is our mathematical framework for describing gravitational fields. It has passed all the experimental tests to this date. One of its most striking predictions, the existence of gravitational waves, was confirmed by the Laser Interferometer Gravitational-Wave Observatory (LIGO). On 14 September 2015, two detectors of LIGO simultaneously observed gravitational waves and a binary black hole merger [4]. Later in 2017, they also announced that they had observed a binary neutron star merger by the Advanced LIGO and Advanced Virgo detectors through gravitational waves [5]. With these new developments and observations, the theory of general relativity has become more relevant when trying to determine the evolution of the Universe and in the physics of massive objects, such as black holes.

As general relativity is a geometric theory of gravitation, the structure of curved spacetimes is explained with a mathematical object, called the *metric tensor*. A metric tensor is a covariant, second-degree, symmetric tensor on a differentiable manifold, often denoted by  $g_{\mu\nu}$ . It encodes both geometrical information about the coordinate system and physical information about the gravitational field. It is used to compute distances and angles, and hence the curvature. The invariant spacetime interval, for instance, is given by

$$ds^2 = g_{\mu\nu} dx^\mu dx^\nu. \quad (1.1)$$

In general relativity, the Einstein field equations relate the curvature of the spacetime to the distribution of matter within the spacetime as follows

$$G_{\mu\nu} = \frac{8\pi G}{c^4} T_{\mu\nu}, \quad (1.2)$$

where  $G_{\mu\nu}$  is the Einstein curvature tensor and  $T_{\mu\nu}$  is the total energy-momentum tensor. The Einstein curvature tensor is defined as

$$G_{\mu\nu} \equiv R_{\mu\nu} - \frac{1}{2} R g_{\mu\nu}, \quad (1.3)$$

where  $R_{\mu\nu}$  is the Ricci tensor and  $R$  is the scalar curvature. Considering the symmetries of the Einstein curvature tensor and the total energy-momentum tensor, the Einstein field equations is a set of second-order, partial differential equations of the metric tensor  $g_{\mu\nu}$ . These equations are not only coupled, but also non-linear in the metric tensor and its first derivatives. However, they are linear in the second derivatives of the metric tensor. In general relativity, the motion of masses is necessarily dictated by the Einstein field equations.

The simplest solution of the Einstein field equations occurs when there are no sources of energy present. This spacetime which is called the *Minkowski spacetime* explains the kinematical rules of special relativity. It is described by the *flat metric*, given by

$$ds^2 = -c^2 dt^2 + dx^2 + dy^2 + dz^2. \quad (1.4)$$

In general relativity, studying isolated systems is very common. Even though it is not always possible to physically isolate a system, it is reasonable to assume that a distant object would not affect the local structure of the spacetime. In other words, at large distances, an isolated gravitational system is described by asymptotically flat geometries where the curvature vanishes at large distances. This means that the spacetime curvature decays to zero when it is far from the matter source. For those asymptotically flat spacetimes, one can define physical invariants such as mass, angular momenta and charge.

The simplest *curved* spacetimes of general relativity are the ones with the most symmetry, e.g., an empty space outside a spherically symmetric source. This geometry is called the *Schwarzschild solution*. The spherically symmetric solution to the Einstein

field equations in vacuum is given by the Schwarzschild metric, which is

$$ds^2 = -c^2 \left(1 - \frac{R_S}{r}\right) dt^2 + \left(1 - \frac{R_S}{r}\right)^{-1} dr^2 + r^2 (d\theta^2 + \sin^2(\theta)d\phi^2), \quad (1.5)$$

where  $R_S$  is Schwarzschild radius defined as

$$R_S \equiv \frac{2GM}{c^2}, \quad (1.6)$$

and the time coordinate  $t \in \mathbb{R}$ , the radial coordinate  $r > R_S$ , and  $\theta$  and  $\phi$  are the standard coordinates on 2-sphere.

The Schwarzschild solution also tells us the strong field behavior of general relativity, i.e., the prescription for the spacetime after the gravitation collapse of a spherical body. The vacuum Schwarzschild solution that describes the aftermath of a gravitational collapse contains a spacetime singularity hidden within a black hole.

Ignoring the constants ( $G = c = 1$ ), the boundary of this black hole, *event horizon*, is located at  $r = 2M$ . For external observers, there are only two relevant regions: on and outside the event horizon. Events that are happening inside the event horizon cannot affect the outside. It is important to point out that the singularity in the Schwarzschild metric at  $r = 2M$  is not a singularity in the geometry of the spacetime, but a singularity in the Schwarzschild coordinates. By using the Eddington-Finkelstein coordinates, for instance, one can rewrite the same metric in a form that is manifestly smooth across the surface  $r = 2M$ .

The presence of an event horizon is one of the defining properties of a black hole and the event horizon plays a significant role in determining those properties. The No-Hair Theorem explains the characterization of black holes as follows:

**Theorem 1 (A black hole has no hair)** *The external gravitational and electromagnetic fields of a stationary black hole are determined uniquely by the black hole's mass  $M$ , charge  $Q$ , and intrinsic angular momentum  $J$  - i.e., a black hole can have no "hair" (no other independent characteristics) [6].*

The theorem shows that the three-parameter family of stationary Kerr-Newmann black hole solutions are the unique, stationary asymptotically flat black hole solutions

of the Einstein-Maxwell theory.

The concept of energy and the conservation laws play a crucial role in physics. In general relativity, the energy properties of matter are represented by the energy-momentum tensor,  $T_{\mu\nu}$ , also known as the stress-energy tensor. Therefore, the local energy density of matter measured by an observer is well-defined. One of the properties of the stress-energy tensor,  $\nabla^\mu T_{\mu\nu} = 0$ , might also be interpreted as local conservation of energy. However, considering the absence of the notion of the energy density of the gravitational field, this property of the stress-energy tensor does not address a global energy conservation law. Yet, there exists, indeed, a notion of total energy for an isolated system.

In general, it is expected to relate the total energy of a physical system to its Hamiltonian. With that regard, a notion of total energy and momentum at spatial infinity on a hypersurface  $\Sigma$  was given in the Hamiltonian formalism by *ADM mass*. The gravitational mass of an asymptotically flat spacetime is

$$M_{\text{ADM}} = -\frac{1}{8\pi} \lim_{S_t \rightarrow \infty} \oint_{S_t} (k - k_0) \sqrt{\sigma} d^2\theta. \quad (1.7)$$

In this notation,  $S_t$  is a two-sphere at spatial infinity with a specific choice of shift and lapse,  $\sigma_{AB}$  is the metric on it,  $k$  is the extrinsic curvature of  $S_t$  embedded in  $\Sigma$ , and  $k_0$  is the extrinsic curvature of  $S_t$  embedded in the flat space. Since the ADM mass is independent of choice of spatial slice, in this thesis, we will refer to it as the total mass of the spacetime even though it is, in fact, the mass of the hypersurface. Additionally, the mass is well-defined for any asymptotically flat spatial hypersurface in the spacetime satisfying appropriate fall-off conditions at spatial infinity.

An alternative definition for the mass for stationary spacetimes was given by Komar [7] in 1959 and hence, known as *Komar mass*, is

$$M_{\text{Komar}} = -\frac{1}{8\pi} \lim_{S_t \rightarrow \infty} \oint_{S_t} \nabla^\alpha \xi_{(t)}^\beta dS_{\alpha\beta}, \quad (1.8)$$

where  $\xi_{(t)}^\alpha$  is the timelike Killing vector field. The surface element is defined as

$$dS_{\alpha\beta} = -2n_{[\alpha} r_{\beta]} \sqrt{\sigma} d^2\theta, \quad (1.9)$$

where  $n_\alpha$  is the timelike and  $r_\alpha$  the spacelike normal of  $S_t$ . For stationary spacetimes, the Komar formalism and the Hamiltonian formalism give equivalent results, and we will simply denote this mass by  $M$ .

Similarly, one can also define the angular momentum for axially symmetric spacetimes in this formalism as

$$J = \frac{1}{16\pi} \lim_{S_t \rightarrow \infty} \oint_{S_t} \nabla^\alpha \xi_{(\phi)}^\beta dS_{\alpha\beta}, \quad (1.10)$$

where  $\xi_{(\phi)}^\alpha$  is the rotational Killing vector field. Since both  $M$  and  $J$  are defined by using integrals over a closed two-surface at infinity, they can be thought of as the properties of the asymptotic structure.

**Theorem 2 (Positive Mass Theorem)** *Assuming the dominant energy condition, the mass of an asymptotically flat spacetime is non-negative. It is zero if and only if the space is flat [8, 9, 10].*

The second law of thermodynamics states that the total entropy of all matter in the Universe cannot decrease in any physically allowed process. A similar statement was given for black holes by Hawking in 1971 [11]. The *black hole area theorem* tells us that the total area of the black hole in the Universe cannot decrease in any physically allowed process. This analogue for black holes of the second law of thermodynamics extends to the other laws of thermodynamics, as well.

The event horizon of a stationary black hole is a Killing horizon, which means it is a null hypersurface  $\mathcal{N}$  whose normal is a Killing vector field. In other words, there is a Killing vector field  $\xi^a$  which becomes null on the event horizon, and the associated one-form  $\xi_a = g_{ab}\xi^b$  is normal (and tangent) to  $\mathcal{N}$ . Let us start with the definition of the *surface gravity* of a stationary black hole

$$\kappa^2 = -\frac{1}{2} \xi^{\alpha;\beta} \xi_{\alpha;\beta} \Big|_{\mathcal{N}}. \quad (1.11)$$

It can be proved that  $\kappa$  is in fact a *constant* over the event horizon of a stationary black hole, just like the temperature being constant throughout body in thermal equilibrium. In fact, the concept of temperature for black holes, introduced by Hawking in his

famous discovery that black holes radiate, is well-defined as follows

$$T = \frac{\hbar}{2\pi} \kappa. \quad (1.12)$$

Therefore, surface gravity  $\kappa$  plays the role of temperature in the black hole physics. Classically speaking, the surface gravity can also be considered the force needed to hold the test particle at rest near the horizon. The surface gravity for the Schwarzschild solution, for instance, is  $\kappa = \frac{1}{4M}$ .

A classic result is the first law of black hole mechanics which states that under small variations in the parameters of a stationary black hole,

$$\delta M = \frac{\kappa}{8\pi} \delta A + \Omega_H \delta J + \Phi_H \delta Q \quad (1.13)$$

which relates the changes in mass with the changes in surface area and angular momentum. Here,  $\Omega_H$  is the angular velocity of the black hole and it measures the rate at which the black hole rotates with respect to a static observer at infinity. Also,  $\Phi_H$  is the (constant) electric potential on the horizon.

Given the importance of electrovacuum solutions of the Einstein-Maxwell field equations, are there solutions with positive mass, but without an event horizon? We emphasize that there are certainly isolated gravitating systems, such as stars, that have positive mass, but these are not vacuum. A *gravitational soliton* is a non-trivial solution of Einstein field equations that is asymptotically flat, globally stationary, and geodesically complete. For gravitational solitons, the positive mass theorem also applies. One feature that separates gravitational solitons from black holes is that they do not have event horizons. A classic result in four-dimensional general relativity by Lichnerowicz tells us that asymptotically flat and electrovacuum gravitational solitons cannot exist [1]. This result can also be shown using the positive mass theorem, Stokes' theorem, and stationary Killing vector field identities, as follows:

Let us consider a simple example of supergravity theory, stationary Einstein-Maxwell system for an asymptotically flat,  $n$ -dimensional, globally hyperbolic spacetime with a timelike everywhere Killing vector field  $K$ . The field equations are then

$$R_{ab} = 2 \left( F_{ac} F_b^c - \frac{1}{2(n-2)} g_{ab} F^2 \right), \quad (1.14)$$

$$dF = 0 \quad \text{and} \quad d \star F = 0 \quad (1.15)$$

where  $F$  is the Maxwell field strength two-form. The interior product  $dF = 0$  tells us that there exists a globally defined electric potential  $\psi$  which comes from the topological assumption that the spacetime is simply connected [12], and  $d\psi$  is a one-form which is exact. On the other hand, the exterior product  $d \star F = 0$  tells us that there exists a closed  $(n-3)$ -form,  $i_K \star F$ , which is only exact if, in four dimensions,  $i_K \star F = d\mu$  is exact.

In four dimensions, by applying the Stokes' theorem to the Komar mass formalism

$$M = -\frac{1}{8\pi} \int_{S_\infty^2} \star dK = -\frac{1}{8\pi} \int_\Sigma d \star dK. \quad (1.16)$$

Using the fact that  $K$  is a Killing vector field

$$M = \frac{1}{4\pi} \int_\Sigma \star Ric(K). \quad (1.17)$$

By using the field equations

$$M = \frac{1}{4\pi} \int_\Sigma d(\mu F). \quad (1.18)$$

We have already established that  $d\psi$  is exact, and in four dimensions,  $d\mu$  is also exact. In the absence of an inner boundary, the mass is zero. By the positive mass theorem, the only allowed spacetime in this case is the Minkowski spacetime. In other words, an isolated self-gravitating system in equilibrium with positive energy must contain a black hole [13]. Gibbons summarized this with the slogan

*“No solitons without horizons.”*

This result extends to higher dimensions for pure vacuum [14], static solitons were ruled out in Einstein-Maxwell theory [15], and no known stationary examples are known (see, e.g., the review [16]). However, gravitational solitons in higher than four dimensions naturally arise in supergravity theories. Explicit examples of asymptotically flat soliton spacetimes with *bubbles* have been shown in [17, 18, 19]. In addition to those supersymmetric solitons (i.e. they admit Killing spinors), non-supersymmetric

solutions in five dimensional spacetimes were also constructed [20, 21, 22]. Due to the *fuzzball conjecture* [23], those gravitational solitons have drawn attention. Similar to the black hole case, soliton first law and Smarr relation was rigorously demonstrated in the asymptotically flat case in [24] extended to a particular example of an asymptotically globally Anti-de Sitter soliton case in [25]. Typically, gravitational solitons are characterized by some non-trivial topology in the spacetime, such as non-collapsing spheres or *bubbles*. A bubble, in the context of solutions to the Einstein equations, refers to a ‘hole’ in a spatial hypersurface in spacetime. Mathematically speaking, it is a non-contractible cycle, that is a closed  $n$ -dimensional submanifold, located at some region of space. For the solutions considered in this thesis, these bubbles are two-dimensional spheres ( $S^2$ ) that cannot be shrunk to a point. The geometries smoothly ‘pinch off’ near a bubble, so the four-dimensional spatial surface near the bubble looks like  $\mathbb{R}^2 \times S^2$  where the  $\mathbb{R}^2$  factor has polar coordinates  $(r, \psi)$ . The bubble is located at  $r = 0$  where the polar angle  $\partial_\psi$  degenerates. For this degeneration to be smooth (no conical singularities), we must impose constraints on the parameters of the solution.

In [24], the first law of black hole mechanics and Smarr relation in a general five dimensional theory of Einstein gravity coupled to an arbitrary number of Maxwell fields  $F^I$  and neutral scalars  $\chi^A$  are derived. The result applies to asymptotically flat spacetimes that could contain both black holes *and* solitons (i.e. an arbitrary number of bubbles as described above). They found that even in the absence of black holes, the mass of a soliton in an asymptotically flat, stationary spacetime is

$$M = \frac{1}{2} \sum_{[C]} \Psi[C] q^I[C] + E_\chi, \quad (1.19)$$

and the mass difference between nearby solitons in phase space satisfies

$$\delta M = \sum_{[C]} \Psi[C] \delta q^I[C]. \quad (1.20)$$

Here, the sum over  $[C]$  denotes a sum over the bubbles, or 2-cycles,  $q[C]$  is a magnetic flux associated to each bubble,  $E_\chi$  is a contribution coming from background scalar fields, and  $\Psi[C]$  is a certain potential associated to each bubble. Thus solitons also satisfy a ‘law of soliton mechanics’ analogous to the well-known black hole first law

discussed above.

*Anti-de Sitter spacetime (AdS)* is a maximally symmetric solution to Einstein field equations with negative scalar curvature. Geometries arising in general relativity that are asymptotically Anti-de Sitter have been of huge interest for the last two decades because of the famous conjectured relationship between Anti-de Sitter spacetimes and conformal field theories, called *the gauge theory/gravity duality* [26]. This conjectured relation asserts that quantum gravity in asymptotically Anti-de Sitter backgrounds is equivalent to a certain type of quantum field theory defined on the boundary of this Anti-de Sitter spacetime. In principle, this provides a formulation of quantum gravity in this setting in terms of a well-defined quantum field theory with many qualitative similarities to the theories describing particle physics. This gives a new approach to describing phenomena in particle physics that cannot be studied using standard techniques.

The metric for  $n$ -dimensional AdS spacetime is given by

$$ds^2 = - \left( 1 + \frac{r^2}{\ell^2} \right) dt^2 + \left( 1 + \frac{r^2}{\ell^2} \right)^{-1} dr^2 + r^2 d\Omega_{n-2}^2, \quad (1.21)$$

where  $\ell$  is the AdS length parameter and  $d\Omega_{n-2}^2$  is the round metric on  $S^{n-2}$ . The Ricci curvature is

$$R_{\mu\nu} = - \frac{(n-1)}{\ell^2} g_{\mu\nu}. \quad (1.22)$$

By using the coordinate transformation

$$t = \ell\tau \quad \text{and} \quad r = \ell \sinh(\rho), \quad (1.23)$$

one can draw the Penrose diagram.

One of the interesting features of AdS spacetimes is that although AdS is maximally symmetric and geodesically complete, it is not a globally hyperbolic spacetime. As it can be seen from the Penrose diagram, AdS has closed timelike curves and  $\rho = \frac{\pi}{2}$ , the spatial infinity is timelike. Hence, there is an information leak to and from infinity, which can be sealed by using reflective boundary conditions.

Finding solutions to (1.22) is significantly more challenging than finding electrovacuum

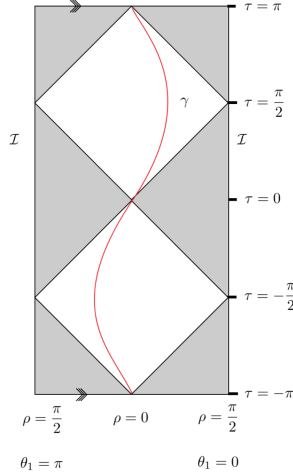


Figure 1.1: Penrose diagram for AdS spacetime

In this diagram, the coordinates  $\theta_1$  and  $\psi$  are suppressed,  $\mathcal{I}$  represents the conformal infinity, and the red curve represents a timelike geodesic. Considering the future and past domain of dependence of a hypersurface and predictability of the set of initial data that hypersurface forms, shaded triangles denote the regions where no prediction can happen.

solutions (mathematically, this is analogous to finding Einstein metrics with non-zero curvature). A natural question is whether black hole solutions exist that are asymptotically AdS. The best known example of this kind is the static and spherically symmetric Schwarzschild-AdS solution

$$ds^2 = - \left( 1 - \frac{2M}{r^{n-3}} + \frac{r^2}{\ell^2} \right) dt^2 + \left( 1 - \frac{2M}{r^{n-3}} + \frac{r^2}{\ell^2} \right)^{-1} dr^2 + r^2 d\Omega_{n-2}^2, \quad (1.24)$$

which reduces to the Schwarzschild solution in the limit of vanishing cosmological constant  $\ell \rightarrow \infty$ . While there is a generalization of these solutions to include angular momenta (the Kerr-AdS black holes), there is no analogue of the no-hair theorems for AdS black holes. This is ultimately tied to the complexity of (1.22).

For asymptotically anti-de Sitter spacetimes, a formalism for calculations of conserved quantities, such as mass and angular momenta, was developed by Ashtekar, Magnon, and Das [27]. In this formalism, given any infinitesimal asymptotic symmetry and

$d - 2$  sphere cross section  $C$  at infinity, a conserved quantity is defined by

$$Q_\xi[C] \equiv -\frac{1}{8\pi G} \frac{\ell}{n-3} \oint_C \mathcal{E}_{ab} \xi^a dS^b, \quad (1.25)$$

where  $\mathcal{E}_{ab}$  is the electric part of the (leading order) Weyl tensor and  $\xi^a$  is the conformal Killing vector field. Effectively, the definition measures the rate of decay of the Weyl tensor as we approach infinity (since AdS is conformally flat and has vanishing Weyl tensor). Applying this to the static Killing field  $\partial_t$  for the Schwarzschild-AdS metric, one finds that its mass is proportional to the parameter  $M$ . Note that the standard Komar mass will diverge for asymptotically AdS spacetimes. The problem of defining well-behaved conserved charges in asymptotically AdS spacetimes remains an active area of research.

Naturally, one might ask whether asymptotically AdS gravitational solitons exist. It has proved harder to find explicit analytic examples in any dimension. A general class of asymptotically globally AdS<sub>5</sub> gravitational solitons was considered in [25]. They are solutions of minimal five-dimensional gauged supergravity, which is essentially Einstein-Maxwell theory with a negative cosmological constant (the precise action will be given later in this thesis). The metric is given by

$$ds^2 = -\frac{r^2 W(r)}{4b(r)^2} dt^2 + \frac{dr^2}{W(r)} + \frac{r^2}{4} (\sigma_1^2 + \sigma_2^2) + b(r)^2 (\sigma_3 + f(r) dt)^2, \quad (1.26)$$

with the metric functions

$$\begin{aligned} b(r)^2 &= \frac{r^2}{4} \left( 1 - \frac{j^2 q^2}{r^6} + \frac{2j^2 p}{r^4} \right), \\ W(r) &= 1 + \frac{4b(r)^2}{\ell^2} - \frac{2}{r^2} (p - q) + \frac{q^2 + 2pj^2}{r^4}, \\ f(r) &= -\frac{j}{2b(r)^2} \left( \frac{2p - q}{r^2} - \frac{q^2}{r^4} \right), \end{aligned} \quad (1.27)$$

where  $p, q, j \in \mathbb{R}$ . Left-invariant one-forms  $\sigma_i$  on SU(2) are

$$\begin{aligned} \sigma_1 &= -\sin \psi d\theta + \cos \psi \sin \theta d\phi, \\ \sigma_2 &= \cos \psi d\theta + \sin \psi \sin \theta d\phi, \\ \sigma_3 &= d\psi + \cos \theta d\phi, \end{aligned} \quad (1.28)$$

satisfying

$$d\sigma_i = \frac{1}{2} \epsilon_{ijk} \sigma_j \wedge \sigma_k, \quad (1.29)$$

with the identifications

$$\begin{aligned} \psi &\sim \psi + \frac{4\pi}{k}, \\ \psi &\sim \psi + 2\pi, \phi \sim \phi + 2\pi, \\ \theta &\in (0, \pi). \end{aligned} \quad (1.30)$$

Since the metric is written in terms of these  $SU(2)$ -invariant forms, it automatically inherits this as its isometry group. In addition it has a  $U(1)$  isometry generated by  $\partial_\psi$ . Therefore, the full set of symmetries is  $\mathbb{R} \times SU(2) \times U(1)$  where the first factor corresponds to time translations. The bubble  $r_0$  is located where the metric functions  $b(r)^2$  and  $W(r)$  have simultaneous zeros. From the metric we see that this means  $\partial_t$  is timelike at  $r = r_0$  but the spacelike Killing field  $\partial_\psi$  degenerates there, much like the axial vector  $y\partial_x - x\partial_y$  degenerates at the origin in  $\mathbb{R}^2$ . The  $(\theta, \phi)$  coordinates then define a  $S^2$  (the ‘‘bubble’’) of radius  $r_0/2$ . This puts restrictions on the parameters as follows:

$$\begin{aligned} 1 - \frac{j^2 q^2}{r_0^6} + \frac{2j^2 p}{r_0^4} &= 0, \\ 1 - \frac{2}{r_0^2} (p - q) + \frac{q^2 + 2pj^2}{r_0^4} &= 0, \end{aligned} \quad (1.31)$$

which means

$$p = \frac{r_0^4 (r_0^2 - j^2)}{2j^4} \quad \text{and} \quad q = -\frac{r_0^4}{j^2}. \quad (1.32)$$

Note that the coordinate singularity for  $r = r_0$  can easily be avoided by using a coordinate transformation. In the original work, only the  $k = 1$  case was considered. Then the geometry is asymptotically globally  $\text{AdS}_5$  (that is, the conformal boundary as  $r \rightarrow \infty$  is  $\mathbb{R} \times S^3$ ). The resulting geometry has the following conserved quantities

$$\begin{aligned} \text{Mass} \quad M &= \frac{\pi}{4} \left( 3(p - q) + \frac{j^2 p}{\ell^2} \right), \\ \text{Electric charge} \quad Q &= -\frac{\sqrt{3}}{2} \pi \frac{r_0^4}{j^2}, \\ \text{Angular momentum} \quad J &= \frac{\pi j}{4} (2p - q), \end{aligned} \quad (1.33)$$

and the following first law holds

$$dM = VdP + \sum_{[I]} \Psi[I]dq[I], \quad (1.34)$$

where  $P, V$  are a ‘thermodynamic pressure’ and ‘volume’ associated to asymptotically AdS spacetimes. The progress that has been completed so far to generalize this work for the general  $k \in \mathbb{N}$  values is presented in Chapter 5.

This thesis is organized as follows:

- In Chapter 2, we construct new supersymmetric, asymptotically globally AdS<sub>5</sub> gravitational soliton solutions of five-dimensional gauged supergravity and show that they contain evanescent ergosurfaces. We argue that this indicates they nonlinearly unstable. This chapter is based on the article “Supersymmetric multicharge solitons in AdS<sub>5</sub>” by Turkuler Durgut and Hari K. Kunduri published on Physical Review D 105, 064068 (2022).
- In Chapter 3, we analyze the family of Eguchi-Hanson-AdS<sub>5</sub> gravitational solitons. These are static soliton solutions of the vacuum Einstein equations with negative cosmological constant. They are characterized by a positive integer  $p \geq 3$  and they are not asymptotically globally AdS<sub>5</sub>, but rather asymptotic to AdS<sub>5</sub>/Z<sub>p</sub>. We study mode solutions of the linear scalar wave equation and show it has a normal mode spectrum. We also study various geometric and thermodynamic properties of these solutions which had not been investigated before. This chapter is based on the article “Phase Transitions and Stability of Eguchi-Hanson-AdS Solitons” by Turkuler Durgut, Robie A. Hennigar, Hari K. Kunduri and Robert B. Mann (Journal of High Energy Physics 114 (2023)).
- In Chapter 4, we construct new supersymmetric gravitational soliton solutions of five-dimensional gauged supergravity coupled to arbitrarily many vector multiplets which are asymptotic to AdS<sub>5</sub>/Z<sub>p</sub>. These can be thought of supersymmetric generalizations of the Eguchi-Hanson-AdS<sub>5</sub> solution. This work is based on an article “Supersymmetric asymptotically locally AdS<sub>5</sub> gravitational solitons” by Turkuler Durgut and Hari K. Kunduri, which is accepted to Annals of Physics 457 (169435) in July 2023.

Finally, in the conclusion we summarize our main results and present some ongoing work on extending the analysis of Chapter 3 to the more general, charged and rotating solitons with local metrics given by (1.21). In particular we discuss progress on solving the linear wave equation, the calculation of the Euclidean action, and new solutions which are asymptotically  $\text{AdS}_5/\mathbb{Z}_p$  for  $p > 1$ .

## 1.1 Supplementary Material

This thesis is written in the manuscript style, and the following chapters are taken directly from the published version of the corresponding articles. They are therefore written for a specialized audience and contain certain field-specific terms which are assumed to be well-known. Here, we provide some background material for the reader unfamiliar with these details.

A *supergravity theory* can be thought of as a theory of gravity that is also invariant under local supersymmetry transformations. It necessarily contains both bosonic fields  $B$ , such as the metric  $g_{ab}$ , which has spin 2, and Maxwell fields  $F^I$ , which are spin 1, and spinorial fields  $F$ , such as the gravitino, which has spin 3/2. In addition to the usual diffeomorphism invariance, the action is invariant under supersymmetry transformations in the form of

$$\delta B = \epsilon F, \quad \delta \psi = D\epsilon \tag{1.35}$$

where  $\epsilon$  can be considered a spinor parametrizing the transformation, and  $D$  denotes the covariant derivative acting on spinors. This is analogous to how a tensor field  $T$  transforms under an infinitesimal transformation generated by a vector field  $X$ , i.e.,  $T \rightarrow T + \epsilon L_X T$ . Since we are interested in classical solutions that are purely bosonic, we consider solutions with  $F = 0$ . In this case, a supergravity theory typically reduces to general relativity plus additional matter fields. For example, the familiar four-dimensional Einstein-Maxwell theory can be thought of as the bosonic part of a supergravity theory.

A subset of bosonic solutions of a supergravity theory (i.e., solutions of the equations

of motion with all fermions set to zero) will also ‘preserve’ some fraction of the supersymmetry. These are called *supersymmetric* or *BPS solutions*. For these solutions, we have  $\delta F = D\epsilon = 0$ . Here, the spin connection  $D$  depends on the metric and possibly other bosonic fields. Solutions  $\epsilon$  to this equation are called *Killing spinors*. The idea here is similar to how geometries admitting a continuous isometry admit a Killing vector field  $K$  satisfying  $D_{(a}K_{b)} = 0$ . Hence, looking at supersymmetric solutions is similar to, for instance, restricting attention to stationary solutions.

A supergravity theory generally admits more than one independent supersymmetry, and is generally labeled by its total number of generators. For example, the five-dimensional supergravity theories considered in this thesis are called ‘ $N = 1$  supergravities’, which perhaps confusingly means they admit eight supercharges (a spinor has eight independent components). A BPS solution will generally only preserve a fraction of these supersymmetries or, equivalently, admit only a smaller number of Killing spinors than the maximal number. In particular, for the theories considered here, it can be proved that BPS solutions can preserve only  $1/4$  or  $1/2$  of the maximal number. It is customary to refer to these solutions as  $1/4$  BPS or  $1/2$  BPS, respectively. Using the algebra satisfied by the supersymmetry generators, one can show that for BPS solutions, the energy  $M$ , charge  $Q$ , and angular momentum  $J$  will be related; such an equation is called a *BPS relation*. For the gauged supergravity theories considered here, the unique solution which preserves the full set of supersymmetries (admitting the maximal number of independent Killing spinors) is global  $\text{AdS}_5$ ; physically, it is interpreted as the ground state, or vacuum, solution. However, this doesn’t guarantee that it is dynamically stable.

If a solution admits a Killing spinor, then the integrability conditions obtained from the first-order equation  $D\epsilon = 0$ , which put a number of differential and algebraic constraints on the bosonic fields. In particular, the field equations (which are second-order) can be shown to hold as a consequence. Therefore, finding BPS solutions is more tractable. A great deal of work has been done to find the necessary and sufficient conditions for the existence of a BPS solution; these conditions are easier to solve than trying to directly solve the field equations and *then* impose supersymmetry. We will use this technology in the thesis with appropriate references to their derivation.

Given a Killing spinor  $\epsilon$ , one can construct an associated vector field  $V^a = \bar{\epsilon}\gamma^a\epsilon$  (here

$\gamma^a$  is a ‘gamma matrix’ which acts on spinors, and  $\bar{\epsilon}$  denotes the conjugate of  $\epsilon$ ). This vector field  $V$  is necessarily a Killing vector field and must be either timelike or null, so we can write  $g_{ab}V^aV^b = -f^2 \leq 0$  for some smooth function  $f$ . For the solution in this thesis, we consider the case where  $V$  is timelike almost everywhere, particularly at infinity, and so we refer to this preferred vector field as the *supersymmetric timelike Killing field*. Note that there are other timelike Killing fields one could construct by taking linear combinations of other Killing fields; it will turn out that ergosurfaces, where an asymptotically timelike Killing vector field becomes null, may exist with respect to one choice but not the other.

Finally, we make some comments on the particular supergravity theories considered in this thesis. We construct BPS solutions of five-dimensional gauged supergravity coupled to  $n - 1$  vector multiplets. The bosonic content of this theory consists of the metric,  $n$  Maxwell fields  $F^I$ , and  $n - 1$  scalar fields  $\Phi^I$ . It is more convenient to work with  $n$  scalar fields  $X^I$  subject to a constraint, namely  $C_{IJK}X^IX^JX^K = 6$ . Here the  $C_{IJK}$  are a set of constants which characterize the theory; for the particular choice  $C_{IJK} = |\epsilon_{IJK}|$  with  $I = 1, 2, 3$  the corresponding supergravity theory is the so-called ‘ $U(1)^3$  gauged  $N = 1$  supergravity ’ that is much studied in the theoretical physics community as it arises as a dimensional reduction on  $S^5$  of the low-energy limit of ten-dimensional Type IIB string theory. This is relevant for studies of AdS-CFT correspondence, although our motivation is purely from the gravitational perspective.

# Chapter 2

## Supersymmetric Multicharge Solitons in $\text{AdS}_5$

This chapter is based on “Supersymmetric multicharge solitons in  $\text{AdS}_5$ ” by Turkuler Durgut and Hari K. Kunduri published in *Phys. Rev. D* 105, 064068 (2022).

### 2.1 Abstract

We construct supersymmetric, asymptotically  $\text{AdS}_5$  gravitational soliton solutions of five-dimensional gauged supergravity coupled to arbitrarily many vector multiplets. These generalize the supersymmetric solitons of  $U(1)^3$  gauged supergravity previously constructed by Chong, Cvetic, Lu, and Pope. We show that the solitons contain evanescent ergosurfaces and give an argument that these solitons should be nonlinearly unstable.

### 2.2 Introduction

A gravitational soliton is a geodesically complete, globally stationary (and horizon-free) non-trivial solution of the Einstein equations, with prescribed asymptotic geometry. It is a classic theorem of Lichnerowicz [1] that asymptotically flat, electrovacuum gravitational solitons cannot exist. The proof is considerably simpler if one employs

the spacetime positive mass theorem [13]. In the pure vacuum case, the result extends to higher dimensions [14], and in Einstein-Maxwell theory, static solitons can be ruled out [15] and no stationary examples are known (see, e.g. the review [16]). On the other hand, within supergravity theories which have Maxwell fields (or higher  $p$ -form field strengths), there are many known families of asymptotically flat solitons carrying mass, angular momenta, and electric charge ‘magnetic fluxes’ which support non-trivial cycles in the spacetime. These charges satisfy variational laws analogous to the first law of black hole mechanics [24].

The majority of these known solutions are asymptotically flat and supersymmetric (i.e., they are supergravity solutions admitting one or more Killing spinors [28]). However, this is likely a result of the fact that the integrability conditions imposed by supersymmetry allow for the construction of explicit solutions (see [29] for classification of supersymmetric black holes and solitons with  $U(1)^2$  isometry in minimal ungauged supergravity). Fewer examples are known in the asymptotically globally AdS setting with conformal boundary  $\mathbb{R} \times S^n$ . Non-supersymmetric examples were constructed in [30] by taking limits of local solutions of gauged supergravity that were first used to obtain charged, rotating asymptotically AdS<sub>5</sub> black holes. As the solitons do not have horizons, they cannot be interpreted as thermal states from the CFT perspective. It is reasonable to interpret them as pure states with non-zero vacuum expectation values for energy and R-charge.

Given the difficulty in constructing solutions of gauged supergravity, it is natural to focus attention on supersymmetric soliton geometries. A general formalism for constructing BPS solutions of minimal gauged supergravity was given in [31] with the purpose of constructing the first examples of supersymmetric AdS<sub>5</sub> black holes. The analysis shows that BPS solutions can be categorized into either a timelike or null class. Solutions in the timelike class can be constructed by first selecting a four-dimensional Kähler base  $B$ ; the remaining field equations are then reduced to geometric equations on  $B$ . This work was extended [32] to the more general setting of gauged supergravity coupled to vector multiplets, which contains the  $U(1)^3$  gauged supergravity as a particular case. Solutions of the latter theory naturally lift to local solutions of Type IIB supergravity compactified on  $S^5$  (or, more generally, a Sasaki-Einstein five-manifold). This was subsequently used to construct a four-parameter family of  $\frac{1}{4}$ -BPS AdS<sub>5</sub> black hole solutions [33]. This led to a strict quantitative test of AdS/CFT: could the semi-classical entropy of these black holes be obtained

by counting the degeneracy of dual BPS CFT states? Remarkably, this computation was recently achieved through different approaches [34, 35, 36] (see also the review article [37]).

The above constructions focused mainly on black hole solutions, but the local metrics of [38] produced as a byproduct the first examples of  $\frac{1}{2}$ - BPS asymptotically globally AdS<sub>5</sub> gravitational solitons. All the known BPS black holes and solitons have a base space which is a particular member of a class of orthotoric Kähler spaces parameterized by two arbitrary functions of a single variable. A systematic approach to classifying BPS solutions in minimal supergravity with this general class of base spaces was carried out in [39]. This analysis reproduced the known solutions as well as producing new families; in particular, the BPS solitons of [38] were rederived and their regularity investigated. The summary was that there is an asymptotically globally AdS<sub>5</sub> soliton with positive energy and non-zero angular momenta and electric charge and no free continuous parameters. The spacetime metric possesses an  $\mathbb{R} \times SU(2) \times U(1)$  isometry group. Interestingly, the Killing spinors are invariant under a different  $SU(2)$  action, and thus if one writes this solution into the canonical supersymmetric form, the base space  $B$  does not inherit this symmetry and is merely toric. Note that recently, a classification of BPS solutions of the minimal theory, which admit an  $SU(2)$  action as isometries, was achieved [40]. In particular, this work established a uniqueness theorem for  $SU(2)$ -invariant BPS AdS<sub>5</sub> black holes of [31].

The purpose of the present work is to construct generalizations of these BPS solitons to the case of gauged supergravity coupled to an arbitrary number of Abelian vector multiplets (referred to as ‘ $U(1)^N$  supergravity’). These new solutions reduce in the case of equal electric charges to the solutions of the minimal theory found by [38]. In the special case of  $U(1)^3$  supergravity, our solutions reduce to the ones obtained in [41] by taking a combined BPS and horizonless limit of a local family of  $SU(2) \times U(1)$ -invariant solutions. The main difficulty in this construction is that in addition to multiple gauge fields, there are also scalar fields that must be determined. The supergravity equations couple these fields together, which makes a systematic analysis of all solutions with the given orthotoric base space along the lines of [39] difficult. We hope to return to a general analysis in the future.

A global analysis of the local metrics reveals a family of everywhere regular solutions parameterized by  $N$  positive moduli subject to one constraint. We also demonstrate

that they must possess an evanescent ergosurface instability. This is an instability of stationary solutions associated with the stable trapping of null geodesics near a timelike hypersurface along which the asymptotically stationary Killing field becomes null. A subtlety here is that in asymptotically  $\text{AdS}_5$  spacetimes, there is more than one such choice of a stationary Killing field, and for a particular choice, this ergosurface is revealed. A second observation is that the subfamily of solutions of  $U(1)^3$ -gauged supergravity can indeed be oxidized to globally smooth solutions of Type IIB supergravity on  $S^5/\mathbb{Z}_p, p \geq 3$  provided the moduli parameterizing the solution is suitably quantized (as previously noted in [41] the case of  $S^5$  leads to a global obstruction to smoothness). The dual CFT duals defined on the  $\mathbb{R} \times S^3$  conformal boundary of these geometries are quivered gauge theories.

Our work is organized as follows. In Section 2.3, we review the construction of supersymmetric solutions of  $U(1)^N$  gauged supergravity and derive our local solutions. We then perform a global analysis of these solutions and compute their conserved charges. We also give a self-contained description of the three-charge BPS soliton solutions of  $U(1)^3$ -supergravity and describe their lifting to ten dimensions. Finally, in Section 2.4, we discuss in some detail the existence of evanescent ergosurfaces and the associated stable trapping on null geodesics. We argue that this provides strong evidence that our solutions must suffer from (at least) a nonlinear instability whose endpoint would be a spacetime containing one or more near-BPS  $\text{AdS}_5$  black holes.

## 2.3 Supersymmetric $\text{AdS}_5$ solitons

### 2.3.1 Supersymmetric solutions to gauged supergravity

The bosonic sector of the theory consists of the metric,  $N$  gauge fields  $A^I$ , and  $N - 1$  real scalar fields, which are represented by  $N$  real scalar fields  $X^I$  subject to the constraint [32, 33]

$$\frac{1}{6}C_{IJK}X^IX^JX^K = 1. \quad (2.1)$$

The  $C_{IJK}$  are constants and as a tensor it is totally symmetric, i.e.  $C_{IJK} = C_{(IJK)}$  with  $I = 1 \dots N$ . A particular combination that often comes up is

$$X_I = \frac{1}{6}C_{IJK}X^JX^K. \quad (2.2)$$

The theory is governed by the action [33]

$$S = \frac{1}{16\pi G} \int \left( R \star_5 1 - Q_{IJ} F^I \wedge \star_5 F^J - Q_{IJ} dX^I \wedge \star_5 dX^J - \frac{1}{6} C_{IJK} F^I \wedge F^J \wedge A^K + 2g^2 V \star_5 1 \right), \quad (2.3)$$

with  $F^I := dA^I$  where  $A^I$  are local  $U(1)$  gauge fields. The matrix  $Q_{IJ}$  is given by

$$Q_{IJ} = \frac{9}{2} X_I X_J - \frac{1}{2} C_{IJK} X^K. \quad (2.4)$$

The  $C_{IJK}$  are assumed to satisfy the following symmetric space condition

$$C_{IJK} C_{J'(LM} C_{PQ)K'} \delta^{JJ'} \delta^{KK'} = \frac{4}{3} \delta_{I(L} C_{MPQ)}. \quad (2.5)$$

This condition ensures that  $Q_{IJ}$  has an inverse

$$Q^{IJ} = 2X^I X^J - 6C^{IJK} X_K, \quad (2.6)$$

with the identification  $C^{IJK} := C_{IJK}$ . This also allows us to invert for  $X^I$  in terms of the  $X_J$ :

$$X^I = \frac{9}{2} C^{IJK} X_J X_K, \quad (2.7)$$

which then implies

$$C^{IJK} X_I X_J X_K = \frac{2}{9}. \quad (2.8)$$

Finally the potential

$$\hat{V} = 27 C^{IJK} \bar{X}_I \bar{X}_J X_K, \quad (2.9)$$

where the  $\bar{X}_I$  are a set of constants. As shown in [32], the vacuum  $\text{AdS}_5$  background with radius  $\ell = 1/g$  corresponds to  $A^I \equiv 0$  and constant scalars  $X^I = \bar{X}^I$ , and

$$\bar{X}^I \equiv \frac{9}{2} C^{IJK} \bar{X}_J \bar{X}_K. \quad (2.10)$$

The special  $U(1)^3$  supergravity case corresponds to  $N = 3$ ,  $C_{IJK} = 1$  if  $(IJK)$  is a permutation of  $(123)$  and  $C_{IJK} = 0$  otherwise and  $\bar{X}^I = 1$ , or equivalently  $\bar{X}_I = 1/3$ . The symmetric space condition (2.5) holds automatically.

Given a Killing spinor, one can show that there is a Killing vector field  $V$ , which is

non-spacelike. So we assume we are in a region where  $V^2 = f^2 < 0$  so that  $f > 0$  for some function  $f$  and the metric can be decomposed as

$$ds^2 = -f^2(dt + \omega)^2 + f^{-1}h_{ab}dx^a dx^b, \quad (2.11)$$

where  $V = \partial/\partial t$ . Supersymmetry implies that the 4d metric  $h$  is Kähler with Kähler form  $J$ , and the orientation of the base space  $B$  chosen so that  $J$  is anti self dual  $\star J = -J$ . The 5-form  $(dt + \omega) \wedge \text{dvol}(h)$  has a positive orientation in the full spacetime.

The Maxwell field has to take the form

$$F^I = d[X^I f(dt + \omega)] + \Theta^I - 9gf^{-1}C^{IJK}\bar{X}_J X_K J, \quad (2.12)$$

and  $\Theta^I$  are self-dual two-forms on  $B$ , and we must have

$$X_I \Theta^I = -\frac{2}{3}G^+, \quad (2.13)$$

and  $G^\pm$  is the (anti-)self dual two-form with  $\star G^\pm = \pm G^\pm$ , defined as

$$G^\pm = \frac{1}{2}f(d\omega \pm \star d\omega). \quad (2.14)$$

Above  $\star$  refers to the Hodge dual with respect to  $(B, h)$ . This can be inverted so that

$$d\omega = f^{-1}(G^+ + G^-). \quad (2.15)$$

Since  $(B, h, J)$  is Kähler, we can define the Ricci two-form

$$\mathcal{R}_{ab} = \frac{1}{2}R_{abcd}J^{cd}. \quad (2.16)$$

Supersymmetry implies that  $\mathcal{R} = dP$  where  $P$  is the one-form

$$P = 3g\bar{X}_I(A^I - fX^I\omega). \quad (2.17)$$

This determines completely the function  $f$  as

$$f = -\frac{108g^2}{R}C^{IJK}\bar{X}_I\bar{X}_J X_K, \quad (2.18)$$

and the following condition holds

$$\mathcal{R} - \frac{R}{4}J = 3g\bar{X}_I\Theta^I. \quad (2.19)$$

All these conditions are necessary and turn out to be sufficient to guarantee the existence of a supercovariantly constant spinor. All the field equations are satisfied provided  $dF^I = 0$  (which is automatically true if we specify potentials), and the Maxwell equations

$$d(Q_{IJ} \star_5 F^J) = -\frac{1}{4}C_{IJK}F^J \wedge F^K \quad (2.20)$$

are satisfied. The Bianchi identity and the Maxwell equation respectively reduce to the following equations on the base space

$$d\Theta^I = 9gC^{IJK}\bar{X}_Jd(f^{-1}X_K) \wedge J, \quad (2.21)$$

and

$$\begin{aligned} d \star_4 d(f^{-1}X_I) = & -\frac{1}{6}C_{IJK}\Theta^I \wedge \Theta^J + 2g\bar{X}_I f^{-1}G^- \wedge J \\ & + 6g^2 f^{-2}(Q_{IJ}C^{JMN}\bar{X}_M\bar{X}_N + \bar{X}_IX^J\bar{X}_J)d\text{vol}(h). \end{aligned} \quad (2.22)$$

For convenience, we also record here an alternate form of the symmetric space condition (2.5) as follows

$$\begin{aligned} C_{IJK}(C^{JLM}C^{KPQ} + C^{JLP}C^{KMQ} + C^{JLQ}C^{KMP}) = & \delta_{IL}C_{MPQ} + \delta_{IM}C_{PQL} \\ & + \delta_{IP}C_{QLM} + \delta_{IQ}C_{LMP}. \end{aligned} \quad (2.23)$$

### 2.3.2 The local solution

We now present the local form of our solution  $(g, F^I, A^I)$ . Our construction is based on the analysis of the supersymmetric solitons of the minimal theory written in terms of the above Kähler decomposition [39] (this corresponds to setting the  $X^I$  constant and setting all the  $F^I$  equal) and a similar analysis of the 3-charge solutions discussed in [41].

Our starting point is a selection of a Kähler base [39], which we take to be the following

orthotoric Kähler base metric, which in terms of local coordinates  $(y, x, \Phi, \Psi)$  is

$$h = g^{-2} \left[ \frac{y-x}{F(x)} dx^2 + \frac{F(x)}{y-x} (d\Phi + y d\Psi)^2 + \frac{y-x}{G(y)} dy^2 + \frac{G(y)}{y-x} (d\Phi + x d\Psi)^2 \right] \quad (2.24)$$

for yet-to-be determined single-variable  $C^2$ -functions  $F = F(x)$  and  $G = G(y)$ .

The vector fields  $\partial_\Phi, \partial_\Psi$  are Killing vector fields of the Kähler space, and we will assume they extend to the whole spacetime. The Kähler form is

$$J = g^{-2} d[(y+x)d\Phi + xy d\Psi]. \quad (2.25)$$

It is explicitly

$$g^2 J = dy \wedge d\Phi + dx \wedge d\Phi + y dx \wedge d\Psi + x dy \wedge d\Psi. \quad (2.26)$$

A natural orthonormal frame is

$$e^1 = g^{-1} \left[ \frac{y-x}{F(x)} \right]^{1/2} dx, \quad e^2 = g^{-1} \left[ \frac{F(x)}{y-x} \right]^{1/2} (d\Phi + y d\Psi), \quad (2.27)$$

$$e^3 = g^{-1} \left[ \frac{y-x}{G(y)} \right]^{1/2} dy, \quad e^4 = g^{-1} \left[ \frac{G(y)}{y-x} \right]^{1/2} (d\Phi + x d\Psi). \quad (2.28)$$

The orientation is chosen so that  $\epsilon_{1234} = -1$ , so the volume form  $\text{dvol}_h = -\frac{1}{2} J \wedge J$ , where

$$J = e^1 \wedge e^2 + e^3 \wedge e^4. \quad (2.29)$$

Then this form is obviously anti-self dual. We will use the same symbol for the  $(1, 1)$  tensor field  $J^a_b$ . It can be easily checked that  $J^a_b J^b_c = -\delta^a_c$ . The Ricci scalar is easily calculated to be

$$R_h = -\frac{g^2(f''(x) + g''(y))}{y-x}. \quad (2.30)$$

We may also identify the other 2 anti self-dual forms:

$$J^2 = e^1 \wedge e^3 - e^2 \wedge e^4 \quad \text{and} \quad J^3 = -e^1 \wedge e^4 - e^2 \wedge e^3. \quad (2.31)$$

These satisfy the algebra (setting  $J^1 := J$ )

$$J^i \cdot J^j = -\delta^{ij} \mathbb{I} + \epsilon^{ijk} J^k, \quad (2.32)$$

where  $\cdot$  indicates matrix multiplication,  $i, j = 1, 2, 3$  and  $\mathbb{I}$  is the identity matrix. The case  $i, j = 1$  has been mentioned above. The Ricci form  $\mathcal{R}$ , defined by

$$\mathcal{R}_{ab} = \frac{1}{2} R_{abcd} J^{cd} \quad (2.33)$$

is closed and hence locally exact, i.e.,  $\mathcal{R} = d\mathcal{P}$ , with

$$\mathcal{P} = -\frac{F'(x)(d\Phi + yd\Psi) + G'(y)(d\Phi + xd\Psi)}{2(y-x)}. \quad (2.34)$$

Having specified the base metric, we now turn to the rest of the fields which determine the full solution. Let  $\mathfrak{q}_I \in \mathbb{R}$  and suppose  $\mathfrak{q}_I > 0$ . The scalar fields  $X_I$  are chosen to take the form

$$f^{-1} X_I = \frac{\bar{X}_I y + \mathfrak{q}_I}{y-x}. \quad (2.35)$$

Using (2.8) we find

$$f = \frac{y-x}{[P(y)]^{1/3}}, \quad P(y) = y^3 + \alpha_2 y^2 + \alpha_1 y + \alpha_0, \quad (2.36)$$

where the  $\alpha_i$  are defined by

$$\alpha_0 = \frac{9}{2} C^{IJK} \mathfrak{q}_I \mathfrak{q}_J \mathfrak{q}_K, \quad \alpha_1 = \frac{27}{2} C^{IJK} \bar{X}_I \mathfrak{q}_J \mathfrak{q}_K, \quad \alpha_2 = \frac{27}{2} C^{IJK} \bar{X}_I \bar{X}_J \mathfrak{q}_K. \quad (2.37)$$

The Kähler metric  $h$  is fully fixed by the choice

$$F(x) = 4\alpha_0(1-x^2), \quad G(y) = 4y(y^2 + (\alpha_0 + \alpha_2)y + \alpha_1). \quad (2.38)$$

Note that the Ricci scalar of  $h$  is

$$R_h = -\frac{8g^2(3y + \alpha_2)}{y-x}, \quad (2.39)$$

and it is easily verified that the BPS constraint (2.18) is satisfied. Note the scalars  $X^I$  are determined as

$$X^I = \frac{9}{2} C^{IJK} X_J X_K = \frac{\bar{X}^I y^2 + 9C^{IJK} \bar{X}_J \mathfrak{q}_K y + \frac{9}{2} C^{IJK} \mathfrak{q}_J \mathfrak{q}_K}{[P(y)]^{2/3}}. \quad (2.40)$$

Thus to specify a supersymmetric solution  $(g, F^I, X^I)$ , it remains to specify the functions  $\omega$  and  $\Theta^I$ , and then actually check that the remaining supersymmetry conditions and field equations are satisfied. For the self-dual two-forms  $\Theta^I$  we take

$$\Theta^I = \frac{(9C^{IJK}\mathfrak{q}_J\mathfrak{q}_K + (x+y)9C^{IJK}\bar{X}_J\mathfrak{q}_K + 2xy\bar{X}^I)}{g(y-x)^2} [dy \wedge (d\Phi + xd\Psi) - dx \wedge (d\Phi + yd\Psi)]. \quad (2.41)$$

It is evident that these forms are self-dual by writing them in terms of the orthonormal frame  $\{e^a\}$ . A long but straightforward computation verifies that the necessary conditions (2.19) and (2.21) are automatically satisfied. To perform this calculation, note that

$$d[(y-x)^{-2}dy \wedge (d\Phi + xd\Psi) - dx \wedge (d\Phi + yd\Psi)] = 0. \quad (2.42)$$

For the one-form  $\omega$ , we take

$$\omega = \omega_\Phi d\Phi + \omega_\Psi d\Psi, \quad (2.43)$$

where

$$\omega_\Phi = \frac{2}{g(y-x)^2} [\alpha_0(1-x^2+xy) + \alpha_1y + y^2(y+\alpha_2)], \quad (2.44)$$

$$\omega_\Psi = \frac{2y}{g(y-x)^2} [\alpha_0 + \alpha_1x + \alpha_2xy + xy^2]. \quad (2.45)$$

Recall that supersymmetry requires  $X_I\Theta^I = -\frac{2}{3}G^+$ . This requires calculating  $\star d\omega$ . It is useful to record that the volume form in the  $(y, x, \Phi, \Psi)$  coordinates is given by

$$d\text{Vol}(h) = \frac{y-x}{g^4} dy \wedge dx \wedge d\Phi \wedge d\Psi. \quad (2.46)$$

and the inverse metric components are

$$h^{yy} = \frac{g^2G(y)}{y-x}, \quad h^{xx} = \frac{g^2F(x)}{y-x}, \quad h^{\Phi\Phi} = \frac{g^2(G(y)x^2 + F(x)y^2)}{F(x)G(y)(y-x)}, \quad (2.47)$$

$$h^{\Phi\Psi} = -\frac{g^2(G(y)x + F(x)y)}{F(x)G(y)(y-x)}, \quad h^{\Psi\Psi} = \frac{g^2(F(x) + G(y))}{F(x)G(y)(y-x)}, \quad (2.48)$$

and hence we compute that

$$\star(dx \wedge d\Phi) = \frac{G(y)x^2 + F(x)y^2}{G(x)(y-x)} dy \wedge d\Psi + \frac{G(y)x + F(x)y}{G(y)(y-x)} dy \wedge d\Phi, \quad (2.49)$$

$$\star(dy \wedge d\Phi) = -\frac{G(y)x + F(x)y}{F(x)(y-x)} dx \wedge d\Phi - \frac{G(y)x^2 + F(x)y^2}{F(x)(y-x)} dx \wedge d\Psi, \quad (2.50)$$

$$\star(dx \wedge d\Psi) = -\frac{G(y)x + F(x)y}{G(y)(y-x)} dy \wedge d\Psi - \frac{F(x) + G(y)}{G(x)(y-x)} dy \wedge d\Phi, \quad (2.51)$$

$$\star(dy \wedge d\Psi) = \frac{F(x) + G(y)}{F(x)(y-x)} dx \wedge d\Phi + \frac{G(y)x + F(x)y}{F(x)(y-x)} dx \wedge d\Psi. \quad (2.52)$$

We now wish to verify that

$$f^{-1}X_I\Theta^I = -\frac{1}{3}(d\omega + \star d\omega), \quad (2.53)$$

The left-hand side is given by the self-dual two-form

$$f^{-1}X_I\Theta^I = \frac{2}{3g(y-x)^3} [(\alpha_1 + (x+y)\alpha_2 + 3xy)y + 3\alpha_0 + (x+y)\alpha_1 + xy\alpha_2] \cdot [dy \wedge (d\Phi + xd\Psi) - dx \wedge (d\Phi + yd\Psi)]. \quad (2.54)$$

We have once again verified that (2.53) is satisfied. It only remains to verify that the Maxwell equation (2.22) holds without any further constraints. This is possible after a tedious calculation, with the use of the identities

$$C_{IJK}\bar{X}^J C^{KPQ}\bar{X}_{PqQ} = \frac{9}{2}C_{IJK}C^{JLM}\bar{X}_L\bar{X}_M C^{KPQ}\bar{X}_{PqQ} = \frac{q_I}{3} + \frac{\alpha_2}{3}\bar{X}_I, \quad (2.55)$$

$$C_{IJK}C^{JLM}C^{KPQ}\bar{X}_Lq_M\bar{X}_{PqQ} = -\frac{1}{9}C_{IJK}\bar{X}^J C^{KMq}q_Mq_Q + \frac{2}{27}\alpha_1\bar{X}_I + \frac{2}{27}\alpha_2q_I, \quad (2.56)$$

$$C_{IJK}C^{JLM}C^{KPQ}q_Lq_M\bar{X}_{PqQ} = \frac{2}{27}(\alpha_0\bar{X}_I + \alpha_1q_I). \quad (2.57)$$

Therefore we have satisfied all the necessary and sufficient conditions to produce a local BPS solution where in particular, the metric takes the canonical form (2.11).

### 2.3.3 Global analysis and conserved charges

The soliton solutions constructed above have an  $SU(2) \times U(1)$  isometry, although this is incompatible with a supersymmetric decomposition [39]. Nonetheless, having the explicit bosonic solution, we can express the metric in a coordinate chart where the symmetry is manifest. To this end define a new chart  $(T, r, \psi, \theta, \phi)$  by

$$r = \left[ \frac{y}{g^2 \alpha_0} \right]^{1/2}, \quad \theta = \arccos x, \quad T = t, \quad \psi = 4\alpha_0 \Psi, \quad \phi = 4\alpha_0 \Phi - 2gt, \quad (2.58)$$

so that in particular we have a Killing vector field

$$\frac{\partial}{\partial T} = \frac{\partial}{\partial t} + \frac{g}{2\alpha_0} \frac{\partial}{\partial \Phi}. \quad (2.59)$$

In this coordinate chart, the metric takes the manifestly  $SU(2) \times U(1)$ -invariant form

$$\begin{aligned} ds^2 = & -\frac{H(r)^{1/3} W(r) dT^2}{\alpha_0 B(r)} + \frac{H(r)^{1/3} \alpha_0 dr^2}{W(r)} + \frac{r^2 B(r)}{4H(r)^{2/3}} (d\psi + \cos \theta d\phi + \Omega(r) dT)^2 \\ & + \frac{H(r)^{1/3}}{4g^2 \alpha_0} (d\theta^2 + \sin^2 \theta d\phi^2), \end{aligned} \quad (2.60)$$

where we have defined

$$\begin{aligned} W(r) &= g^4 \alpha_0^2 r^4 + g^2 \alpha_0 r^2 (\alpha_2 + \alpha_0) + \alpha_1, & B(r) &= g^4 \alpha_0^2 r^4 + g^2 r^2 \alpha_2 \alpha_0 + \alpha_1, \\ H(r) &= \alpha_0 (g^6 \alpha_0^2 r^6 + g^4 \alpha_2 \alpha_0 r^4 + g^2 \alpha_1 r^2 + 1), & \Omega(r) &= -\frac{2g\alpha_0}{B(r)}. \end{aligned} \quad (2.61)$$

In these coordinates, we may identify the geometry in the asymptotic region  $r \rightarrow \infty$  with  $\text{AdS}_5$  with radius  $g^{-1}$ . This is realized by shifting the radial coordinate as  $r^2 = R^2 - \alpha_2/(3\alpha_0 g^2)$  so that as  $R \rightarrow \infty$ , the metric has the expansion

$$\begin{aligned} ds^2 \rightarrow & -(1 + g^2 R^2 + O(R^{-2})) dt^2 + \frac{dr^2}{1 + g^2 R^2 + O(R^{-2})} \\ & + \frac{R^2 + O(R^{-2})}{4} (d\psi + \cos \theta d\phi + O(R^{-4}) dT)^2 + \frac{R^2 + O(R^{-2})}{4} (d\theta^2 + \sin^2 \theta d\phi^2), \end{aligned} \quad (2.62)$$

and hence to recover an asymptotically globally  $\text{AdS}_5$  spacetime we must take  $\psi \in (0, 4\pi)$ ,  $\phi \sim \phi + 2\pi$ , and  $\theta \in (0, \pi)$  (with standard coordinate singularities at  $\theta = 0, \pi$

corresponding to the poles of the  $S^3$ ). Note that

$$\left(\frac{\partial}{\partial T}\right)^2 = g_{TT} = -\frac{\alpha_0^2 g^6 r^6 + \alpha_0 g^4 (\alpha_0 + \alpha_2) r^4 + \alpha_1 g^2 r^2 + 1}{H^{2/3}} < 0, \quad (2.63)$$

and hence  $\partial_T$  is strictly timelike everywhere. A similar computation shows that  $(dT)^2 = g^{TT} < 0$  everywhere, and hence the function  $T$  may be identified a time function on the spacetime, which is stably causal. Timelike surfaces of constant  $r > 0$  have topology  $\mathbb{R} \times S^3$ .

The functions  $W(r), H(r), B(r) > 0$  from the requirement  $\mathbf{q}_I > 0$ . Hence the metric is non-degenerate for all  $r > 0$ . As  $r \rightarrow 0$ ,  $g_{\psi\psi} = O(r^2)$  and the Killing vector field  $\partial/\partial\psi$  degenerates. To ensure a smooth degeneration of the  $S^1$  generated by this vector field, we must impose the regularity constraint

$$\alpha_0 = \alpha_1. \quad (2.64)$$

This places one algebraic constraint on  $\mathbf{q}_I$ . Thus, a member of this family of globally smooth asymptotically AdS<sub>5</sub> gravitational soliton is parameterized by the  $N$  positive real constants  $\mathbf{q}_I$  subject to (2.64). The 2-cycle at  $r = 0$  is a round  $S^2$  of radius  $r_{S^2} = (2g\alpha_0^{1/3})^{-1}$ . With the condition (2.64) the full soliton spacetime metric extends to a global metric on  $\mathbb{R} \times \mathbb{CP}^2 \setminus \{\text{pt}\}$  where the first factor corresponds to the time direction and the second to spacelike Cauchy surfaces  $\Sigma_t$  induced on the level sets of constant  $t$ . The topology of  $\Sigma_t$  is easiest to read off by noting that the induced metric is toric and the resulting toric diagram (rod structure) is that of  $\mathbb{CP}^2$  with one vertex removed corresponding to the point ‘at infinity’. Equivalently  $\Sigma_t$  has the topology of Taub-Bolt space  $O(-1) \rightarrow S^2$ , i.e., the tautological bundle over  $\mathbb{CP}^1$  [39].

Physically, the 2-cycle is prevented from collapse by the magnetic fluxes

$$\mathcal{D}^I = \frac{1}{2\pi} \int_{S^2} F^I = \frac{9}{2g\alpha_0} C^{IJK} \mathbf{q}_J \mathbf{q}_K. \quad (2.65)$$

The total mass of the spacetime may be computed using the conformal mass of Ashtekar-Magnon-Das [27]. Setting  $\Omega = 1/(gR)$  and defining the conformal metric  $\bar{g}_{ab} = \Omega^2 g_{ab}$  with conformal boundary at  $\Omega = 0$  ( $R \rightarrow \infty$ ), we define the electric

part of the Weyl tensor to be

$$\bar{\mathcal{E}}_b^a = (g\Omega)^{-2} \bar{g}^{cd} \bar{g}^{ef} n_d n_f C_{cbe}^a, \quad (2.66)$$

where  $n = d\Omega$ . The conserved quantity associated with a Killing vector field  $\xi$  is

$$Q[\xi] = \frac{1}{16\pi g} \int_{S^3} \bar{\mathcal{E}}_b^a \xi^b dS_a, \quad (2.67)$$

where the integral is taken over the  $S^3$  of radius  $g^{-1}$  at conformal infinity with unit timelike normal  $dT$ . The mass is associated to  $\xi = \partial_T$ , which is non-rotating at infinity. A computation reveals that as  $R \rightarrow \infty$ , the relevant components of the Weyl tensor decay as

$$C_{RTR}^T = \frac{2\alpha_2}{g^4 \alpha_0 R^6} + O(R^{-8}), \quad (2.68)$$

and we obtain the mass

$$E := Q[\partial_T] = \frac{\pi \alpha_2}{4g^2 \alpha_0}. \quad (2.69)$$

Next, consider the electric charges  $Q_I$ . Note that

$$\star F = -f^{-2} \star_4 d(X^I f) + e^0 \wedge (X^I f \star_4 d\omega + \Theta^I + 9f^{-1} g C^{IJK} \bar{X}_J X_K J) \quad (2.70)$$

where  $e^0 = f(dt + \omega)$ . We define

$$Q_I = \frac{1}{8\pi} \int_{S_\infty^3} Q_{IJ} \star F^J, \quad (2.71)$$

where the integral is taken over the boundary sphere as  $r \rightarrow \infty$  on a spatial hypersurface defined by  $t = T = \text{constant}$ . One finds as  $y \rightarrow \infty$  that, pulled back to a surface  $y = \text{constant}$ ,

$$\star F^J = \left[ \frac{4\alpha_0}{g^2} (\alpha_2 \bar{X}^I - 9C^{IJK} \bar{X}_J \mathfrak{q}_K) + O(y^{-1}) \right] dx \wedge d\Phi \wedge d\Psi. \quad (2.72)$$

Using the fact that  $Q_{IJ} = \frac{9}{2} \bar{X}_I \bar{X}_J - \frac{1}{2} C_{IJK} \bar{X}^K + O(y^{-1})$  as  $y \rightarrow \infty$ , we find

$$Q_I = -\frac{3\pi \mathfrak{q}_I}{4g^2 \alpha_0}. \quad (2.73)$$

Note that the mass (2.69) of these supersymmetric solutions satisfies the BPS relation

$$E = |\bar{X}^I Q_I| = \frac{\pi \alpha_2}{4g^2 \alpha_0}. \quad (2.74)$$

The angular momentum associated to the Killing vector field  $\eta = 2\partial_\psi$ , which has  $2\pi$ -periodic closed orbits, is computed from the Komar integral

$$J = \frac{1}{16\pi} \int_{S_\infty^3} \star d\eta = \frac{\pi}{2\alpha_0 g^3}. \quad (2.75)$$

where we have used the expansion

$$\star d\eta|_{S_\infty^3} = \left( \frac{1}{2\alpha_0 g^3} + O(r^{-1}) \right) \sin\theta d\theta \wedge d\psi \wedge d\phi. \quad (2.76)$$

This corresponds to equal angular momenta in two orthogonal planes of rotation at spatial infinity. Note that the angular momentum associated to the Killing vector field  $\partial_\phi$  vanishes.

### 2.3.4 The $U(1)^3$ supergravity theory

Of particular interest in the class of supergravity theories is the  $\mathcal{N} = 1$  gauged supergravity coupled to two Abelian vector multiplets, which has gauge group  $U(1)^3$  that arises as a reduction of Type IIB supergravity on  $S^5$  (one keeps the maximal Abelian subgroup  $U(1)^3$  of the of maximal 5d  $SO(6)$ -gauged supergravity). At least locally, a five-dimensional solution to this theory can be oxidized to a solution of type IIB supergravity theory reduced appropriately on  $S^5$ . In this special case, the solutions presented here were previously obtained [41] by performing a BPS limit of a more general family of local supergravity solutions [38]. The theory is recovered by setting  $I = i = 1, 2, 3$  with  $\bar{X}_i = 1/3$  (or equivalently  $\bar{X}^i = 1$ ), and  $C^{ijk} = |\epsilon_{ijk}|$  where  $\epsilon_{123} = \pm 1$  is totally antisymmetric. For simplicity, we rescale our dimensionless charge parameters  $\mathfrak{q}_i \rightarrow \mathfrak{q}_i/3$ . We then have the simplified expressions

$$\alpha_0 = \mathfrak{q}_1 \mathfrak{q}_2 \mathfrak{q}_3, \quad \alpha_1 = \mathfrak{q}_1 \mathfrak{q}_2 + \mathfrak{q}_1 \mathfrak{q}_3 + \mathfrak{q}_2 \mathfrak{q}_3, \quad \alpha_2 = \mathfrak{q}_1 + \mathfrak{q}_2 + \mathfrak{q}_3. \quad (2.77)$$

The parameters  $\mathfrak{q}_i$  are subject to the regularity condition is simply  $\mathfrak{q}_1 \mathfrak{q}_2 \mathfrak{q}_3 = \mathfrak{q}_1 \mathfrak{q}_2 + \mathfrak{q}_1 \mathfrak{q}_3 + \mathfrak{q}_2 \mathfrak{q}_3$ . The solution then takes the canonical supersymmetric form (2.11) in the

$(t, y, x, \Phi, \Psi)$  coordinates with

$$f = \frac{y-x}{(H_1 H_2 H_3)^{1/3}} \quad \text{and} \quad H_i = y + \mathfrak{q}_i, \quad (2.78)$$

and the scalar fields are given by

$$X_i = \frac{f}{3} \cdot \frac{y + \mathfrak{q}_i}{y - x}, \quad (2.79)$$

or equivalently

$$X^1 = \frac{y^2 + (\mathfrak{q}_2 + \mathfrak{q}_3)y + \mathfrak{q}_2 \mathfrak{q}_3}{(H_1 H_2 H_3)^{2/3}} \quad (2.80)$$

with similar expressions for  $X^2, X^3$  with the natural permutations of the  $\mathfrak{q}_i$ . The Kähler base space metric  $h$  is given by (2.24) where

$$\begin{aligned} F(x) &= 4\mathfrak{q}_1 \mathfrak{q}_2 \mathfrak{q}_3 (1 - x^2), \\ G(y) &= 4y (y^2 + (\mathfrak{q}_1 \mathfrak{q}_2 \mathfrak{q}_3 + \mathfrak{q}_1 + \mathfrak{q}_2 \mathfrak{q}_3)y + \mathfrak{q}_1 \mathfrak{q}_2 + \mathfrak{q}_1 \mathfrak{q}_3 + \mathfrak{q}_2 \mathfrak{q}_3). \end{aligned} \quad (2.81)$$

The one-form  $\omega$  is given by (2.43) where the constants  $\alpha_i$  are given by (2.77). The Maxwell fields  $F^i$  are then determined by (2.12) where the Kähler form  $J$  is given by (2.25), and the self-dual forms  $\Theta^i$  by

$$\Theta^1 = \frac{2xy + (x+y)(\mathfrak{q}_2 + \mathfrak{q}_3) + 2\mathfrak{q}_2 \mathfrak{q}_3}{g(y-x)^2} [dy \wedge (d\Phi + yd\Psi) - dx \wedge (d\Phi + yd\Psi)], \quad (2.82)$$

with similar expressions for  $\Theta^2, \Theta^3$  with the obvious permutations of the  $\mathfrak{q}_i$ .

In the coordinate system  $(T, r, \theta, \psi, \phi)$  the metric takes the form (2.60) where the functions  $W(r), B(r)$  and  $\Omega(r)$  are given by (2.61) with the constants  $\alpha_i$  given by (2.77) and the function  $H$  factors as

$$H(r) = \mathfrak{q}_1 \mathfrak{q}_2 \mathfrak{q}_3 (1 + g^2 \mathfrak{q}_1 \mathfrak{q}_2 r^2)(1 + g^2 \mathfrak{q}_1 \mathfrak{q}_3 r^2)(1 + g^2 \mathfrak{q}_2 \mathfrak{q}_3 r^2). \quad (2.83)$$

The conserved charges and angular momentum are given by

$$E = \frac{\pi}{4g^2 \mathfrak{q}_1 \mathfrak{q}_2 \mathfrak{q}_3} (\mathfrak{q}_1 + \mathfrak{q}_2 + \mathfrak{q}_3), \quad Q_i = -\frac{\pi \mathfrak{q}_i}{4g^2 \mathfrak{q}_1 \mathfrak{q}_2 \mathfrak{q}_3}, \quad J = \frac{\pi}{2g^3 \mathfrak{q}_1 \mathfrak{q}_2 \mathfrak{q}_3}, \quad (2.84)$$

and the angular momentum is associated to the Killing vector field  $m = 2\partial_\psi$ . The angular momentum associated to the Killing field  $\partial_\phi$  vanishes,  $J_\phi = 0$ . We note that

the parameters  $q_i$  used in [41] (c.f. (3.28) of that work) are related to the ones used here by  $q_i = \mathbf{q}_i / (g^2 \mathbf{q}_i \mathbf{q}_2 \mathbf{q}_3)$ . The magnetic dipole fluxes out of the  $S^2$  are given by

$$\mathcal{D}^i = \frac{|\epsilon^{ijk}| \mathbf{q}_j \mathbf{q}_k}{2g(\mathbf{q}_i \mathbf{q}_2 \mathbf{q}_3)} = \frac{1}{g\mathbf{q}_i}. \quad (2.85)$$

From this and the regularity condition it follows that

$$\frac{g}{4\pi} \int_{S^2} \sum_i^3 F^i = \frac{g}{2} \sum_{i=1}^3 \mathcal{D}^i = \frac{1}{2}, \quad (2.86)$$

which is the Dirac quantisation condition appropriate for a manifold with a  $\text{spin}^c$  structure.

Above, we mentioned that the  $U(1)^3$  solutions could be locally uplifted to Type IIB supergravity along a Sasaki-Einstein five-manifold  $Y_5$ . However, in the case that the five-dimensional spacetime has a non-trivial topology, there will generically be global obstructions to producing a smooth ten-dimensional metric. Indeed, it was observed in [41] that the solutions constructed here could not be lifted along the simplest Sasaki-Einstein manifold,  $S^5$  (in contrast, to the three-charge supersymmetric  $\text{AdS}_5$  black holes [33]). In the equal charge case ( $\mathbf{q}_i = \mathbf{q}$ ), the solutions above become solutions of minimal gauged supergravity. It was proved there that in this case, globally regular oxidization was indeed possible along more general *regular* Sasaki-Einstein manifolds [39]. In particular, suppose that  $Y_5$  is a circle bundle over a Fano Kähler-Einstein  $M_4$  with Fano index  $I$  (e.g.  $\mathbb{C}\mathbb{P}^2$  has  $I = 3$ ). Suppose for generality, we allow the coordinate  $\psi$  to have period  $4\pi/p$  ( $p = 1$  corresponds to the asymptotically globally  $\text{AdS}_5$  case we have hitherto assumed). A regular oxidization can be achieved provided  $kp/I \in \mathbb{Z}$  where  $k \in \mathbb{Z}$  divides  $I$ , with  $k = 1$  if and only if  $Y_5$  is simply connected [39]. For a concrete example, take the asymptotically globally  $\text{AdS}_5$  case  $p = 1$  and  $M_4 = \mathbb{C}\mathbb{P}^2$ . In this case  $k = 3$  and  $Y = S^5/\mathbb{Z}_3$ , with the boundary CFT being a quiver gauge theory living on  $\mathbb{R} \times S^3$ . More generally a del Pezzo surface  $M_4 = dP_i$ ,  $3 \leq i \leq 9$  has  $I = 1$  (hence  $k = 1$ ) and the boundary CFT is placed on  $S^3/\mathbb{Z}_p$  for any  $p \geq 1$ .

In the general case of unequal charge parameters  $\mathbf{q}_i$ , however, we are not aware of a compactification of Type IIB supergravity on a general Sasaki-Einstein manifold  $Y_5$  which reduces to the  $U(1)^3$  gauged supergravity theory. A compactification on  $S^5$  is

known, and since the isometry group has a maximal torus of rank 3, the three gauge fields to be naturally incorporated into the ten-dimensional metric [42]. In particular, one takes as Type IIB fields

$$\begin{aligned}
g_{10} &= W^{1/2} ds_5^2 + W^{-1/2} \sum_{i=1}^3 (X^i)^{-1} [d\mu_i^2 + \mu_i^2 (d\phi^i + gA^i)^2], \\
F_5 &= (1 + \star_{10}) \left( 2g \sum_{i=1}^3 ((X^i)^2 \mu_i^2 - W X^i) d\text{Vol}_5 - \frac{1}{2g} \sum_{i=1}^3 (X^i)^{-1} \star_5 dX^i \wedge d\mu_i^2 \right. \\
&\quad \left. + \frac{1}{2g^2} \sum_{i=1}^3 (X^i)^{-2} d\mu_i^2 \wedge (d\phi^i + gA^i) \wedge \star_5 F^i \right) \quad (2.87)
\end{aligned}$$

where  $W := \sum_i^3 \mu_i^2 X^i > 0$ , and  $(\mu_i, \phi^i)$  are coordinates on  $S^5$  where the ‘direction cosines’ satisfy the constraint  $\mu_1^2 + \mu_2^2 + \mu_3^2 = 1$ . To cover  $S^5$ , the angles  $\phi^i$  must each be identified with period  $2\pi$ . More precisely, the 3-torus parameterized by  $\phi^i$  is defined by the identifications  $T_1 : (\phi^1, \phi^2, \phi^3) \sim (\phi^1 + 2\pi, \phi^2, \phi^3)$  with similar expressions for  $T_2, T_3$ . Since the compactification is purely local, we can also use<sup>1</sup> this embedding with  $S^5/\mathbb{Z}_p$  replacing  $S^5$ , provided we define the lattice with the identifications  $\hat{T} : (\phi^1, \phi^2, \phi^3) \sim (\phi^1 + 2\pi/p, \phi^2 + 2\pi/p, \phi^3 + 2\pi/p)$  along with any two of the original identifications  $T_1, T_2, T_3$ . These identifications can be straightforwardly derived by relating the above standard coordinates on  $S^5$  with those used in writing  $S^5$  as a  $U(1)$  bundle over  $\mathbb{CP}^2$ . The Killing vector field  $\partial_\psi = \frac{1}{3}(\partial_{\phi^1} + \partial_{\phi^2} + \partial_{\phi^3})$  is non-vanishing and generates the  $U(1)$  fibre. The  $\mathbb{Z}_p$  quotient corresponds to identifying  $\psi \sim \psi + 6\pi/p$ , with  $S^5$  corresponding to  $p = 1$ . The ten-dimensional metric extends globally to a smooth manifold provided that the connection on the  $\mathbb{T}^3$ -bundle is globally defined. This requires

$$\frac{g}{2\pi} \int_{S^2} F^i = \frac{k^i}{p}, \quad k^i \in \mathbb{Z} \quad (2.88)$$

which from (2.85) implies  $k_i = p/q_i > 0$ . However the regularity constraint (2.86) imposes the condition

$$k_1 + k_2 + k_3 = p. \quad (2.89)$$

It is clear  $p = 1$  is not allowed. In the case of equal charges previously investigated in [39],  $k_i = 1$  and  $p = 3$  corresponding to uplifting on  $S^3/\mathbb{Z}_3$ . We have therefore demonstrated that general members of this family of asymptotically globally  $\text{AdS}_5$

---

<sup>1</sup>We thank J. Lucietti for this observation.

BPS soliton spacetimes can also be uplifted, provided  $q_i = p/k_i$  and (2.89) is satisfied.

## 2.4 Evanescent ergosurface and stable trapping

As observed above, there is a strictly timelike Killing vector field  $\partial_T$ , which is static in the asymptotically globally AdS<sub>5</sub> region. This differs from the supersymmetric Killing vector field  $V = \partial_t$  associated to the bilinear of a Killing spinor field  $\epsilon$  via  $V^a \sim \bar{\epsilon}\gamma^a\epsilon$ . The Killing vector field  $V$  is everywhere causal:

$$|V|^2 = \left(\frac{\partial}{\partial t}\right)^2 = -f^2 = -\frac{(y-x)^2}{P(y)^{2/3}} \leq 0. \quad (2.90)$$

and  $|V|^2$  vanishes if and only if  $y = x$ . This relation defines a smooth timelike hypersurface  $\mathcal{S}$  along which  $V$  is null. Hence  $\mathcal{S}$  may be identified as an *evanescent ergosurface* [43, 44, 45]. The geometry of  $\mathcal{S}$  is simplest to see in the  $(T, r, \theta, \phi, \psi)$  coordinate chart, as  $\partial_T$  remains timelike. The induced metric on the timelike hypersurface  $\mathcal{S}$  is

$$ds^2 = H(r)^{1/3} \left[ -\frac{W(r)dT^2}{\alpha_0 B(r)} + \frac{H(r)dr^2}{W(r)(1-g^4\alpha_0^2 r^4)} + \frac{r^2 B(r)}{4H(r)} (d\psi + g^2\alpha_0 r^2 d\phi + \Omega(r)dT)^2 + \frac{(1-g^4\alpha_0^2 r^4)d\phi^2}{4g^2\alpha_0} \right] \quad (2.91)$$

A simple analysis of the fixed points sets of the torus action generated by  $(\partial_\psi, \partial_\phi)$  reveals that the constant  $T$ -surfaces have  $S^3$ -topology and an inhomogeneous metric. To see, this observe that the metric in the above coordinates is smooth and positive definite when the radial coordinate takes value in  $0 < r < (g\sqrt{\alpha_0})^{-1}$ .  $\mathcal{S}$  intersects the  $S^2$  bubble at  $r = 0$ , where  $\partial_\psi$  smoothly degenerates, and at  $r = (g\sqrt{\alpha_0})^{-1}$  the Killing vector field  $\partial_\phi - \partial_\psi$  smoothly degenerates.

The supersymmetric Killing vector field  $V$  is easily seen to be tangent to affinely parametrized null geodesics on  $\mathcal{S}$ :

$$\nabla_V V|_{\mathcal{S}} = -\frac{1}{2}d(|V|^2)|_{\mathcal{S}} = 0 \quad (2.92)$$

since  $V$  has a second-order zero on  $\mathcal{S}$ . With respect to an observer at infinity moving along the orbits of  $V$ , the conserved energy along these geodesics must vanish because

$E = -V \cdot V = 0$  on  $\mathcal{S}$ , that is,  $V$  is tangent to zero-energy geodesics on the evanescent ergosurface. Such geodesics are also *stably trapped* as proved in [44]. We will briefly overview their elegant argument, which employs the Jacobi equation for geodesic deviation and the fact that  $V$  is a Killing vector field such that  $-|V|^2$  is minimized on  $\mathcal{S}$ .

Given a energy-minimizing null geodesic  $\gamma$  on  $\mathcal{S}$  with tangent vector field  $V$ , consider a one-parameter family of causal geodesics  $\gamma_s$  with  $\gamma_0 = \gamma$  and associated causal tangent vector fields  $X_s$  and geodesic deviation vector field  $Y$ . The geodesic deviation equation on  $\gamma$

$$\nabla_V \nabla_V Y^a|_\gamma = R^a{}_{bcd} V^b V^c Y^d|_\gamma \quad (2.93)$$

admits a first integral as a consequence of the Killing property of  $V$

$$|\mathcal{L}_V Y|^2 + H_{ab} Y^a Y^b = C, \quad (2.94)$$

where  $C$  is a constant on  $\gamma$ , and  $H_{ab}$  is the Hessian of  $-V^2/2$ , i.e.,  $H_{ab} = \nabla_a \nabla_b (-V^2/2)$ . Using the fact that  $|X_s|^2$  is maximized on  $\gamma$ , it can be shown that  $V \cdot Y$  is a constant on  $\gamma$ . Thus

$$V \cdot \mathcal{L}_V Y = 0, \quad (2.95)$$

from which it follows that  $\mathcal{L}_V Y$  is spacelike or null on  $\gamma$ . Hence, the first term in (2.94) is non-negative. Moreover a direct computation shows that

$$H_{ab} = 4g^2 n_a n_b, \quad (2.96)$$

where the spacelike unit normal to  $\mathcal{S}$  is given by

$$n = \frac{1}{2gH^{1/3}} d(g^2 \alpha_0 r^2 - \cos \theta). \quad (2.97)$$

Hence  $H_{ab}$  is a positive-definite metric on the space on the vectors normal to  $\mathcal{S}$  and vanishes on those vectors tangent to  $\mathcal{S}$ . In particular, (2.94) implies that  $C \geq 0$  and

$$H_{ab} Y^a Y^b = 4g^2 (n \cdot Y)^2 \leq C, \quad (2.98)$$

where  $n \cdot Y$  measures the component of the deviation vector field  $Y$  normal to  $\mathcal{S}$ . Therefore the normal component of  $Y$  remains bounded on the evanescent ergosurface.

This demonstrates the stable trapping property, namely, that initially nearby causal geodesics to  $\gamma$  remain sufficiently close.

The phenomena of stable trapping provide a geometric obstruction to the establishment of sufficiently strong decay statements for solutions of wave equations [44, 45, 46]. Intuitively, since the behavior of high-frequency waves can be approximated by null geodesics, the trapping property should lead to the clumping of energy in a bounded region. In particular, a fast (e.g., polynomial) decay of such solutions is widely expected to be required for nonlinear stability. On the other hand, unstable trapping, such as that which occurs at the photon sphere  $r = 3M$  of the Schwarzschild spacetime, is known not to prevent sufficiently fast decay. As shown above for the gravitational solitons considered here, however, the trapping is stable, and in addition, there is no event horizon to aid in decay.

In the stationary, asymptotically flat case, Moschidis has rigorously proved that provided an energy boundedness statement is true for solutions of the linear wave equation, then the local energy of waves must decay at least inverse logarithmically [47]. The question arises whether, in a given spacetime, such a decay statement is sharp or whether one can prove faster decay. For supersymmetric microstate geometries with evanescent ergosurfaces (and hence fall outside the hypotheses of Moschidis' theorem), Keir rigorously established that a stronger decay statement cannot exist and indeed any spacetime possessing an evanescent ergosurface but no event horizon exhibits a linear instability [45] (see also his analysis of a particular family of supersymmetric microstate geometries [48]). Analogous results have been established for non-supersymmetric microstate geometries that exhibit stable trapping despite not having an evanescent ergosurface [49] (in fact, the energy of solutions to the linear wave equation are uniformly bounded).

In the asymptotically Anti-de Sitter case, slow decay of waves caused by stable trapping has been investigated by Holzegel and Simulivici in Kerr-AdS<sub>4</sub> spacetimes [50, 51]. Here the underlying geometric obstruction to decay is a combination of unstable trapping near the horizon and the lack of dispersion at null infinity (assuming standard reflective boundary conditions). In the present case for the family of asymptotically globally AdS<sub>5</sub> solitons considered there, one has both the combined effect of stable trapping at an evanescent ergosurface along with the usual lack of dispersion at infinity, and moreover, there is no horizon to help with decay. These considerations

strongly suggest that these solutions, despite being supersymmetric, are nonlinearly unstable and likely also unstable at the linear level, as is generically the case for similar asymptotically flat and asymptotically Kaluza-Klein spacetimes [45]. Indeed, even the maximally supersymmetric AdS vacuum is now known to be nonlinearly unstable to arbitrarily small, generic perturbations that lead to the formation of black holes [52, 53, 54], and therefore it is reasonable to expect the endpoint of instability of supersymmetric globally AdS<sub>5</sub> solitons would be a near-BPS, asymptotically AdS<sub>5</sub> black hole spacetime.

# Chapter 3

## Phase Transitions and Stability of Eguchi-Hanson-AdS Solitons

This chapter is based on “Phase Transitions and Stability of Eguchi-Hanson-AdS Solitons” by Turkuler Durgut, Robie A. Hennigar, Hari K. Kunduri and Robert B. Mann published in JHEP 114 (2023).

### 3.1 Abstract

The Eguchi-Hanson-AdS<sub>5</sub> family of spacetimes are a class of static, geodesically complete asymptotically locally AdS<sub>5</sub> soliton solutions of the vacuum Einstein equations with negative cosmological constant. They have negative mass and are parameterized by an integer  $p \geq 3$  with a conformal boundary with spatial topology  $L(p, 1)$ . We investigate mode solutions of the scalar wave equation on this background and show that, similar to AdS<sub>5</sub>, the geometry admits a normal mode spectrum (i.e. solutions that neither grow or decay in time). In addition, we also discuss other geometric properties of these soliton spacetimes, including the behaviour of causal geodesics and their thermodynamic properties. We also point out a surprising connection with the AdS soliton.

## 3.2 Introduction

A classic theorem of Wang [55] states that Anti-de Sitter (AdS) spacetime is the unique conformally compact (globally) static solution to the vacuum Einstein equations  $G_{ab} + \Lambda g_{ab} = 0$  where  $\Lambda < 0$  and with spherical conformal spatial boundary. The theorem holds in situations where the positive mass theorem for asymptotically hyperbolic manifolds is valid (see also [56, 57]). This result lends support to the expectation that AdS spacetime is the appropriate ‘ground state’ amongst the class of all solutions with the same asymptotic behaviour. A putative ground state would, in turn, be expected to be dynamically stable, and indeed studies of the wave equation on a fixed AdS background are consistent with this intuition. However, the remarkable result of Bizon et al. [52] demonstrates that, in fact, AdS is nonlinearly unstable under arbitrarily small perturbations whose endpoint is the formation of black holes - that is, small amounts of energy tend to concentrate at shorter and shorter scales, rather than dissipating as in Minkowski spacetime [52, 53].

A natural question is whether the vacuum Einstein equations with negative cosmological constant admit other static solutions that are asymptotically locally AdS but with a different conformal boundary. The family of AdS soliton spacetimes provides such an example with toroidal conformal spatial boundary [58, 59]. Clarkson and Mann considered the problem of finding static solutions asymptotic to a freely acting discrete quotient of AdS [60, 61]. They succeeded in constructing solutions in odd dimensions (referred to as Eguchi-Hanson-AdS spacetimes) that are asymptotic to  $\text{AdS}_{d+1}/\mathbb{Z}_p$ . These spacetimes have negative energy relative to that of pure AdS. In five spacetime dimensions,  $p \geq 3$  (see below) and spatial cross sections of the conformal boundary are lens spaces  $L(p, 1)$  equipped with the standard round metric. Clarkson and Mann conjectured that these metrics are the states of lowest energy in their asymptotic class [60].

The Eguchi-Hanson-AdS<sub>5</sub> geometry, in addition to being static, has a local  $SU(2) \times U(1)$  isometry group, which acts with three-dimensional orbits. Hence its spatial sections belong to the biaxial Bianchi IX class of geometries. Dold exploited this symmetry to study the evolution of initial data within this symmetry class [62]. In addition to showing that the resulting system of equations forms a well-posed initial-boundary value problem (with the fields satisfying an appropriate Dirichlet condition

at conformal infinity), he rigorously proved that the maximal development of this restricted class of initial data sufficiently close to Eguchi-Hanson-AdS<sub>5</sub> data cannot form a horizon in the future. Assuming that Eguchi-Hanson-AdS<sub>5</sub> is indeed the only static solution within its conformal class, this implies that the endpoint of the evolution must generically be a spacetime containing a naked singularity.

In the present article, we will take a different perspective and study mode solutions to the massless Klein-Gordon equation

$$\square_g \Phi = 0 \tag{3.1}$$

on the fixed Eguchi-Hanson-AdS<sub>5</sub> background. One advantage of this approach is that we do not need to make any special symmetry restrictions on  $\Phi$ . It is easy to see that (3.1) is separable and so it is relatively straightforward to reduce the problem to a single radial Schrödinger-type equation. Since the background is static, it is straightforward to show that there is a conserved energy and hence a uniform bound for the energy associated with the field  $\Phi$  in terms of its initial energy. This kind of bound, however, does not tell us if the field is being concentrated within a compact region as a result of some geometric mechanism (e.g. trapping).

For simplicity we will study quasinormal mode solutions of (3.1). We will show that, similar to AdS spacetime, Eguchi-Hanson-AdS<sub>5</sub> admits normal mode solutions (i.e. they neither grow nor decay in time). Our results will be based on a robust numerical approach as well as analytic methods.

In addition to the Klein-Gordon test field, we consider many other aspects of these solutions that have not been addressed to date in the literature. We begin with an analysis of the mechanical properties of these solitons. We compute their mass and show that these solutions have a non-trivial thermodynamic volume of topological origin [63, 25]. Examining the thermodynamics in the canonical ensemble, we show that there is an analog of the Hawking-Page phase transition [64]. The two relevant states in the phase transition are the Eguchi-Hanson-AdS<sub>5</sub> soliton and the black hole resulting from performing  $\mathbb{Z}_p$  identifications to the spherical AdS black hole. We then study the geodesics in the spacetime, which is relevant for two reasons. First, we seek to find whether or not there exists stable trapping of null geodesics (the confinement of null geodesics to a compact subregion of space) in the Eguchi-Hanson-AdS<sub>5</sub> spacetime. Stable trapping presents an obstruction to proving strong decay

statements for solutions of the wave equation [51, 65]. For example, decay might be no faster than inversely logarithmic in time, rather than inverse polynomial [48]. The latter is expected to be necessary if there is any hope of demonstrating nonlinear stability. In particular, stable trapping has been shown in several examples of families of horizonless soliton spacetimes, which typically have some nontrivial spatial topology (e.g., two-cycles or ‘bubbles’) [48, 25, 49] or ultracompact objects [46]. However, we find that stable trapping is absent in the Eguchi-Hanson-AdS<sub>5</sub> spacetime. Second, we investigate the light-crossing time of the geometry and find that it turns out to be relevant to understanding the spacing between overtones for the normal mode solutions of the Klein-Gordon equation.

A recurring theme throughout each aspect of our work is a connection between the Eguchi-Hanson-AdS<sub>5</sub> soliton and the AdS soliton that has not been pointed out in the literature. Namely, starting with the former with spatial boundary metric (the round  $L(p, 1)$  lens space), we find that formally taking the  $p \rightarrow \infty$  limit gives the (universal cover of the) AdS soliton as the limiting solution. As such, we show how the relevant quantities of the AdS soliton govern the asymptotics of the corresponding quantities for the Eguchi-Hanson soliton.

The outline of our paper is as follows. In Section 3.3, we review the basic structure of the Eguchi-Hanson soliton and show its limit is AdS soliton as  $p \rightarrow \infty$ . In Section 3.4, we analyze the mass and thermodynamic behaviour of the soliton, and in Section 3.5, we consider the behaviour of timelike and null geodesics in this spacetime. We find that both massive and null particles oscillate between the edge of the soliton and infinity, with no stable trapping regions. In Section 3.6, we proceed with the main purpose of our paper, that of analyzing the scalar wave equation in the Eguchi-Hanson soliton spacetime. As an analytic solution is apparently intractable, we solve the equation numerically, checking our results against various approximations in certain limits. Amongst our most intriguing results is that the normal modes interpolate between those of a scalar wave on the orbifold AdS<sub>5</sub>/ $\mathbb{Z}_2$  and on the AdS soliton as the parameter  $p$  is varied. We close our paper with some concluding remarks in Section 3.7. Several appendices contain details showing how we arrived at our results.

### 3.3 Metric and Structure

Clarkson and Mann [60] obtained a solution of the  $D = 5$  Einstein equations with negative cosmological constant, namely

$$R_{ab} = -\frac{4}{\ell^2}g_{ab} , \quad (3.2)$$

given by

$$ds^2 = -g(r)dt^2 + r^2 f(r) \left[ d\psi + \frac{\cos(\theta)}{2} d\phi \right]^2 + \frac{dr^2}{f(r)g(r)} + \frac{r^2}{4} d\Omega_2^2 \quad (3.3)$$

$$g(r) = 1 + \frac{r^2}{\ell^2} \quad \text{and} \quad f(r) = 1 - \frac{a^4}{r^4}. \quad (3.4)$$

This is a cohomogeneity-one metric with local isometry group  $\mathbb{R} \times SU(2) \times U(1)$ . When  $a = 0$  this reduces to the  $\text{AdS}_5$  metric with spherical boundary when  $t \in \mathbb{R}$ ,  $r > 0$ ,  $\psi \in (0, 2\pi)$ ,  $\theta \in (0, \pi)$  and  $\phi \in (0, 2\pi)$  with a standard apparent singularity at  $r = 0$ , where the  $(\psi, \theta, \phi)$  part of the metric degenerates, representing the origin of coordinates. However, for  $a \neq 0$  (we fix  $a > 0$  without loss of generality) the metric extends globally to a manifold with non-trivial topology, provided that certain regularity conditions are satisfied. The Killing vector field  $\partial/\partial\psi$  becomes degenerate at  $r = a$ ; examining the  $(r, \psi)$  sector of the geometry, absence of conical singularities requires the identification

$$\psi \sim \psi + \frac{2\pi}{2\sqrt{g(a)}}. \quad (3.5)$$

This ensures that the geometry smoothly ‘pinches off’ leaving a round  $S^2$  of radius  $a/2$ . This condition must be combined with the independent condition, arising from regularity of the constant  $(t, r)$  surfaces, that demands

$$\psi \sim \psi + \frac{2\pi}{p}, \quad (3.6)$$

where  $p \in \mathbb{Z}$  (this ensures the geometry is that of  $L(p, 1)$ ). Satisfying both conditions requires that

$$a^2 = \left( \frac{p^2}{4} - 1 \right) \ell^2. \quad (3.7)$$

Thus regularity requires that we must have  $p \geq 3$ . This means that asymptotically the boundary metric is a lens space  $L(p, 1)$  ( $p = 1$  would be  $S^3$ ). Thus, we have a gravitational soliton (a geodesically complete, strictly stationary solution) that has a 2-cycle in the interior region and has a lens space as its boundary. The above metric is often referred to as the ‘Eguchi-Hanson-AdS<sub>5</sub>’ soliton as constant time hypersurfaces generalize the well-known four-dimensional Eguchi-Hanson gravitational instanton metric which must have  $p = 2$  [66].

### 3.3.1 The Large $p$ Limit of the Metric: AdS Soliton

As we have just seen, the Eguchi-Hanson-AdS<sub>5</sub> soliton is characterized by a single integer  $p$ . For several reasons, it will be fruitful to consider these solutions for large values of  $p$ .

Beginning with the Eguchi-Hanson-AdS<sub>5</sub> metric (3.3), we perform the following transformations

$$t = \frac{2\tau}{p}, \quad r = az, \quad \theta = \frac{4\rho}{p}, \quad \varphi = \psi + \frac{p}{2}\phi, \quad (3.8)$$

and then take the limit  $p \rightarrow \infty$ . The result is

$$ds^2 = -z^2 d\tau^2 + \frac{\ell^2 dz^2}{z^2 f(z)} + \frac{\ell^2 z^2 f(z)}{4} d\varphi^2 + \ell^2 z^2 [d\rho^2 + \rho^2 d\phi^2] + \mathcal{O}\left(\frac{1}{p}\right) \quad (3.9)$$

where

$$f(z) = 1 - \frac{1}{z^4}. \quad (3.10)$$

One can then convert the polar coordinates on the  $\mathbb{R}^2$  to standard Cartesian coordinates, giving

$$ds^2 = -z^2 d\tau^2 + \frac{\ell^2 dz^2}{z^2 f(z)} + \frac{\ell^2 z^2 f(z)}{4} d\varphi^2 + \ell^2 z^2 [dx^2 + dy^2] + \mathcal{O}\left(\frac{1}{p}\right). \quad (3.11)$$

In the strict  $p \rightarrow \infty$  limit, this is an AdS<sub>5</sub> soliton belonging to the class first reported in [67], in coordinates such that the location of the bubble is at  $z = 1$ . One can easily check that the coordinate  $\varphi$  is periodic with period  $2\pi$ . Strictly speaking, there are several topologically distinct solitons that can be obtained from the same local metric (3.11) depending on identifications performed on the auxiliary flat directions

$(x, y)$  — see, e.g., [68]. In this case, the soliton corresponding to the large  $p$  limit of Eguchi-Hanson-AdS has no identifications on these coordinates, i.e. the spatial part of the boundary metric is  $\mathbb{S}^1 \times \mathbb{R}^2$ . This is the same configuration first considered in [67], and henceforth we will refer to this case as “the” AdS soliton. To the best of our knowledge, this connection between the Eguchi-Hanson-AdS<sub>5</sub> soliton and the AdS soliton has not been previously reported on<sup>1</sup>.

Regularity of the solution requires that  $p \geq 3$  is an integer. Therefore, the  $p \rightarrow \infty$  limit may be most cautiously considered as a ‘formal’ limit. Nonetheless, it is difficult to overstate the utility of this result. As we will see in the subsequent sections, many of the quantities of interest cannot be evaluated exactly for the Eguchi-Hanson-AdS<sub>5</sub> soliton, but the asymptotics of these quantities can be effectively captured by the corresponding quantities for the AdS soliton. Said another way, Eguchi-Hanson-AdS<sub>5</sub> solitons for large values of  $p$  behave in a manner similar to the AdS soliton.

## 3.4 Soliton Mechanics

### 3.4.1 Smarr Relation & First Law

While it is well-known that black holes satisfy a first law and Smarr relation, similar relationships can be found for solitons and soliton-black hole configurations. This was rigorously demonstrated in the asymptotically flat case in [24], and extended to a particular example of an asymptotically globally AdS soliton in [25]. Here we apply these considerations to the Eguchi-Hanson-AdS<sub>5</sub> soliton. While the mass was calculated in the original manuscript [60], the notion of thermodynamic volume [63] — which proves crucial for deriving the Smarr relation and first law in this case — was at that point not developed. We note also that considerations of extended thermodynamics have been previously carried out for Eguchi-Hanson-dS soliton in [70]. In Section 3.8 we compare the results of these computations with the formalism of holographic renormalization.

Let  $\xi = \partial_t$  be the stationary Killing field. It has zero divergence so  $d \star \xi = 0$ , where  $\star$  is the Hodge dual. It follows that one can write the closed four-form  $\star \xi = -d \star \varpi$  for

---

<sup>1</sup>The connection between the Eguchi-Hanson and AdS soliton geometries could be inferred from the results for lensed CFT partition functions [69]. We are grateful to Edgar Shaghoulian who, after this work was completed, brought this reference to our attention.

some locally defined 2-form  $\varpi$ , or equivalently

$$\xi = \star d \star \varpi. \quad (3.12)$$

On the other hand a basic identity is

$$d \star d\xi = 2 \star \text{Ric}(\xi) = \frac{8}{\ell^2} d \star \varpi \quad (3.13)$$

where the second equality follows from the Einstein equation  $R_{ab} = -\frac{4}{\ell^2} g_{ab}$  and (3.12). This means we have the conservation equation

$$d \star \left[ d\xi - \frac{8}{\ell^2} \varpi \right] = 0 \quad (3.14)$$

which we will integrate over a spatial hypersurface  $t = \text{constant}$ . If we introduce the basis

$$\begin{aligned} e^0 &= \sqrt{g} dt, & e^1 &= \frac{dr}{\sqrt{fg}}, & e^2 &= r\sqrt{f} \left( d\psi + \frac{\cos\theta}{2} d\phi \right), \\ e^3 &= \frac{r}{2} d\theta, & e^4 &= \frac{r}{2} \sin\theta d\phi \end{aligned} \quad (3.15)$$

and assume  $\varpi$  takes the form

$$\varpi = A(r) e^0 \wedge e^1 + B(r) e^1 \wedge e^2 \quad (3.16)$$

then a calculation gives

$$A(r) = \frac{1}{\sqrt{f}} \left( \frac{r}{4} + \frac{C_1}{r^3} \right), \quad B(r) = \frac{C_2}{r^2 \sqrt{g}} \quad (3.17)$$

so that

$$\varpi = \frac{1}{f} \left( \frac{r}{4} + \frac{C_1}{r^3} \right) dt \wedge dr + \frac{C_2}{rg} dr \wedge \left( d\psi + \frac{\cos\theta}{2} d\phi \right). \quad (3.18)$$

whose Hodge dual is

$$\star \varpi = -\frac{1}{4} \left( \frac{r^4}{4} + C_1 \right) \sin\theta d\psi \wedge d\theta \wedge d\phi + \frac{C_2}{4} \sin\theta dt \wedge d\theta \wedge d\phi. \quad (3.19)$$

Note that the degeneracy of  $\partial/\partial\psi$  at the ‘centre’  $r = a$  implies that  $\star\varpi$  is not well defined there unless  $C_1$  is chosen to be  $C_1 = -a^4/4$ . However, as is typical — and as we will see below — regularity is not the correct prescription for fixing the parameter

$C_1$ .

Next, we integrate the closed form defined by (3.14) over a hypersurface  $\Sigma$  defined as a surface of constant time,  $t = \text{constant}$ , over the region  $R_0 \leq r \leq \infty$  with  $R_0 > a$ . On this region  $\varpi$  is well-defined and we can apply Stokes' theorem. The identity gives

$$0 = \int_{\Sigma} d \left[ \star \left( d\xi - \frac{8}{\ell^2} \varpi \right) \right] = \int_{\partial_{\infty}\Sigma} \star \left( d\xi - \frac{8}{\ell^2} \varpi \right) - \int_{\partial\Sigma_{R_0}} \star \left( d\xi - \frac{8}{\ell^2} \varpi \right) \quad (3.20)$$

where  $\partial_{\infty}\Sigma$  and  $\partial\Sigma_{R_0}$  represent the asymptotic and inner boundaries respectively.

Let us first focus on the contribution at conformal infinity. A calculation shows that as  $r \rightarrow \infty$ ,

$$\star d\xi = \left( -\frac{r^4}{2\ell^2} + \frac{a^4}{2\ell^2} + O(1/r^2) \right) \sin\theta d\psi \wedge d\theta \wedge d\phi, \quad (3.21)$$

and we note that the divergent term is precisely cancelled by the corresponding divergent term of  $\star\varpi$  when the two terms are combined as in (3.20). We identify a renormalized Komar mass as [63]

$$M_{\text{Komar}} := -\frac{3}{32\pi} \int_{\partial_{\infty}\Sigma} \star \left( d\xi - \frac{8}{\ell^2} \varpi \right) = -\frac{3\pi}{8\rho\ell^2} (a^4 + 4C_1). \quad (3.22)$$

The fact that the free parameter  $C_1$  appears in the Komar mass can be understood as an ambiguity in the ground state energy. We will now fix this ambiguity.

We can ensure the integral over the asymptotic boundary evaluates to the mass by choosing  $C_1$  appropriately. To calculate this we use the Ashtekar-Magnon procedure [71] which is well-defined in this setting. The relevant component of the Weyl tensor is

$$C^t{}_{tr} = -\frac{a^4}{(r^2 + \ell^2)(r^4 - a^4)} = -\frac{a^4}{r^6} + O(r^{-8}) \quad (3.23)$$

as  $r \rightarrow \infty$ . Setting  $\Omega = \ell/r$  and defining the conformal metric  $\bar{g}_{ab} = \Omega^2 g_{ab}$  with  $\Omega = 0$  as  $r \rightarrow \infty$ , the Ashtekar-Magnon mass is then defined as

$$Q[\partial_t] = \frac{\ell}{16\pi} \int_{\partial M} \bar{\mathcal{E}}^a{}_b(\partial_t)^b dS_t \quad (3.24)$$

where  $dS_t$  is a constant time slice of the conformal boundary, which has a round lens

space metric of radius  $\ell$ . The quantity  $\bar{\mathcal{E}}^a_b$  is the electric part of the Weyl tensor

$$\bar{\mathcal{E}}^a_b = \frac{\ell^2}{\Omega^2} \bar{g}^{cd} \bar{g}^{ef} n_d n_f C^a_{cbe}, \quad (3.25)$$

with unit spacelike normal  $n = d\Omega$ .

Noting that  $\bar{g}^{rr} = r^4 \ell^2$ , it is then a straightforward matter to obtain the relevant component

$$\bar{\mathcal{E}}^t_t = \frac{r^6}{\ell^6} C^t_{rtr} = -\frac{a^4}{\ell^6} \quad (3.26)$$

yielding

$$M := Q[\partial_t] = \frac{\ell}{16\pi} \int_{\partial M} \left( -\frac{a^4}{\ell^6} \right) \ell^3 \frac{\sin \theta}{4} d\psi d\theta d\phi = -\frac{\pi a^4}{8\ell^2 p} \quad (3.27)$$

so the mass is negative, a fact already observed in [60] — c. f. eq.(10) of that work. Comparing the above with the result of the Komar integration implies  $C_1 = -a^4/6$ .

Once the Komar mass has been computed, the thermodynamic volume is identified by evaluating the integral of the Killing potential over the inner boundary, and taking the limit  $R_0 \rightarrow a$ . This gives:

$$V = - \int_{\partial \Sigma_R} \star \varpi = \frac{\pi^2}{2p} (a^4 + 4C_1) = \frac{\pi^2 a^4}{6p}. \quad (3.28)$$

using the choice  $C_1 = -a^4/6$ . For some black hole solutions the thermodynamic volume can be interpreted as the volume of a Euclidean ball of radius  $a$  that is removed from the spatial hypersurface [72]. This interpretation is not available in this case because there is no ‘ball’ in Euclidean space for which a lens space is its boundary. In this case, the thermodynamic volume  $V$  has a topological origin: it arises not due to the presence of an horizon, but instead because the choice of constant  $C_1$  that leads to the correct mass leads to a Killing potential that is not regular at the location of the bubble.

Noting that thermodynamic pressure is [72]

$$P := -\frac{\Lambda}{8\pi} = \frac{3}{4\pi\ell^2} \quad (3.29)$$

then we have

$$M = -PV \quad (3.30)$$

which is the Smarr formula for this system. Using the regularity condition (3.6) and the mass (3.27) we have

$$dM = -\frac{\pi}{4p} \left( \frac{p^2}{4} - 1 \right)^2 \ell d\ell \quad (3.31)$$

Alternatively, using (3.28), (3.29), and the regularity condition (3.6), we have

$$VdP = -\frac{\pi}{4p} \left( \frac{p^2}{4} - 1 \right)^2 \ell d\ell \quad (3.32)$$

and consequently

$$dM = VdP \quad (3.33)$$

which is the expression of the first law for the Eguchi-Hanson-AdS<sub>5</sub> soliton.

The fact that the regularity condition is required for the validity of the first law is consistent with previous studies of (extended) mechanics of smooth geometries [24, 73, 25]. It is worth remarking that in some cases, e.g., for accelerating black holes or spacetimes containing Misner strings, it is possible to formulate the Smarr relation and first law without requiring the regularity condition to hold [74, 75]. It may be interesting to better understand when, exactly, regularity of the geometry is crucial for formulating a sensible first law and Smarr relation.

### 3.4.2 Euclidean action

By sending  $t \rightarrow i\tau$  the Eguchi-Hanson-AdS<sub>5</sub> solution (3.3) may be analytically continued to produce a Riemannian (positive signature) Einstein metric:

$$ds^2 = g(r)d\tau^2 + r^2 f(r) \left[ d\psi + \frac{\cos\theta}{2} d\phi \right]^2 + \frac{dr^2}{f(r)g(r)} + \frac{r^2}{4} d\Omega_2^2. \quad (3.34)$$

The geometry is smooth and complete with an  $S^2$ -bolt at  $r = a$  provided the regularity condition (3.7) is imposed. We now periodically identify the  $\tau$ -coordinate as  $\tau \sim \tau + \beta$  so that it parameterizes an  $S^1$ . The vector field  $\partial_\tau$  is nowhere vanishing since  $g(r) > 0$  and therefore this  $S^1$  does not degenerate. In particular there is no condition on  $\beta$ . The underlying manifold will therefore be  $S^1 \times T^*S^2$  (the latter factor being the cotangent bundle of  $S^2$ ). The metric is conformally compact with conformal boundary

$S^1 \times L(p, 1)$  equipped with the conformal boundary metric

$$\gamma = d\tau^2 + \ell^2 \left[ \left( d\psi + \frac{\cos \theta}{2} d\phi \right)^2 + \frac{d\Omega_2^2}{4} \right]. \quad (3.35)$$

The metric on the boundary  $L(p, 1)$  is the round metric.

We may easily produce a Riemannian Einstein metric with the same conformal boundary by taking appropriate angular identifications of the Euclidean Schwarzschild-AdS<sub>5</sub> metric to obtain an Einstein metric on  $\mathbb{R}^2 \times L(p, 1)$ :

$$ds^2 = U(r)d\tau^2 + U(r)^{-1}dr^2 + r^2 \left[ \left( d\psi + \frac{\cos \theta}{2} d\phi \right)^2 + \frac{d\Omega_2^2}{4} \right] \quad (3.36)$$

where  $U(r) = 1 - \mu/r^2 + r^2/\ell^2$ . We take, as above,  $\psi \sim \psi + 2\pi/p$  and  $\theta \in (0, \pi)$ ,  $\phi \in (0, 2\pi)$  and  $r > r_+$  where  $r_+$  is the largest root of  $U(r)$ . As is well known, regularity at  $r = r_+$ , the largest root of  $U(r)$ , requires that the angle  $\tau$  must be identified as  $\tau \sim \tau + \beta$  with

$$\beta = \frac{2\pi\ell^2 r_+}{2r_+^2 + \ell^2}. \quad (3.37)$$

Thus for fixed temperature  $T = \beta^{-1}$  there are two possible black holes

$$r_+ = \frac{\pi\ell^2 \pm \ell\sqrt{\pi^2\ell^2 - 2\beta^2}}{2\beta} \quad (3.38)$$

provided  $T > T_{min}$  where

$$T_{min} = \frac{\sqrt{2}}{\pi\ell}. \quad (3.39)$$

Note that rather than closing smoothly to an  $S^1 \times S^2$  ‘bolt’ as in Euclidean Eguchi-Hanson-AdS<sub>5</sub>, the above space has a  $L(p, 1)$  bolt.

We now follow the standard procedure [76, 77] to compare the finite Euclidean on-shell actions for these two possible infilling metrics for fixed temperature  $T = \beta^{-1}$ . The renormalized Euclidean action is

$$I = -\frac{1}{16\pi G} \left[ \int_M \left( R_g + \frac{12}{\ell^2} \right) d\text{Vol}(g) + 2 \int_{\partial M} \left( \text{Tr}K - \frac{3}{\ell} - \frac{\ell R_h}{4} \right) d\text{Vol}(h) \right] \quad (3.40)$$

where  $h$  is the metric induced on a hypersurface  $r = R$  and  $R_g, R_h$  are the respective scalar curvatures of the metrics  $g$  and  $h$ .

For Eguchi-Hanson-AdS<sub>5</sub> we have

$$I_{EH} = \frac{\beta\ell^2 \text{Vol}(L(p, 1))}{16\pi G} \left[ \frac{3}{4} - \left( \frac{p^2}{4} - 1 \right)^2 \right] \quad (3.41)$$

where  $\text{Vol}(L(p, 1)) = 2\pi^2/p$  is the volume of the boundary  $L(p, 1)$ . For the Euclidean black hole metric (3.36) a computation gives

$$I_{BH} = \frac{\beta\ell^2 \text{Vol}(L(p, 1))}{16\pi G} \left[ \frac{3}{4} + \frac{r_+^2}{\ell^2} \left( 1 - \frac{r_+^2}{\ell^2} \right) \right]. \quad (3.42)$$

With the actions at hand, simple calculations reveal that the situation is analogous to the Hawking-Page transition [64]. At low temperature the Eguchi-Hanson-AdS<sub>5</sub> soliton has the least action and dominates the canonical ensemble, whereas at sufficiently large temperatures, it is a large black hole that dominates. When the actions are equal there is a transition analogous to the Hawking-Page transition. The temperature at which the phase transition occurs can be shown to be<sup>2</sup>

$$T_{\text{EHB}} = \frac{1}{2\pi\ell} \frac{4 + \sqrt{p^4 - 8p^2 + 20}}{\sqrt{2 + \sqrt{p^4 - 8p^2 + 20}}}. \quad (3.43)$$

At large values of  $p$  this has the asymptotic form

$$T_{\text{EHB}} = \frac{p}{2\pi\ell} \left[ 1 + \frac{1}{p^2} + \frac{5}{2p^4} + \dots \right]. \quad (3.44)$$

In the strict  $p \rightarrow \infty$  limit, this phase transition is related to that which occurs between the toroidal AdS black hole and the AdS soliton [80].

### 3.5 Geodesics

In this section we consider the behaviour of null and timelike geodesics in the Eguchi-Hanson-AdS<sub>5</sub> geometry. Our primary interest is to investigate instabilities in this horizonless spacetime. As is now well established, there is a close connection between the geometrically induced stable trapping of null geodesics and instabilities due to the

---

<sup>2</sup>See also [78, 79] where an analogous computation was performed. We thank the referee for bringing these references to our attention.

clumping of wave energy. In the geometric optics approximation, the propagation of solutions to the wave equation in a fixed background can be described by the trajectory of null geodesics. Stable trapping is a phenomena by which properties of the geometry create obstacles forcing null geodesics to be confined in a spatially compact region.

The prototypical example of null trapping is the photon sphere at  $r = 3M$  in the Schwarzschild spacetime; null geodesics exist in circular orbits at fixed radius. Such trapping, however is unstable because any small perturbation of the orbit will cause the null geodesics to either fall towards the horizon or escape to infinity. By contrast, stable trapping occurs when small perturbations of the orbits remain small so the trapping region is ‘attractive’. Stable trapping has been shown to lead to inverse-logarithmic time decay of wave energy in both asymptotically flat [65, 48, 49] and asymptotically AdS spacetimes [51]. As discussed in the introduction, this is suggestive of a non-linear instability, as linear stability typically requires decay that is an inverse polynomial function of time.

To exploit the local  $\mathbb{R} \times SU(2) \times U(1)$  isometry of the Eguchi-Hanson-AdS<sub>5</sub> spacetime, it is convenient to (3.3) in the form

$$ds^2 = -g(r)dt^2 + \frac{dr^2}{f(r)g(r)} + \frac{r^2 f(r)}{4} [d\bar{\psi} + \cos(\theta)d\phi]^2 + \frac{r^2}{4} d\Omega_2^2 \quad (3.45)$$

where we have defined a new coordinate  $\bar{\psi} = 2\psi$ . Then  $(\bar{\psi}, \theta, \phi)$  become the familiar Euler angles, with  $\theta \in (0, \pi)$ ,  $\bar{\psi} \in (0, 4\pi/p)$ ,  $\phi \in (0, 2\pi)$ , and the metric can be expressed as

$$ds^2 = -g(r)dt^2 + \frac{dr^2}{f(r)g(r)} + \frac{r^2}{4} (\sigma_1^2 + \sigma_2^2) + \frac{r^2 f(r)}{4} \sigma_3^2 \quad (3.46)$$

where  $\sigma_i$  are left-invariant one-forms on  $SU(2)$  defined by

$$\sigma_1 = -\sin \bar{\psi} d\theta + \cos \bar{\psi} \sin \theta d\phi, \quad (3.47)$$

$$\sigma_2 = \cos \bar{\psi} d\theta + \sin \bar{\psi} \sin \theta d\phi, \quad (3.48)$$

$$\sigma_3 = d\bar{\psi} + \cos \theta d\phi. \quad (3.49)$$

Explicitly, the spatial Killing vector fields are given by

$$R_1 = \cot \theta \cos \phi \partial_\phi + \sin \phi \partial_\theta - \frac{\cos \phi}{\sin \theta} \partial_\psi \quad (3.50)$$

$$R_2 = -\cot \theta \sin \phi \partial_\phi + \cos \phi \partial_\theta + \frac{\sin \phi}{\sin \theta} \partial_\psi \quad (3.51)$$

$$R_3 = \partial_\phi, \quad L_3 = \partial_\psi. \quad (3.52)$$

The trajectories of geodesics of mass  $\hat{m}$  are easily found using this symmetry and the Hamilton-Jacobi method as outlined in [81]. In particular the Hamiltonian for the motion of uncharged particles is  $H = g^{ab} p_a p_b$  where  $p_a$  are the canonical momenta. The Hamiltonian system is Liouville integrable as there are five Poisson commuting functions associated with the local isometries (there is an additional conserved quantity associated with a reducible Killing tensor). The Hamilton-Jacobi equation is

$$\frac{\partial S}{\partial \lambda} + g^{ab} \frac{\partial S}{\partial x^a} \frac{\partial S}{\partial x^b} = 0 \quad (3.53)$$

where  $\lambda$  is an affine curve parameter and it is clear one can express the Hamilton-Jacobi function  $S$  in the separable form

$$S = \hat{m}^2 \lambda - Et + p_\psi \psi + p_\phi \phi + \Theta(\theta) + R(r) \quad (3.54)$$

where  $(E, p_\psi, p_\phi)$  correspond to conserved energy and angular momenta along particle trajectories, with  $p_a = \partial_a S$ . Omitting details, we simply present the resulting curve equations for  $x^a(\lambda)$ :

$$\begin{aligned} \dot{t} &= \frac{2E}{g(r)} & \dot{\psi} &= -\frac{8 \cot \theta}{r^2} \left[ \frac{p_\phi}{\sin \theta} - \cot \theta p_{\bar{\psi}} \right] \\ \dot{\phi} &= \frac{8}{r^2 \sin \theta} \left[ \frac{p_\phi}{\sin \theta} - \cot \theta p_{\bar{\psi}} \right] \end{aligned} \quad (3.55)$$

and

$$\dot{r}^2 = 4E^2 f(r) - \frac{16g(r)}{r^2} p_{\bar{\psi}}^2 - 4\hat{m}^2 f(r)g(r) - \frac{16C}{r^2} f(r)g(r) \quad (3.56)$$

$$\dot{\theta}^2 = \frac{64}{r^2} \left[ C - \left( \cot \theta p_{\bar{\psi}} - \frac{p_\phi}{\sin \theta} \right)^2 \right] \quad (3.57)$$

where  $C$  is another constant of the motion associated with the existence of the reducible Killing tensor.

We will now perform more detailed studies of the geodesics.

### 3.5.1 Time-like Geodesics: Negative Mass Repulsion

Let us begin with a consideration of time-like geodesics, i.e.  $\hat{m} \neq 0$ . To illustrate some similarities/differences with time-like geodesics in AdS, we will restrict attention here to radial time-like geodesics. After defining  $\mathcal{E} = E/\hat{m}$  and rescaling the affine parameter accordingly, we arrive at the equation

$$\dot{r}^2 = f(r) [\mathcal{E}^2 - g(r)] . \quad (3.58)$$

We immediately see that the large- $r$  turning point of the motion is exactly the same as it is for AdS<sup>3</sup>:

$$r_{\max} = \ell\sqrt{\mathcal{E}^2 - 1} . \quad (3.59)$$

This result is sensible — the space is asymptotically locally AdS and so at large enough distances the radial motion should approach that of AdS. There is a further constraint to consider since the only physically relevant cases are those for which  $r_{\max} \geq a$ . This in turn enforces that the energy must be larger than a given threshold,

$$\mathcal{E} \geq \mathcal{E}_{\min} = \frac{p}{2}, \quad \text{where} \quad \frac{a}{\ell} = \sqrt{\frac{p^2}{4} - 1} . \quad (3.60)$$

A second turning point arises due to the presence of the bubble, this is at  $r = a$ , where  $f(r) = 0$ . The motion of a massive particle is therefore oscillatory, bouncing back and forth on the interval  $a \leq r \leq r_{\max}$ .

The presence of the bubble has implications for the motion at smaller values of  $r$ . To highlight this, consider the acceleration

$$\ddot{r} = -\frac{r}{\ell^2} - \frac{a^4}{r^3\ell^2} + \frac{2a^4(\mathcal{E}^2 - 1)}{r^5} \quad (3.61)$$

where the first term on the right-hand side is the acceleration term present in pure AdS. This makes manifest the well-known fact that the motion of time-like geodesics in AdS is periodic with period  $2\pi\ell$ . Further, note that the sign of the acceleration

---

<sup>3</sup>Of course, the radial coordinate for the soliton is not the same as the radial coordinate for pure AdS. These differences disappear at sufficiently large  $r$ , as can be confirmed by putting the metric into Fefferman-Graham form. What we mean here is that the functional form of  $r_{\max}$  is identical.

in pure AdS is *always negative* — a stone tossed in AdS will always be returned to sender.

The additional acceleration terms for  $a \neq 0$  have interesting consequences. The last term in the above always makes a positive contribution, since  $\mathcal{E} \geq \mathcal{E}_{\min} > 1$ . Close to the bubble this positive term actually dominates, leading to a region where the acceleration is positive, indicating a repulsion.

It is a simple matter to prove this. First, note that for sufficiently large  $r$ , the leading AdS term will always dominate, meaning that  $\ddot{r} < 0$  at large  $r$ . Next, let us consider the possibility of solutions to the equation  $\ddot{r} = 0$ . Define a new variable  $r = \ell(x + \alpha)$  where  $\alpha = a/\ell$ . Then, the equation  $\ddot{r} = 0$  becomes equivalent to the polynomial equation<sup>4</sup>

$$x^6 + 6\alpha x^5 + 15\alpha^2 x^4 + 20\alpha^3 x^3 + 16\alpha^4 x^2 + 8\alpha^5 x + 2\alpha^4 (1 - \mathcal{E}^2 + \alpha^2) = 0. \quad (3.62)$$

Every term in this polynomial is manifestly positive except for the very last one. It will vanish for

$$\mathcal{E} = \mathcal{E}_{\min} = \frac{p}{2}. \quad (3.63)$$

For  $\mathcal{E} > \mathcal{E}_{\min}$  the last term is negative. In this case, applying Descartes' rule of signs tells us that there will be a single positive value of  $x$  where the above polynomial has a zero. There are no zeros for positive  $x$  under other circumstances. Undoing our substitutions,  $x > 0$  implies  $r > a$ . Thus, we have concluded that there is exactly one zero for the acceleration for  $r > a$ . Since we know from the above analysis that  $\ddot{r} < 0$  for sufficiently large  $r$ , we then conclude that in a neighbourhood of the bubble the acceleration is positive for particles with  $\mathcal{E} > p/2$ . Since this corresponds to the minimum possible energy, it follows that *all* massive particles feel a repulsion in the vicinity of the bubble, except those for which  $\mathcal{E}$  is *exactly*  $\mathcal{E}_{\min}$  as these particles just sit at the bubble without motion.

The extent of this repulsion is bounded and approaches a constant, as can be seen by expanding the acceleration in the vicinity of the bubble:

$$\ddot{r} = \frac{(4\mathcal{E}^2 - p^2)}{\ell\sqrt{p^2 - 4}} + \mathcal{O}(r - a). \quad (3.64)$$

---

<sup>4</sup>While an explicit solution for  $x$  in this equation can be obtained, it is sufficiently complicated that it is not beneficial to present it here.

The origin of this effect is the negative mass of the bubble. To see this, it is instructive to re-write the expression for the acceleration in terms of the mass given in (3.27). It is a simple matter to show that it then takes the form,

$$\ddot{r} = -\frac{r}{\ell^2} - \frac{8pM}{\pi} \frac{(2r_{\max}^2 - r^2)}{r^5}, \quad (3.65)$$

where  $r_{\max}$  was introduced in eq. (3.59). Since  $r \leq r_{\max}$  we see directly that if it were possible to have positive mass, then the acceleration would always be attractive. However, since the mass is necessarily negative, there is a competition between the confining potential of AdS and the negative mass repulsion of the bubble. This leads to a thin layer in the vicinity of the bubble where massive particles find themselves accelerated away from the bubble.

Finally, it is important to emphasize that the repulsion does not result in a situation where a (positive energy) particle ‘hovers’ at some fixed position  $r > a$ . When  $\mathcal{E} > \mathcal{E}_{\min}$  the velocity is necessarily non-zero at the point where the acceleration vanishes. The only case when it is possible for  $\dot{r} = \ddot{r} = 0$  simultaneously is when  $\mathcal{E} = \mathcal{E}_{\min}$ , corresponding to a particle at the location of the bubble.

The (radial) motion of massive particles in Eguchi-Hanson-AdS<sub>5</sub> is therefore qualitatively similar to the motion of massive particles in AdS. The motion is forever oscillatory, with particles confined in some layer surrounding the bubble, the thickness of which depends on the energy of the particle. Unsurprisingly, this suggests that Eguchi-Hanson-AdS<sub>5</sub> may suffer from a similar non-linear instability as global AdS, however, here without the possibility of forming horizons [62].

### 3.5.2 Null Geodesics: Absence of Stable Trapping

Consider, now, null geodesics. These are obtained by setting  $\hat{m} = 0$  in (3.56), yielding

$$\dot{r}^2 = 4f(r) - \frac{16g(r)\eta^2}{r^2} - \frac{16\hat{C}}{r^2}f(r)g(r) \quad (3.66)$$

where  $\eta := p_\psi/E$  and  $\hat{C} = C/E^2$  and we have performed an appropriate rescaling of the affine parameter. For convenience, we will work with dimensionless parameters

by scaling out  $\ell$  (this is equivalent to fixing  $\ell = 1$ ). Doing so produces

$$r^2 = V(x) = \frac{4}{x^3}P(x), \quad P(x) = c_3x^3 + c_2x^2 + c_1x + c_0. \quad (3.67)$$

where  $x = r^2$  and

$$c_3 = 1 - 4\hat{C} - 4\eta^2, \quad c_2 = -4(\hat{C} + \eta^2), \quad c_1 = -a^4(1 - 4\hat{C}), \quad c_0 = 4a^4\hat{C}. \quad (3.68)$$

Trajectories are only allowed in regions where the effective potential  $V(r) > 0$  with turning points at the zeroes, whereas regions with  $V(r) < 0$  are forbidden. Stable trapping will occur if there exist  $x_1, x_2$  such that  $0 < a^2 \leq x_1 < x_2$  with  $V(x_i) = 0$ ,  $V(x) > 0$  for  $x \in (x_1, x_2)$ , and  $V(x) < 0$  in neighbourhoods to the left of  $x_1$  and right of  $x_2$  (see [49, Fig 2]). This translates into similar conditions on the cubic  $P(x)$ . First note that  $\hat{C} \geq 0$  by definition. Observe that

$$P(0) = 4a^4\hat{C} \geq 0, \quad P(a^2) = -4a^4(1 + a^2)\eta^2 \leq 0. \quad (3.69)$$

We now consider several distinct cases.

**Case 1:**  $\eta, \hat{C} \neq 0$

From above, we have  $P(0) > 0$  and  $P(a^2) < 0$ . Thus there must be at least 1 root  $x_0$  with  $0 < x_0 < a^2$ . For stable trapping we will need two further positive roots  $x_1, x_2$  each strictly greater than  $a^2$ . As  $x \rightarrow \infty$ , the sign of  $P$  is controlled by  $c_3$ . If  $c_3 > 0$  then it is clear there cannot be a 2nd root  $x_2$ . This occurs if

$$0 < \hat{C} < \frac{1}{4} - \eta^2 < \frac{1}{4} \quad (3.70)$$

Thus we find there is no stable trapping in this case. Now, suppose that  $c_3 < 0$ . then

$$\hat{C} > \frac{1}{4} - \eta^2 \quad (3.71)$$

Now consider Descartes' rule of signs. We are assuming  $c_3 < 0$ , and  $c_2 < 0$ , whereas  $c_0 > 0$  automatically. Thus there is only one sign flip between adjacent coefficients: if  $c_1 > 0$  there is a sign flip between the  $x^2$  and  $x$  coefficients, and if  $c_1 < 0$  there is a sign flip between the  $x$  and  $x^0$  coefficients. Thus the rule of signs indicates there

can be only one positive root, but we already know one exists in  $(0, a^2)$ . Thus stable trapping cannot occur in this case either.

Finally suppose  $c_3 = 0$  so that

$$\hat{C} = \frac{1}{4} - \eta^2 > 0 \quad (3.72)$$

in which case we must have  $\eta^2 < 1/4$ . Writing  $\eta^2 = 1/4 - \epsilon$  for  $0 < \epsilon < 1/4$ , we have

$$P(x) = -x^2 + a^4(4\epsilon - 1)x + 4a^4\epsilon \quad (3.73)$$

which is a downward-pointing parabola. It is easy to see that the only turning point has to be for  $x < 0$ ; in particular there cannot be two roots to the right of  $x = a^2$ . Thus there is no stable trapping here either.

**Case 2:**  $\hat{C} = 0$

In this case we get

$$P(x) = x((1 - 4\eta^2)x^2 - 4\eta^2x - a^4). \quad (3.74)$$

Then  $x = 0$  is automatically a root. Suppose that  $\eta^2 = 0$ . Then  $P = x(x - a^2)(x + a^2)$  for which we easily read off the roots and find stable trapping cannot occur. Hence assume  $\eta^2 > 0$ . To get stable trapping we need the quadratic  $Q(x) = (1 - 4\eta^2)x^2 - 4\eta^2x - a^4$  to have two roots that are greater than  $a^2$ . From Descartes' rule of signs we see that there can be at most 1 sign flip between adjacent coefficients, and hence only one positive root. Thus there is no stable trapping here either.

**Case 3:**  $\eta = 0$

We have

$$P(x) = (1 - 4\hat{C})(x - a^2)(x + a^2) \left( x - \frac{4\hat{C}}{1 - 4\hat{C}} \right) \quad (3.75)$$

If  $C = 1/4$  then this is just

$$P = -(x - a^2)(x + a^2) \quad (3.76)$$

which is a downward pointing parabola and there is no stable trapping here. Hence assume  $\hat{C} \neq 1/4$ . There is a root  $x_- = -a^2$  and  $x_1 = a^2$ . Then the only way we have the final root  $x_2$  to the right of  $x = a^2$  is if

$$\frac{4\hat{C}}{1-4\hat{C}} > a^2 \quad (3.77)$$

which, since  $\hat{C} > 0$  implies we must have  $1 - 4\hat{C} > 0$ . But then  $P'(x_2) > 0$ , which cannot occur for stable trapping.

The above cases exhaust all possibilities, establishing that stable trapping does not occur.

### 3.5.3 Null Geodesics: Light-Crossing Time

In AdS, a light ray sent from a given point completes a round-trip to infinity and back in finite time coordinate time. Taking this point to be the origin, we have

$$T_{\text{AdS}} = 2 \int_{r=0}^{r=\infty} dr \frac{\dot{t}}{\dot{r}} = 2 \int_0^\infty \frac{dr}{g(r)} = \pi\ell. \quad (3.78)$$

This in turn defines a fundamental frequency naturally associated with AdS:

$$\omega_{\text{AdS}}\ell = \frac{2\pi\ell}{T_{\text{AdS}}} = 2. \quad (3.79)$$

This is relevant because the fundamental frequency matches the spacing for the overtones of scalar normal modes in AdS. Since we will study scalar normal modes in the next section, it is relevant to understand if a similar effect occurs for the soliton.

The computation for the light-crossing time in the soliton proceeds along the same lines. The integral to evaluate is now

$$T_p = 2 \int_a^\infty \frac{1}{g(r)\sqrt{f(r)}} dr, \quad (3.80)$$

where here the subscript  $p$  refers to the integer defining regularity of the geometry.

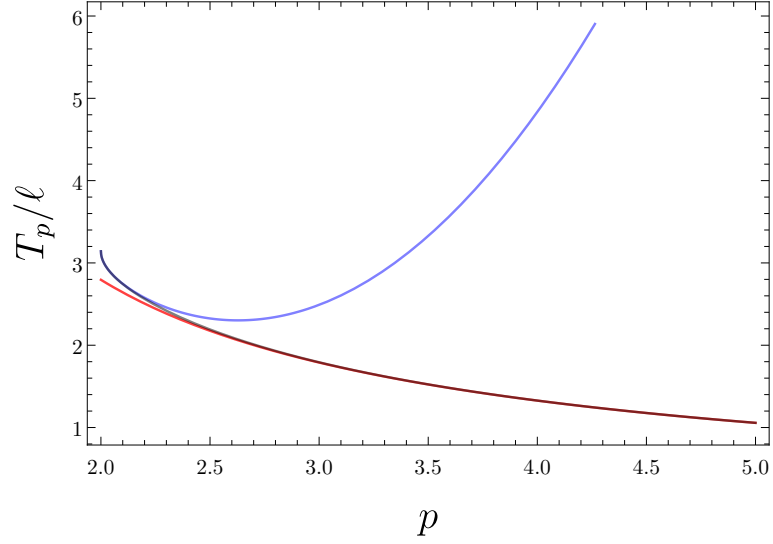


Figure 3.1: A plot of the light-crossing time  $T_p$  as a function of  $p$  (black curve) compared with the asymptotic approximations as  $p \rightarrow 2$  (blue curve) and as  $p \rightarrow \infty$  (red curve). In each case we include the first three terms of the approximation. We see that the large  $p$  approximation is quite accurate for all physical values of  $p \geq 3$ .

This integral actually has a closed form expression,

$$\begin{aligned} \frac{T_p}{\ell} = & \frac{1}{48\sqrt{2\pi}(p^2-4)^{3/2}} \left\{ 48(p^2-4)^2 \Gamma\left(\frac{3}{4}\right)^2 \left[ {}_2F_1\left(-\frac{1}{4}, 1, \frac{1}{4}, \frac{16}{(p^2-4)^2}\right) - 1 \right] \right. \\ & \left. + \Gamma\left(\frac{1}{4}\right)^2 \left[ 48(p^2-4) + \frac{256}{p\sqrt{p^2-8}} {}_2F_1\left(\frac{1}{2}, \frac{3}{4}, \frac{7}{4}, \frac{16}{(p^2-4)^2}\right) \right] \right\}. \end{aligned} \quad (3.81)$$

Expanding this in different limits is more useful. First, for  $p \rightarrow 2$ , the expansion is

$$\frac{T_p}{\ell} = \pi - \sqrt{\frac{2}{\pi}} \Gamma\left[\frac{3}{4}\right]^2 \sqrt{p-2} - \frac{4\pi\Gamma[1/4] + 3\sqrt{2}\Gamma[3/4]^3}{24\sqrt{\pi}\Gamma[3/4]} (p-2)^{3/2} + \frac{\pi}{2} (p-2)^2 + \mathcal{O}(p-2)^{5/2}. \quad (3.82)$$

The other limit of interest where this can be expanded is  $p \rightarrow \infty$ . In this case the expansion reads,

$$\frac{T_p}{\ell} = \frac{\Gamma[1/4]^2}{\sqrt{2\pi}p} + \sqrt{\frac{2}{\pi}} \frac{\Gamma[1/4]^2 - 8\Gamma[3/4]^2}{p^3} + \frac{3(17\Gamma[-3/4]^2 - 256\Gamma[3/4]^2)}{8\sqrt{2\pi}p^5} + \mathcal{O}(p^{-6}). \quad (3.83)$$

We show in Figure 3.1 a plot of the exact evaluation of the light crossing time, compared with the approximate forms described above. Here we have plotted the result treating  $p$  as a continuous parameter. It must be kept in mind that regular geometries exist only for integer  $p \geq 3$ . First, we note that the light-crossing time for the soliton is always less than that of pure AdS. Regarding the approximations, for  $p \sim 2$  the approximation is accurate in the close vicinity of  $p = 2$ , but is a poor approximation for larger, physical values of  $p$ . The large  $p$  approximation is much better suited for all cases  $p \geq 3$ . Finally, in the limit  $p \rightarrow \infty$ , we recover the light-crossing time of the AdS soliton,  $\tau_{\text{AdS}} = \Gamma[1/4]^2/(2\sqrt{2\pi})$ .<sup>5</sup> This is observed after performing the shift of the time coordinate necessary for that limit  $\tau = pt/2$  — see Section 3.3.1.

### 3.6 Wave Equation on Eguchi-Hanson Solitons

A massive Klein-Gordon field  $\Phi$  obeys the equation

$$\nabla^\mu \nabla_\mu \Phi = \hat{M}^2 \Phi \quad (3.84)$$

in the spacetime background metric (3.3). We use the separation ansatz

$$\Phi = e^{-i\omega t} e^{im\psi} Y(\theta, \phi) R(r) \quad (3.85)$$

where  $Y(\theta, \phi)$  is an eigenfunction of the charged scalar Laplacian on  $S^2 = CP^1$ , satisfying

$$D^2 Y(\theta, \phi) = -\mu Y(\theta, \phi) \quad (3.86)$$

where  $A_\mu$  is a one-form on  $S^2$  defined as  $A_\mu = \frac{\cos\theta}{2} d\phi$ , and the connection is  $D_\mu = \nabla_{S^2_\mu} - imA_\mu$ . The spectrum of this operator, and the associated eigenfunctions have been studied [83, 84, 85], and the spectrum is

$$\mu = l(l+2) - m^2, \quad (3.87)$$

$$l = 2k + |m|, \quad (3.88)$$

$$k = 0, 1, 2, \dots \quad (3.89)$$

---

<sup>5</sup>See, for example, [82].

Requiring  $\Phi$  to be smooth implies  $m = np$ , as  $\psi$  is identified with period  $2\pi/p$ . With this observation, the problem reduces to that of a single radial equation, which reads

$$\frac{1}{r} \frac{d}{dr} \left( f(r)g(r)r^3 \frac{dR(r)}{dr} \right) + \left[ \frac{\omega^2 r^2}{g(r)} - \frac{m^2}{f(r)} - \hat{M}^2 r^2 - \mu \right] R(r) = 0. \quad (3.90)$$

The radial equation (3.90) can be cast into Schrödinger equation form. To see this, we introduce a new independent variable  $x$

$$\frac{dx}{dr} = \frac{1}{g\sqrt{f}}, \quad x(a) = 0 \quad (3.91)$$

and a dependent variable  $\Psi$

$$\Psi = f^{1/4} r^{3/2} R. \quad (3.92)$$

This puts the radial equation into a formally self-adjoint form

$$-\frac{d^2\Psi}{dx^2} + V(r(x))\Psi = \omega^2\Psi \quad (3.93)$$

with potential

$$V(r) = -\frac{gf^{1/4}}{r^{3/2}} \frac{d}{dr} \left[ r^3 fg \frac{d}{dr} (f^{-1/4} r^{-3/2}) \right] + \frac{g}{r^2} \left( \frac{m^2}{f} + \mu + \hat{M}^2 r^2 \right). \quad (3.94)$$

We now seek solutions of this equation. We have not been able to find an analytic solution, and so we proceed with a combination of numerical and approximate techniques.

### 3.6.1 Approximate Solution: WKB Analysis

In the limit of large eigenvalues the differential equation can be solved approximately using, for example, the WKB method [86]. Here we set the mass parameter  $\hat{M} = 0$ . For the purposes of this analysis, it is useful to rewrite the differential equation (3.90) by defining

$$r = za, \quad (3.95)$$

which maps the domain to  $z \in [1, \infty)$ . After this transformation and applying the regularity condition, the resulting equation is given by

$$0 = z(z^4 - 1) (4 + (p^2 - 4)z^2) R''(z) + (4 - (p^2 - 4)z^2 + 12z^4 + 5(p^2 - 4)z^6) R'(z) + 4z^3 \left[ -4k^2 - 2np - 4k(1 + np) + \frac{n^2 p^2 z^4}{1 - z^4} + \frac{(p^2 - 4)z^2 \ell^2 \omega^2}{4 + (p^2 - 4)z^2} \right] R(z). \quad (3.96)$$

We work here in an approximation where the overtone number  $N$  is larger than the other fixed quantum numbers characterizing the problem, i.e.  $N \gg n, k$ . In this case, by defining a new function and variable according to

$$z = 1 + e^x, \quad (3.97)$$

and

$$\Psi = \sqrt{\frac{z}{(z+1)(z^2+1)(4+z^2(p^2-4))}} R(z), \quad (3.98)$$

the differential equation takes the form of a Schrödinger equation,

$$-\frac{1}{(\omega\ell)^2} \frac{d^2\Psi}{dx^2} + V\Psi = 0, \quad (3.99)$$

with potential

$$V = \frac{4z^4(z-1)(p^2-4)}{(4+z^2(p^2-4))^2(z+1)(z^2+1)} \quad (3.100)$$

in the limit of large  $(\omega\ell)$ . The transformation (3.97) has mapped the problem to the interval  $(-\infty, \infty)$ , which allows for direct comparison with the analysis of [86]. Examining the potential as a function of  $x$  we see that it vanishes at the boundaries  $x \rightarrow \pm\infty$ , and there are no turning points on the interior domain. We can then apply directly the results of [86, Sec. 10.5] for the quantization condition of normal mode solutions in the geometric optics approximation:

$$\omega\ell \int_{-\infty}^{\infty} \sqrt{V(x)} dx = \left(N + \frac{1}{2}\right) \pi + \mathcal{O}\left(\frac{1}{\omega}\right), \quad (3.101)$$

where  $N$  is a non-negative integer. Written as an integral over  $z$ , the left-hand side

of the above becomes

$$\int_{-\infty}^{\infty} \sqrt{V(x)} dx = \int_1^{\infty} \frac{2z^2}{(4 + z^2(p^2 - 4))} \sqrt{\frac{p^2 - 4}{z^4 - 1}} dz = \frac{T_p}{2\ell}, \quad (3.102)$$

where in the last equality we recognize the integral as being identical to that defining the light crossing time of the soliton geometry given in (3.80). Therefore, applying the quantization condition as above, we have in the geometric optics approximation the following result for the frequencies:

$$\omega = \left(N + \frac{1}{2}\right) \frac{2\pi}{T_p} = \left(N + \frac{1}{2}\right) \omega_{\text{fun}}, \quad (3.103)$$

where the fundamental frequency  $\omega_{\text{fun}} = 2\pi/T_p$  for the Eguchi-Hanson-AdS<sub>5</sub> soliton. We expect this relationship to be accurate in the limit of large overtone number, since we have assumed that  $\ell\omega$  is large. Later, in our numerical results, we will verify this is remarkably accurate even at small overtone number.

As explained below (3.80), the light crossing time can be evaluated analytically and was presented in Eq. (3.81). While this closed-form solution for the light-crossing time (or, equivalently, the fundamental frequency) is convenient, it is not necessarily illuminating. Therefore in Table 3.1 we list the numerical values for the fundamental frequency for a few values of  $p$ . Since the asymptotics of  $T_p$  are dominated by a  $1/p$  term, we have factored out an overall multiple of  $p$  in the numerical expressions for  $\omega_{\text{fun}}$ . This allows one to see more clearly the limiting behaviour for larger values of  $p$ . The results in this table should be compared with the fundamental frequency for the AdS soliton, which is

$$\ell\omega_{\text{fun}}^{\text{AdSS}} = \frac{4\sqrt{2}\pi^{3/2}}{\Gamma[1/4]^2} = \lim_{p \rightarrow \infty} \frac{2\ell\omega_{\text{fun}}}{p} \approx 2.39628. \quad (3.104)$$

That is, at large values of  $p$ , the fundamental frequency, which governs the normal modes at large overtone number  $N \gg k, n$ , asymptotically approaches  $p/2$  times the fundamental frequency of the AdS soliton. This is directly related to the fact that there is a sense in which the AdS soliton is formally the large  $p$  limit of the Eguchi-Hanson-AdS<sub>5</sub> soliton, as explained in Section 3.3.1. The factor of  $2/p$  is precisely the factor required to match the time coordinates between the two geometries.

Numerical values of $\omega_{\text{fun}}$								
$p$	3	4	5	6	7	8	8	10
$\ell\omega_{\text{fun}}/p$	1.16822	1.18337	1.18917	1.19207	1.19375	1.19481	1.19553	1.19604

Table 3.1: A selection of numerically obtained  $\omega_{\text{fun}}$  values.

### 3.6.2 Numerical Solution: Boundary Conditions & Regularity

To implement our numerical methods, it is essential to understand the behaviour of the solutions to the radial equation in the vicinity of the bubble and asymptotically. It will also be more convenient to compactify the semi-infinite domain to a finite interval. We therefore begin our numerical analysis of the radial equation with an analysis of the asymptotic behaviour of the solutions and boundary conditions. For the sake of comparison with the broader literature, here we will re-instate the mass parameter  $\hat{M}$  in our formulas.

We begin by introducing a new coordinate

$$u = \frac{2(r-a)}{r+a} - 1, \quad (3.105)$$

which maps the semi-infinite domain  $r \in (a, \infty)$  to the interval  $u \in [-1, 1]$ . To understand the singularity structure, we perform a Frobenius analysis. Near  $r = a$  we write,

$$R(u) = (u+1)^s \sum_{i=0}^{\infty} a_i (u+1)^i \quad (3.106)$$

and extract  $s$  by solving the differential equation near  $u = -1$ . Provided that  $m \neq 0$ , the equation allows for two solutions, corresponding to the values

$$s = \pm \frac{m}{2p}. \quad (3.107)$$

We require regularity of the solution as  $u \rightarrow -1$ , and therefore only one of the above solutions is physically acceptable, depending on the sign of  $m$ . In general, for  $m \neq 0$  we have the regular behaviour  $s = |m|/(2p)$ .

The case  $m = 0$  must be treated separately, since the Frobenius method gives a

degenerate root in that case. Since the degenerate root corresponds to  $s = 0$ , from the general theory of Frobenius analysis, we can conclude in this case that the solution must be of the form

$$R(u) = \sum_{i=0} a_i (u+1)^i + \log(u+1) \sum_{i=0} b_i (u+1)^i. \quad (3.108)$$

It can easily be shown that this ansatz leads to a consistent series solution in the vicinity of  $u = -1$ . Regularity of the solution there forces us to set  $b_0 = 0$ , and so when  $m = 0$ , the solution approaches a constant as  $r \rightarrow a$ . This behaviour is in fact captured by the result above,  $s = |m|/(2p)$ , in the case  $m = 0$ .

The asymptotic analysis near  $u = 1$  (i.e.  $r \rightarrow \infty$ ) is more standard. We can again proceed via Frobenius analysis. Taking the Frobenius ansatz

$$R(u) = (u-1)^{\hat{s}} \sum_{i=0} a_i (u-1)^i, \quad (3.109)$$

expanding the differential equation near  $u \rightarrow 1$  and demanding a solution of the indicial equation, we find

$$\hat{s} = 2 \pm \sqrt{2 + (\hat{M}\ell)^2}. \quad (3.110)$$

Requiring the solution to be real gives the well-known Breitenlohner-Freedman bound [87],  $(\hat{M}L)^2 > -2$ . As usual, we proceed by taking the normalizable solution,

$$\hat{s} = 2 + \sqrt{2 + (\hat{M}\ell)^2}. \quad (3.111)$$

With the asymptotic behaviours understood, we now recast the differential equation into a form that is more amenable to numerical solution. To this end, we define a new function

$$R(u) = (1-u)^{2+\sqrt{2+(\hat{M}\ell)^2}} (1+u)^{|m|/(2p)} h(u). \quad (3.112)$$

We then recast (3.90) in terms of the new function  $h(u)$ . The resulting expression is somewhat messy, and so we do not present it here. The prefactors implement the appropriate fall-off conditions in the two relevant limits, and therefore the only requirement on  $h(u)$  is that it should be regular. Demanding this, a series solution

near either  $u \rightarrow -1$  or  $u \rightarrow +1$  results in Robin boundary conditions

$$h'(-1) = \left[ \frac{(4 + p^2)(m^2 + 2|m|p) + 4p^4 + 8\omega^2 + 2p^2(\mu - \omega^2)}{2p^3(|m| + p)} \right] h(-1) \quad (3.113)$$

$$h'(1) = \left( 1 + \frac{|m|}{4p} \right) h(1) \quad (3.114)$$

that must be imposed on the function  $h(u)$ .

Before moving on, it is worth commenting in a bit more detail about the solution in the near bubble regime  $r \rightarrow a$ . In this regime, the radial solution behaves as  $R(r) \sim (r - a)^{n/2}$ , and so it appears to be continuous but not smooth there. To study this more carefully, we carry out the transformation

$$\rho = \frac{4\sqrt{r - a}}{p\sqrt{f'(a)}}, \quad \varphi = p\psi \quad (3.115)$$

which yields

$$ds^2 = d\rho^2 + \rho^2 d\varphi^2 \quad (3.116)$$

namely the standard polar metric on  $\mathbb{R}^2$  as  $r \rightarrow a$ , with  $\varphi \sim \varphi + 2\pi$  due to the  $2\pi/p$  periodicity of  $\psi$ .

Consider next the solution to the wave equation as  $r \rightarrow a$ . Focusing just on the terms with  $r$  and  $\psi$  dependence, and transforming these according to the polar coordinates (3.115) defined above, we obtain

$$\phi(r, \psi) \sim \rho^n e^{in\varphi}. \quad (3.117)$$

Despite the fact that neither  $\rho$  nor  $\varphi$  are themselves smooth functions — as can be confirmed by transforming these quantities to a Cartesian frame — the combinations as appearing here are indeed smooth. The solutions have the same structure as Bessel functions.

### 3.6.3 Numerical Solution: Normal Modes

We can now perform a numerical analysis of the radial equation (3.90), which we carry out for the case  $\hat{M} = 0$ . To solve this equation, we have employed two different numerical schemes. Our primary method has been a pseudospectral method for obtaining

the eigenvalues of the differential operator. However, we have also cross-checked and benchmarked this method with a simpler shooting method. In Section 3.9 we compare the two techniques.

For an in-depth review of the pseudospectral method we refer to various references, e.g. [88, 89, 90]. After the transformations (3.105) and (3.112), the radial equation is a problem on the interval  $[-1, 1]$ . On this interval, we introduce a grid consisting of  $\mathcal{N} + 1$  grid points  $u_i$ , which we take to be the Gauss-Lobatto points,

$$u_i = \cos \frac{i\pi}{\mathcal{N}} \quad \text{for } i = 0, \dots, \mathcal{N}. \quad (3.118)$$

We then discretize the differential equation. The eigenfunction  $h(u)$  becomes a vector defined at the Gauss-Lobatto points,  $h_i := h(u_i)$ , and the derivatives appearing in the differential equation are replaced with the corresponding Chebychev differentiation matrices<sup>6</sup>  $D_{i,j}$ . The differential equation then reduces to a generalized eigenvalue problem,

$$H_{i,j}h_j = \omega^2 V_{i,j}h_j \quad (3.119)$$

where  $H_{i,j}$  is the discretization of the differential operator and  $V_{i,j}$  is the matrix discretization of the terms multiplying  $\omega^2$  in the original differential equation. To implement the Robin boundary conditions, we replace the first row of the above with the discretization of equation (3.114), and the last row with the discretization of equation of (3.113).

After the differential equation has been discretized, we utilize the built-in eigenvalue solvers of Mathematica to obtain the eigenvalues  $\omega$ . For a given choice of  $\mathcal{N}$  we will obtain a set of eigenvalues  $\{\omega\}_{\mathcal{N}}$  for the generalized eigenvalue problem described above. Of course, for any discretization of the differential equation, the eigenvalues of the corresponding matrix equation will differ from the true eigenvalues of the differential operator. We expect that the error in this discretization will become smaller as  $\mathcal{N}$  is increased. We monitor convergence in the following way. We set *a priori* a tolerance that we regard as the minimum acceptable absolute error in the eigenvalue  $\omega$ . We then choose a number of grid points  $\mathcal{N}$  and compute the spectrum  $\{\omega\}_{\mathcal{N}}$  first for  $\mathcal{N}$  and then the spectrum  $\{\omega\}_{\mathcal{N}+1}$  for a grid with  $\mathcal{N} + 1$  points. For each eigenvalue in  $\{\omega\}_{\mathcal{N}}$  we assess whether there is a corresponding eigenvalue in  $\{\omega\}_{\mathcal{N}+1}$  that is within

---

<sup>6</sup>We refer to, for example, [89] for an explicit form of these objects — c.f. section 2.4.2 therein.

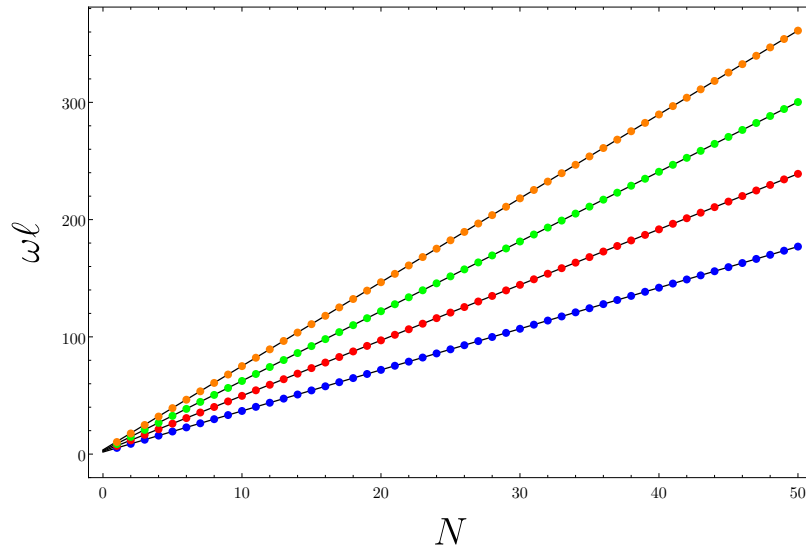


Figure 3.2: A comparison of the WKB approximate results for  $n = k = 0$  (black lines) with the numerically computed eigenvalues for  $p = 3, 4, 5, 6$  corresponding to the blue, red, green and orange dots, respectively.

the specified tolerance. If it is, then we conclude that this particular eigenvalue has been determined to the specified tolerance. We continue in this way, identifying each eigenvalue in  $\{\omega\}_{\mathcal{N}}$  that has converged within the specified tolerance. For most of our results the tolerance has been set to  $10^{-5}$ , meaning the eigenvalues are accurate to *at least* five decimal places. In most cases, we have repeated the above procedure for several values of  $\mathcal{N}$  to gain a better understanding of the convergence properties. In Section 3.11 we present additional details on convergence for particular cases. Furthermore, in Section 3.9 we compare the results obtained via the pseudospectral method with those obtained via the shooting method, to ensure consistency.

When confusion may arise, when referring to a particular element of  $\{\omega\}$  we will use the notation  $\omega_{N,k,n}^{(p)}$  to indicate the dependence on the various parameters that appear in the equation. Here  $N$  is a non-negative integer indicating the overtone, and  $n = m/p$ . Since the equations and boundary conditions are invariant under  $m \rightarrow -m$ , we will without loss of generality consider only the case where  $n$  is a non-negative integer. When there is less risk of confusion, we will suppress additional data attached to the spectral element  $\omega_{N,k,n}^{(p)}$  to avoid unnecessary bulky notation.

To begin our discussion of the numerical results, we compare the output of the pseudospectral method with the approximate results obtained via the WKB method. In

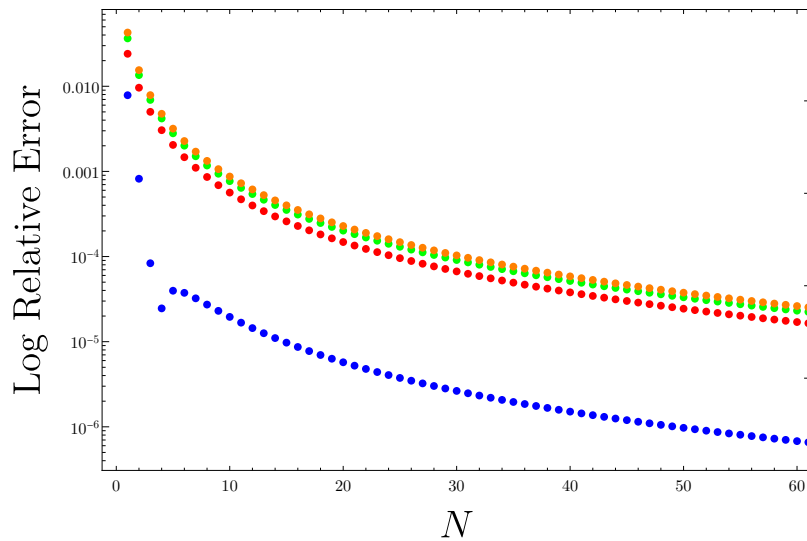


Figure 3.3: A plot showing the error in the WKB approximation as a function of overtone number for  $p = 3, 4, 5, 6$  corresponding to the blue, red, green and orange dots, respectively. Here we show the logarithm of the relative absolute error,  $|\omega_{\text{WKB}} - \omega_{\text{Num}}|/\omega_{\text{Num}}$ .

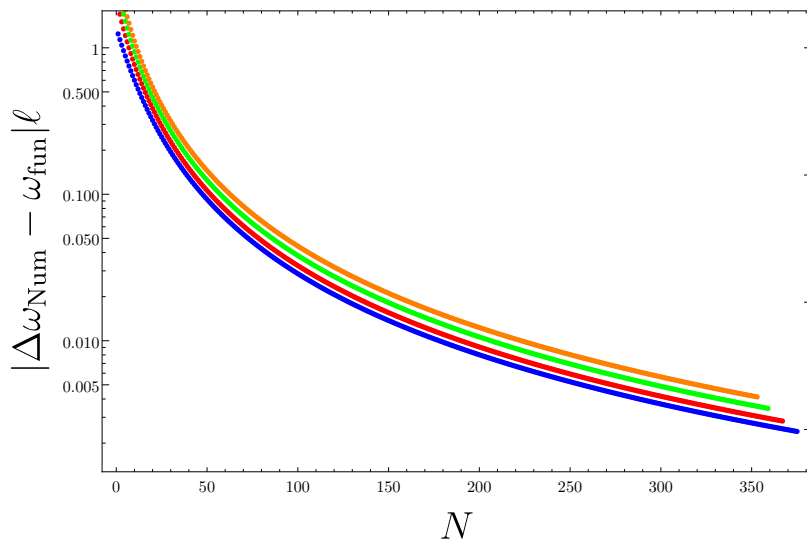


Figure 3.4: A plot showing the difference between the overtone spacing for the numerically computed frequencies  $\Delta\omega_{\text{Num}} = \omega_{N+1} - \omega_N$  and the fundamental frequency  $\omega_{\text{fun}}$  on a logarithmic scale. The plot shows the case  $n = 20, k = 0$  for  $p = 3, 4, 5, 6$  corresponding to the blue, red, green and orange dots, respectively. The results are consistent with the fundamental frequency governing the spacing between successive overtones provided that  $N \gg n, k$ .

the case of modes with  $n = k = 0$ , the WKB approximation is rather accurate for all overtone numbers. This is shown in Figure 3.2, where we show the output of the numerical methods (coloured dots) with the analytic approximation provided by the WKB method (black lines). The plot shows this comparison for overtones up to  $N = 50$  for  $p = 3, 4, 5$  and  $6$ . In all cases, the agreement between the WKB result and the more accurate numerical approach is superb. This is further backed up by Figure 3.3, which shows the relative error between the WKB approximation and the numerical result for the same set of  $p$  values. This plot shows that the WKB approximation is most accurate for the  $p = 3$  case, but in all cases is accurate to about one part in one-thousand for overtone number  $N \geq 10$ . As expected, the accuracy of the WKB approximation becomes better the larger the overtone number becomes.

When  $n$  and  $k$  are non-vanishing, the WKB result no longer provides particularly good agreement, and we will discuss these cases at greater length below. However, it is important to note that even in these cases the WKB approach yields the correct spacing between overtones, provided the overtone number is sufficiently large compared to the values of  $n$  and  $k$ . We illustrate this in Figure 3.4, which compares the overtone spacing  $\omega_{N+1} - \omega_N$  as obtained numerically to the fundamental frequency, which governs the overtone spacing in the WKB approximation. The plot shows this comparison as a function of overtone number for the  $n = 20$  and  $k = 0$  mode for the cases of  $p = 3, 4, 5$  and  $6$ . We see in all cases that the absolute difference between the numerically determined spacing and the fundamental frequency is a monotonically decreasing function of the overtone number. This result, which we have verified in more examples in our numerical computations, is consistent with the notion that the fundamental frequency universally governs the spacing between overtones in the large overtone limit.

As mentioned, the WKB results provide a good approximation to the eigenvalues when  $n = k = 0$ , and more generally allow us to understand the spacing between overtones in the limit of large overtone number. However, there are a number of instances when the approximate solutions obtained in this way are insufficient. We move on to discuss these cases now. While the Eguchi-Hanson-AdS<sub>5</sub> soliton is defined only for integer  $p \geq 3$ , the radial equation is sensible from a mathematical perspective under more general circumstances. To understand the spectrum  $\{\omega\}$  for the soliton, we have found it useful to analyse the radial equation for real values of  $p \in [2, \infty)$ . The main reason for this is that it is possible, through a combination of numerical

and analytical techniques, to obtain simple asymptotic forms for  $\omega$  as  $p \rightarrow 2$  and as  $p \rightarrow \infty$ . By piecing together these approximate forms in various ways it is possible to get a good handle on the spectra over the full range of parameters.

In the limit  $p \rightarrow 2$  we find the following behaviour:

$$\omega_{0,k,n}^{(p)} \approx 2(2+k+n) + n(p-2) + \left[ \frac{6(2n^2 - n - k)}{(k+n)(1+2k+2n)(-1+2k+2n)} \right] (p-2)^2 + \dots \quad (3.120)$$

where the first term has been obtained analytically; the analysis is outlined in Section 3.11. Essentially, in the strict  $p = 2$  limit, the radial equation reduces to that of a Klein-Gordon field on the orbifold  $\text{AdS}_5/\mathbb{Z}_2$ . That problem is obviously analytically solvable, and leads to the first term in the above. We find excellent numerical agreement between the  $p \rightarrow 2$  limit of the numerical results and this analytically derived result, as detailed in Section 3.11.

The second and third terms in (3.120) have been inferred from the numerical results. For simplicity, we have focused here only on the fundamental mode, and have not worked out the dependence for the overtones due to the complexity. Our procedure to determine these corrections was the following. We have computed, for numerous choices of  $n$  and  $k$ , the spectrum on the interval  $p \in (2, 3]$ . For a given choice of  $n$  and  $k$ , we then fit the numerical results to a polynomial in  $(p-2)$ . Adjusting the order of the polynomial fit, we see that the coefficients converge rapidly to particular values<sup>7</sup>. We take this as an indication that a series in  $(p-2)$  captures accurately the behaviour of the spectrum in the close vicinity of  $p = 2$  for given values of  $n$  and  $k$ . By comparing the results of this procedure across several different values of  $n$  and  $k$ , we arrive at a collection of values  $c_{n,k,i}$  for the coefficients of the  $(p-2)^i$  term in the polynomial fit. We then study the way the different  $c_{n,k,i}$  depend on  $n$  and  $k$ , and from this infer their analytical dependence. The analytic dependence is then cross-checked against numerical results for values of  $n$  and  $k$  that were not part of the sample used when deducing the candidate analytic form. This process becomes more involved as the power  $i$  is increased. However, for the linear and quadratic terms, the dependence is simple enough that it can be inferred, giving the results presented above<sup>8</sup>. The fact

---

<sup>7</sup>For example, including terms up to order  $(p-2)^{10}$  in the fit we find that the coefficient of the linear term  $(p-2)$  converges to five decimal places.

<sup>8</sup>We have also found that the behaviour of the  $(p-2)^3$  term can be deduced in certain limits. For

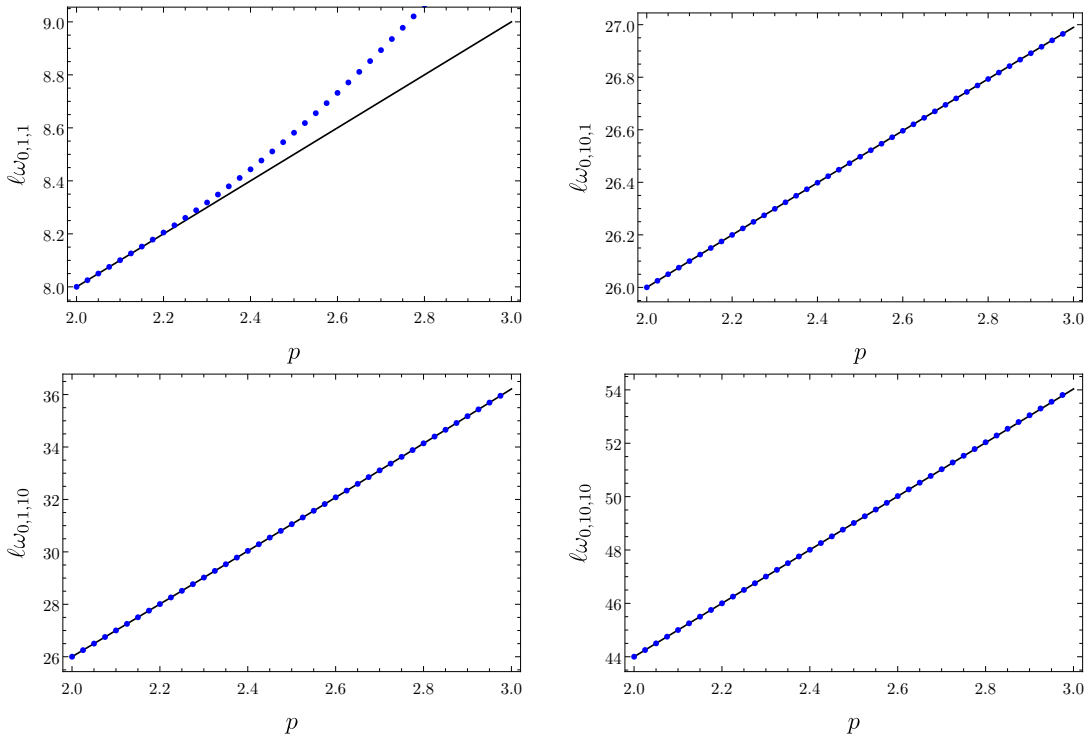


Figure 3.5: Here we compare the approximate form of fundamental mode (black line) against the numerically determined spectra (blue dots) over the range  $p \in (2, 3]$ . The plots show the cases  $n = 1, k = 1$  (top left),  $n = 1, k = 10$  (top right),  $n = 10, k = 1$  (bottom left) and  $n = 10, k = 10$  (bottom right). The plots indicate that the approximate form is valid over a larger range of  $p$  values as the value of  $n$  or  $k$  is made larger.

that the dependence of these terms on  $n$  and  $k$  appears so simple suggests that it may be possible to determine these corrections analytically, though we shall not pursue this any further.

In Figure 3.5, we compare the analytic approximation (3.120) with the numerical results for different values of  $n$  and  $k$ , over the interval  $p \in [2, 3)$ . While this range of  $p$  does not correspond to regular five-dimensional geometries, it does concisely summarize important information about this approximation. First, we see that the approximate form is quite accurate over this interval. Second, we note that the approximation does better for large values of  $n$  and  $k$ . The reason for this second fact seems to be the following. For large  $n$  or  $k$ , the coefficient of the quadratic term in

---

example, we have found that for  $n = 0$  the coefficient of this term is  $-3/(4k^2 - 1)$  while for  $k = 0$  the coefficient of this term is  $3/(2n + 1)^2$ . However, the functional form of the cubic term for general values of  $n$  and  $k$  has eluded us.

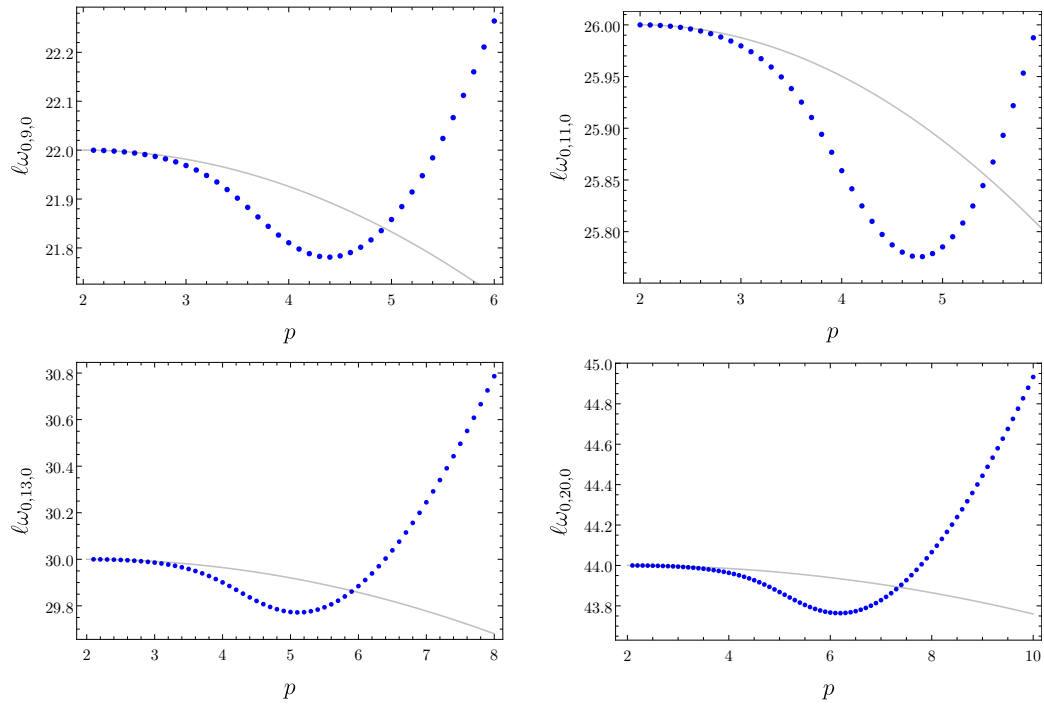


Figure 3.6: Plots of the frequencies vs.  $p$  for  $n = 0$  and  $k = 9, 11, 13$  and  $20$  (top left, top right, bottom left, bottom right, respectively). These plots highlight the fact that, for  $k > 2n^2 - n$ , it is possible for the eigenvalue to initially decrease as  $p$  increases. In all cases, the light gray line indicates the analytic approximation (3.120), while the blue dots indicate numerical data.

(3.120) behaves like  $1/n$  or  $1/k^2$ , respectively. This suggests that series (3.120) — if it is convergent — converges more rapidly for large values of these quantum numbers, or — if it is an asymptotic series rather than a convergent one — that the series approximates the true function for a large range of  $p$  values in this limit.

A careful analysis of the analytic approximation shows that the quadratic term is *negative* whenever  $k > 2n^2 - n$ . This leads to some interesting structure in the spectrum, but does not lead to any complex eigenvalues. Namely, we find that in some circumstances the eigenvalues can initially *decrease* as a function of  $p$ . However this behaviour is ultimately reversed when  $p$  becomes large — for sufficiently large  $p$ , the eigenvalues are monotonically increasing as a function of  $p$ , as we will discuss below. Examples are shown in Figure 3.6 for  $n = 0$  and different choices of  $k$ . For all values of  $k$  that we have explored, the shape of the eigenvalue curve as a function of  $p$  is qualitatively the same. At larger values of  $k$ , the ‘dip’ occurs at larger values of  $p$ . In all cases, the depth of the dip is rather small, and in no cases do the eigenvalues

come close to crossing through zero. In practice, we observe this effect for physical values of  $p$  only in the case  $n = 0$ . For  $n \neq 0$ , the small  $p \rightarrow 2$  approximation is less accurate for  $k > 2n^2 - n$ . Indeed, for any fixed values of  $n$  and  $k$ , the approximate form derived in the  $p \rightarrow 2$  limit will ultimately become bad when  $p$  is sufficiently large. Roughly, this occurs when the quadratic piece in the approximation dominates.

When  $p$  becomes sufficiently large compared to the quantum numbers  $n$  and  $k$ , the approximate form derived in the  $p \rightarrow 2$  limit fails to accurately capture the details of the spectrum. In this regime, we can make progress by understanding the solution of the radial equation in the limit of large  $p$ . Numerical experiments suggest that, when  $p \gg n, k$  the eigenvalues exhibit a linear dependence on  $p$ . This observation can be explained analytically. As described in Section 3.3.1, in the large  $p$  limit, there is a formal sense in which the geometry limits to the AdS soliton. The normal modes of the AdS soliton then govern the slope of the eigenvalues  $\omega_{N,k,n}$ . Explicitly, we have the following relation that holds for large  $p$ :

$$\frac{d\omega_{N,k,n}^{(p)}}{dp} = \alpha_{N,n} + \dots \quad \text{as } p \rightarrow \infty, \quad (3.121)$$

where the dots denote terms that are subleading as  $p \rightarrow \infty$ . Here  $\alpha_{N,n}$  are the normal modes of the AdS soliton which, unfortunately, cannot be determined analytically<sup>9</sup>. We tabulate in Section 3.10 the numerically determined values of these normal modes and overtones for several values of  $n$ . We also note that the WKB approximation gives a reasonably accurate approximation when  $N \gg n$ ,

$$\ell\alpha_{N,n} \approx \frac{2\sqrt{2}\pi^{3/2}}{\Gamma[1/4]^2} \left( N + \frac{1}{2} \right). \quad (3.122)$$

Note that the fact that the quantum number  $k$  is absent in the above expressions is result of neither an assumption nor a typo. There is an ‘emergent degeneracy’ that appears for sufficiently large  $p$  that eliminates any dependence on  $k$  in the leading expressions.

While (3.121) provides a good approximation for the slope, additional details are required to determine the intercept and thereby obtain a good approximation to the eigenvalues themselves, rather than just their slope. One simple — and surprisingly

---

<sup>9</sup>Strictly speaking,  $\alpha_{N,n}$  are the normal modes for the AdS soliton when the time coordinate is rescaled by a factor of 2 from the usual value.

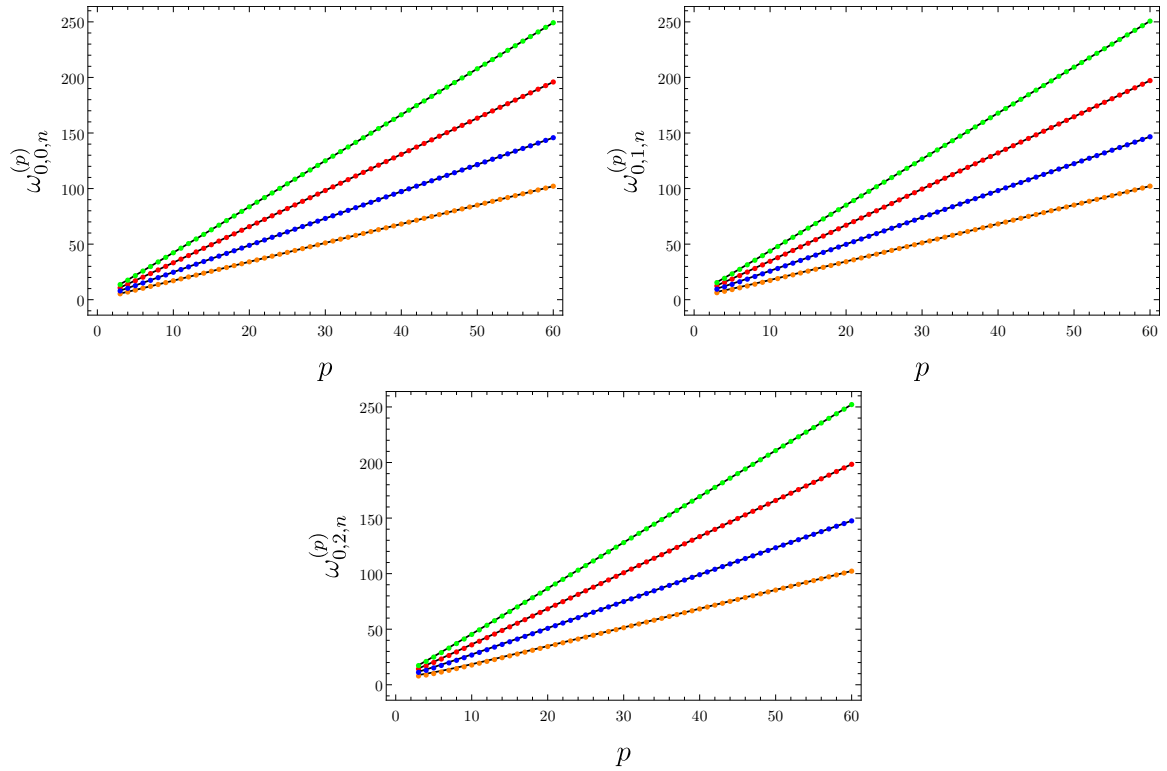


Figure 3.7: Plot of the fundamental mode for  $k = 0$  (top left),  $k = 1$  (top right), and  $k = 2$  (bottom). In all cases, the curves correspond to  $n = 0, 1, 2, 3$  in order from bottom to top (or, in colour order, orange, blue, red, and green). The solid black lines correspond to an analytic approximation to the curves, while the coloured discs correspond to the results of the numerical computation.

accurate — option is to combine this large  $p$  approximation with the fact that we know as  $p \rightarrow 2$  the eigenvalues approach  $2(2 + n + k + N)$ . Choosing the constant of integration to be such that the eigenvalues have this point as the intercept, we obtain the approximation:

$$\omega_{N,k,n}^{(p)} \approx (p - 2)\alpha_{N,n} + 2(2 + n + k + N). \quad (3.123)$$

This approximate form gives very good agreement with the numerically determined eigenvalues over the full range of physical  $p$  values, provided that  $n$  is sufficiently large. In this sense, one may consider (to a first approximation) that the normal modes of Eguchi-Hanson-AdS interpolate between the normal modes of  $\text{AdS}_5/\mathbb{Z}_2$  and the AdS soliton as the parameter  $p$  is varied.

A more accurate approximation can be obtained by carrying out the same series of steps that we followed in the  $p \rightarrow 2$  limit. That is, through a combination of numeric and analytic techniques, we can determine the next-to-leading order terms in the large  $p$  expansion. If instead we do this, we obtain the following:

$$\omega_{N,k,n}^{(p)} \approx p\alpha_{N,n} + \frac{n(2k + 1)}{\alpha_{N,n}} + \mathcal{O}(1/p). \quad (3.124)$$

We show this approximation for a few representative cases in Figure 3.7 for small values of  $n$ .

Despite the constant term being heuristically derived, the approximation (3.123) actually does a better job than one might naively expect, at least for the fundamental mode. One reason for this is the following. Though we have not been able to prove this behaviour analytically, we numerically observe that as  $n$  becomes large,  $\alpha_{0,n} \approx n$ . Therefore, in this limit, the large  $p$  approximation given in (3.123) approaches

$$\omega_{0,k,n}^{(p)} \approx 2(2 + n + k) + n(p - 2) \quad \text{for } n \rightarrow \infty. \quad (3.125)$$

If we compare this result with the large  $n \rightarrow \infty$  limit of the  $p \rightarrow 2$  approximation given in (3.120) we see that the two expressions are exactly the same. Therefore, the approximate forms derived in the  $p \ll n$  and  $p \gg n$  limits are identical. This explains why both approximate forms do better than expected for large values of  $n$ .

For the sake of completeness, we tabulate a number of the numerically determined

normal modes in Section 3.12.

### 3.7 Conclusions

Eguchi-Hanson-AdS solitons are conjectured to be the ground states for anti de Sitter gravity with lens space  $L(p, 1)$  boundary conditions at infinity, analogous to how the AdS soliton is the conjectured ground state for toroidal boundary conditions at infinity. In this manuscript, we have considered various aspects of Eguchi-Hanson-AdS<sub>5</sub> solitons. Our primary objective, which we have initiated here, is to understand to what extent these geometries are likely to be stable or not. In this sense, it is known [62] that under certain circumstances perturbations of the geometry may result in the formation of naked singularities. However, the precise mechanism underlying such an instability remains unknown. Since relatively little is understood about these geometries, our study here has focused on other related properties as well.

A key observation we have made concerns the relationship between the Eguchi-Hanson-AdS<sub>5</sub> solitons and the AdS soliton. We demonstrated that in the limit where the lens space  $L(p, 1)$  parameter  $p \rightarrow \infty$ , the geometry becomes identically equal to that of the AdS soliton, up to a rescaling of the time coordinate. This observation is more than a curiosity, as we have found here this allows one to obtain approximations for various quantities of interest in terms of those same quantities for the simpler AdS soliton geometry.<sup>10</sup>

We have studied the conserved quantities of the Eguchi-Hanson-AdS<sub>5</sub> solitons and constructed the extended first law of soliton mechanics. In doing so, we observe that these solitons possess a non-trivial thermodynamic volume, despite having vanishing entropy. Commensurate with a previous study of thermodynamic volume for asymptotically globally AdS<sub>5</sub> solitons [25], the source of this quantity is topological in nature, and has to do with the structure of the Killing potential in the vicinity of the bubble. It would be interesting to extend these observations for other examples of solitons, as it may allow for further elucidation of the role and interpretation of thermodynamic volume in gravitational thermodynamics.

---

<sup>10</sup>After the first version of this manuscript appeared, Edgar Shaghoulian brought to our attention [69], where the same observation was made for the partition functions of CFTs on lens spaces. Our result for the connection between Eguchi-Hanson-AdS and the AdS soliton could be inferred from these results.

We also considered the thermodynamics of Eguchi-Hanson-AdS<sub>5</sub> solitons in the canonical ensemble. After computing the on-shell action, we showed that for low temperatures the soliton dominates the canonical ensemble, while at higher temperature a Schwarzschild-AdS-type black hole with lens space horizon dominates. The phase transition between these two states is of the same type as studied for the toroidal AdS black hole and the AdS soliton first studied in [80].

We examined the geodesics of the Eguchi-Hanson-AdS<sub>5</sub> solitons, finding no evidence suggestive of instability such as trapping of null geodesics. However, the time-like geodesics exhibit oscillatory behavior analogous to geodesics in global AdS. Thus, an instability of the type shown in [52] for pure AdS may be present also for these solitons. Investigating this in more detail is something we hope to return to in the future.

Finally, we studied the separable solutions to the massless Klein-Gordon equation on this background. Via numerical and approximate analytical methods, we find a set of modes that oscillate, never decaying, analogous to AdS. We find no evidence of frequencies with a non-vanishing imaginary component. Using the WKB approximation, we have been able to study the separation between successive overtones, showing that it is well-approximated by the light-crossing time of the geometry by radial null geodesics. We have found it possible to understand the normal mode frequencies by piecing together two approximations. The first involves an analysis of the equation in the vicinity of the value  $p \rightarrow 2$ . While this does not correspond to a physical soliton solution, the radial equation in this limit reduces to that for AdS<sub>5</sub>/Z<sub>2</sub>, which admits analytic solutions. The second approximation involves the  $p \rightarrow \infty$  limit of the radial equation, which reduces to the wave equation on the AdS soliton. Joining the two approximations together gives a quite accurate approximation for the normal modes of the Eguchi-Hanson-AdS<sub>5</sub> solitons for any physical value of  $p$  in terms of a single parameter that must be numerically determined: the normal modes for the AdS soliton. In an approximate sense, one can then consider the normal modes of the Eguchi-Hanson solitons as interpolating between those of the orbifold AdS<sub>5</sub>/Z<sub>2</sub> and the AdS soliton.

There remain a number of areas for future investigation. First among these, along the lines of understanding potential mechanisms for instability, would be an understanding of the gravitational perturbations of the geometry. This task is simplified since the

solution is cohomogeneity-one, allowing for the techniques of [91] to be used. An understanding of these perturbations may hint toward the existence of ‘resonating’ solutions constructible as non-linear extensions of the normal mode solutions [92, 93]. It would furthermore be interesting to understand the implications of these geometries within the AdS/CFT correspondence, where they may be relevant for understanding aspects of confined phases of CFTs on lens space geometries [94, 95, 82]. It would also be interesting to understand the role of higher-curvature corrections for these geometries [96, 97, 98].

## Acknowledgements

We would like to thank Roberto Emparan, Edgar Shaghoulian, and Eric Woolgar for helpful discussions, comments, and correspondence. The work of RAH received the support of a fellowship from “la Caixa” Foundation (ID 100010434) and from the European Union’s Horizon 2020 research and innovation programme under the Marie Skłodowska-Curie grant agreement No 847648” under fellowship code LCF/BQ/PI21/11830027. HKK acknowledges the support of the NSERC Grant RGPIN-2018-04887. The work of TD and RBM was supported by the Natural Sciences and Engineering Research Council of Canada.

The lands on which Memorial University’s campuses are situated are in the traditional territories of the Beothuk, Mi’kmaq, Innu, and Inuit of the province of Newfoundland and Labrador. McMaster University is located on the traditional territories of the Mississauga and Haudenosaunee nations and within the lands protected by the “Dish with One Spoon” wampum agreement. University of Waterloo is situated on the traditional territory of the Neutral, Anishinaabeg and Haudenosaunee peoples.

## 3.8 Appendix A: Comparison of Komar Mass with Holographic Renormalization

In the main text, the mass was computed via the Komar approach which required the gauge fixing of the Killing potential. We chose a gauge for the Killing potential so that the Komar and Ashtekar-Magnon mass agree. This method of gauge fixing

is standard in black hole chemistry, and was first implemented in this fashion in [99] (see also [100]). In this section, we briefly compare this computation with holographic renormalization, and in particular map the choice of gauge to a choice of quadratic counterterms.<sup>11</sup>

Consider the following counterterm action,

$$I_{\text{ct}} = \frac{1}{8\pi G} \int d^4x \sqrt{h} \left[ \frac{3}{\ell} + \frac{\ell}{4} R + \ell^3 (\alpha_1 R^2 + \alpha_2 R_{ab} R^{ab} + \alpha_3 \chi_4) \right], \quad (3.126)$$

where  $\chi_4 = R_{abcd} R^{abcd} - 4R_{ab} R^{ab} + R^2$  is the Gauss-Bonnet density. This counterterm action includes the terms necessary to cancel all divergences coming from the bulk action and Gibbons-Hawking-York boundary terms. The quadratic terms included here are not necessary to cancel divergences. Nonetheless, these terms can have the effect of shifting the action by a solution-independent constant, as we will now show.

Without presenting details, the computation of the Euclidean action proceeds in exactly the same manner as discussed in the main text. Now, with the quadratic counterterms we arrive at the final result

$$I_{\text{E}} = -\frac{\pi a^4 \beta}{8\ell^2 p G} + \frac{3\pi \ell^2 \beta}{32pG} (1 + 96\alpha_1 + 32\alpha_2), \quad (3.127)$$

where the contributions from the quadratic counterterms are manifest. It is then a trivial matter to obtain the mass,

$$M = -\frac{\pi a^4}{8\ell^2 p G} + \frac{3\pi \ell^2}{32pG} (1 + 96\alpha_1 + 32\alpha_2), \quad (3.128)$$

$$= M_{\text{AM}} + \frac{3\pi \ell^2}{32pG} (1 + 96\alpha_1 + 32\alpha_2). \quad (3.129)$$

Here, in the second line, we have introduced  $M_{\text{AM}}$  which denotes the Ashtekar-Magnon mass computed in the main text. In the absence of the quadratic counterterms, the mass computed via holographic renormalization differs from the AM mass by a constant term,

$$M_0 = \frac{3\pi \ell^2}{32pG}. \quad (3.130)$$

---

<sup>11</sup>We thank the anonymous referee for encouraging us to elaborate on this connection.

This term has the same origin as the Casimir energy present for global AdS with spherical boundary — see e.g. [76]. By restricting to the family of quadratic counterterms

$$I_{\text{ct}}^{\text{quad}} = \frac{1}{8\pi G} \int d^4x \sqrt{h} \left[ \ell^3 \left( \alpha_1 R^2 - \left( \frac{1}{32} + 3\alpha_1 \right) R_{ab} R^{ab} + \alpha_3 \chi_4 \right) \right], \quad (3.131)$$

the  $M_0$  term can be eliminated and the mass computed via holographic renormalization agrees with the Ashtekar-Magnon mass. We can also identify the gauge ambiguity in the Komar mass (3.22) in terms of the coefficients of the quadratic counterterms introduced above. Comparing the mass computed via holographic renormalization with (3.22) we identify

$$C_1 = -\frac{a^4}{6} - \left( 6\alpha_1 + 2\alpha_2 + \frac{1}{16} \right) L^4. \quad (3.132)$$

We then see how the appropriate choice of quadratic counterterms described above yields the value of  $C_1$  chosen in the main text.

A few comments are in order. The main thing we have done here is to show how the gauge ambiguity in the Komar potential can be directly related to the coefficients of certain quadratic terms in the counterterm action. The relationship between the AM mass and holographic renormalization has been previously explored in certain cases [27, 101]. A term such as  $M_0$  is present only for even boundary dimensions. In odd boundary dimensions the Ashtekar-Magnon mass agrees with that mass computed via holographic renormalization using the standard counterterms. It would be interesting to perform a similar analysis for the Komar mass, in particular demonstrating how the gauge ambiguity is related to ambiguities in the counterterm action under more general circumstances.

### 3.9 Appendix B: Solution of the Radial Equation via the Shooting Method

In this section, we provide independent confirmation for the results obtained via the pseudospectral method. To this end, we consider the solution of the radial equation via the shooting method.

We construct two numerical solutions of the radial equation. One solution begins

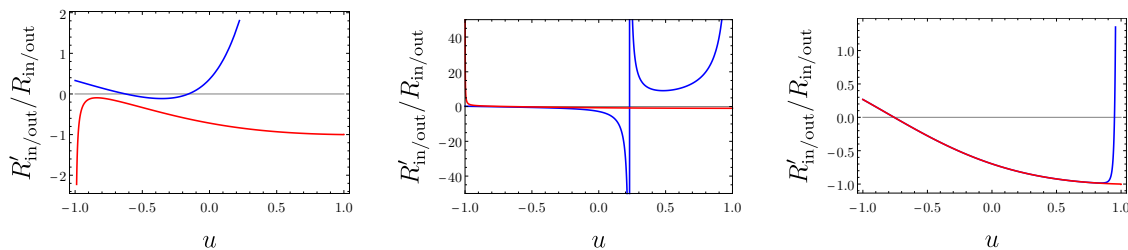


Figure 3.8: Plots of the logarithmic derivative of the numerical solutions. The blue curves correspond to solutions integrated from  $u = -1$ , while the red curves correspond to solutions integrated from  $u = +1$ . In this case, we have set  $p = 3$ ,  $n = 0$ ,  $k = 0$ . The plots correspond to  $\omega = 5.2, 5.4, 5.2985999$  in order of left to right.

near the bubble at  $r = a$ , using a power series solution of the differential equation in this neighbourhood to construct initial conditions, along with an initial guess for the eigenvalue  $\omega$ . This solution is integrated outward, toward  $r = \infty$ , using the standard built-in numerical methods of Mathematica. The second numerical solution proceeds in much the same way, but begins near the asymptotic boundary, and is integrated inward toward  $r = a$ .

The idea is simple: if  $\omega$  has been chosen correctly, then the solution must be everywhere regular, and moreover, the two numerical solutions should agree over the domain. However, since the equation is linear, and both  $R(r)$  and  $cR(r)$  for some constant  $c$  are equally valid solutions, it is not so simple to directly compare the solutions obtained by integrating from either end. (As there is no simple way to ensure consistent normalization from the different starting points.) Instead, we compare a logarithmic derivative,

$$\frac{R'_{\text{in/out}}}{R_{\text{in/out}}}, \quad (3.133)$$

of the numerical solutions at intermediate points. In this way, differences in the normalization of the solution can be eliminated. Matching of the logarithmic derivatives of the two numerically constructed solutions over the domain is taken to mean the correct value of  $\omega$  has been identified.

As the purpose of this method is to serve as independent confirmation of the pseudospectral results, we will not perform an exhaustive analysis here. Rather, we will present a few instances that demonstrate consistency of the two approaches.

We show in Figure 3.8 an example of how the process works. The graphs show the

logarithmic derivative of the solution over the domain  $u \in [-1, 1]$ . The blue curves are those solutions obtained by numerically integrating the equation beginning at  $u = -1$ , while the red curves are those solutions obtained by numerically integrating the equation beginning from  $u = +1$ . The three graphs correspond to three different choices of the eigenvalue  $\omega$ , while we have set  $p = 3$ ,  $n = 0$  and  $k = 0$  here. The pseudospectral method outputs a value  $\omega_{\text{PS}} = 5.2985999$  — this choice of  $\omega$  appears in the rightmost graph. The leftmost graph corresponds to the choice  $\omega = 5.2$ , while the center one corresponds to  $\omega = 5.4$ . For both cases shown where  $\omega$  is different from  $\omega_{\text{PS}}$ , the two solutions are clearly in disagreement. However, for the choice  $\omega = \omega_{\text{PS}}$  the curves are visually indistinguishable over much of the domain, except for very near the end points<sup>12</sup>. This is consistent with  $\omega = \omega_{\text{PS}}$  being the correct choice for a consistent solution.

It is also insightful to understand the difference in the in/out solutions as a function of  $\omega$ , to ensure that the implementation of the pseudospectral method is not missing certain overtones, or returning incorrect eigenvalues. To this end, it is useful to introduce an integrated residual. Of course, for any finite resolution, we expect that the numerical solution that begins from  $u = -1$  to blow up sufficiently close to  $u = +1$ , and vice versa for the solution that begins from  $u = +1$ . Therefore, an integrated residual should focus on an intermediate domain where both solutions can be expected to be accurate. For this, we (arbitrarily) choose  $u \in [-1/2, 1/2]$ . Another issue is the following. When  $\omega$  becomes larger than the fundamental frequency, the solution possesses a zero somewhere in the domain. (The number of zeros increases as  $\omega$  becomes larger than the various overtones). This leads to poles in the logarithmic derivative — see the center plot of Figure 3.8 for an example. To remedy this, it is convenient to work with an integrated *reciprocal* residual,

$$\text{Res}(\omega) = \int_{-1/2}^{1/2} \frac{du}{|\partial_u \log R_{\text{out}} - \partial_u \log R_{\text{in}}|}. \quad (3.134)$$

Viewed as a function of  $\omega$ , the residual  $\text{Res}(\omega)$  will peak when the difference between the two solutions tends to zero. We can identify those peaks as the values of  $\omega$  where a consistent solution exists.

We show a few representative examples in Figure 3.9. In these plots, the peaks

---

<sup>12</sup>Quantitatively, the difference in solutions is on the order of  $10^{-6}$  over the interval  $u \in [-1/2, 1/2]$ .

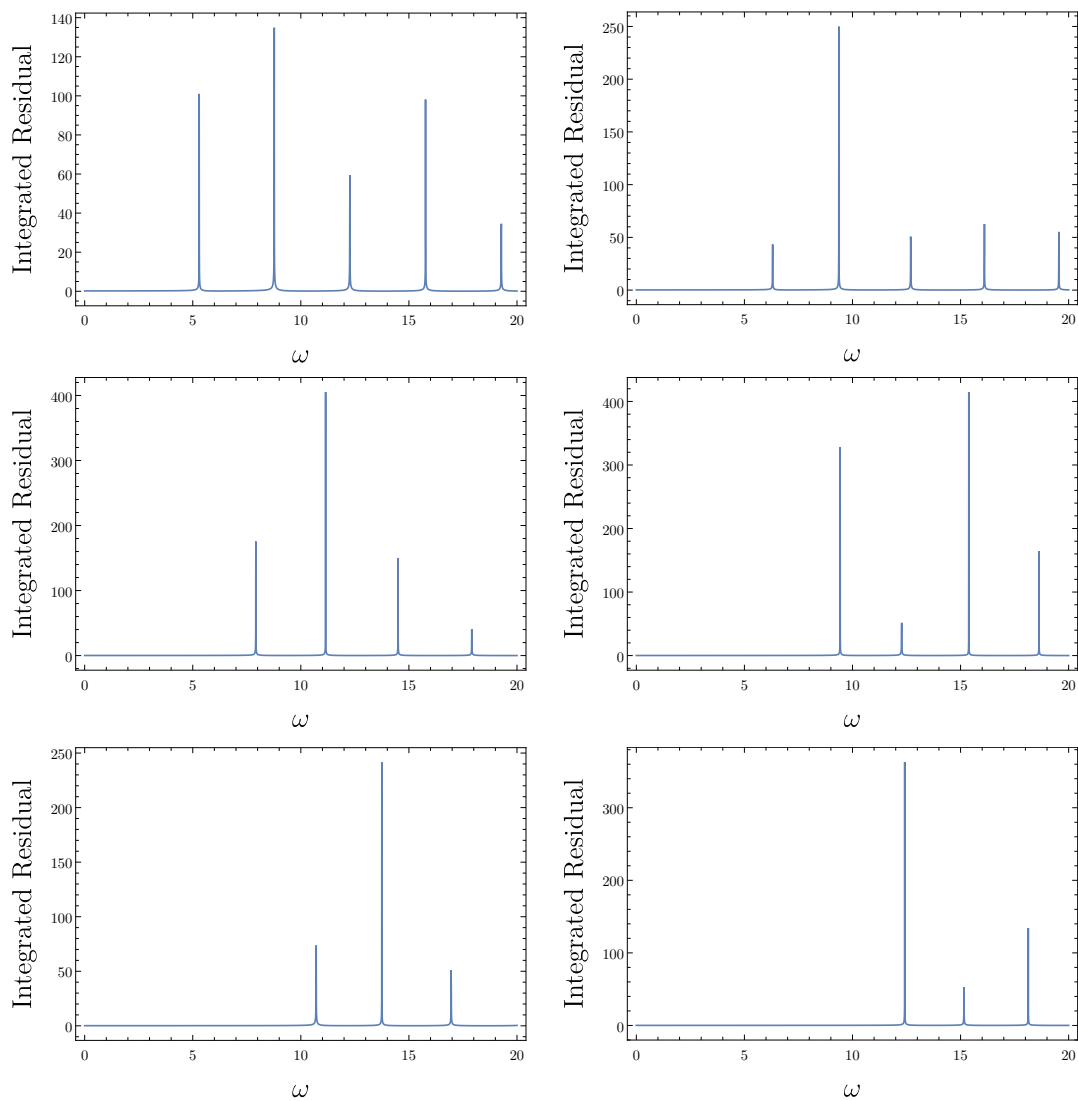


Figure 3.9: Plots of the integrated (reciprocal) residual for  $n = 1, 2, 3$  (first, second, and third rows, respectively) and  $k = 0, 1$  (first and second columns, respectively). In all cases,  $p = 3$  has been chosen. The reciprocal residual peaks at the values of  $\omega$  for which a consistent solution exists — the absolute heights of the peaks shown in the graphs is meaningless. In all cases, the peaks correspond precisely to those values of  $\omega$  determined via the pseudospectral method.

correspond to values of  $\omega$  for which the boundary value problem admits a sensible solution. In all cases, these peaks correspond exactly to those values of  $\omega$  obtained via the spectral method. No additional values of  $\omega$  have been obtained, and no errors have been determined.

### 3.10 Appendix C: Radial Equation at Large $p$ : Extracting the Slope of the Eigenvalues

As discussed in the numerical solution of the radial equation, it is fruitful to consider the radial equation for arbitrary values of  $p$ . In particular, we have discussed the numerical observation that the behaviour of the eigenvalue  $\omega$  rapidly becomes dominated at large  $p$  by a linear dependence. This fact can be explored in more detail, semi-analytically, to give a better understanding of that result.

Consider the radial equation (3.90) and perform the transformation

$$r = za, \quad (3.135)$$

which maps the domain to  $z \in [1, \infty)$ . After this transformation, the resulting equation is given by

$$0 = z(z^4 - 1) (4 + (p^2 - 4)z^2) R_p''(z) + (4 - (p^2 - 4)z^2 + 12z^4 + 5(p^2 - 4)z^6) R_p'(z) + 4z^3 \left[ -4k^2 - 2np - 4k(1 + np) + \frac{n^2 p^2 z^4}{1 - z^4} + \frac{(p^2 - 4)z^2 \ell^2 \omega^2}{4 + (p^2 - 4)z^2} \right] R_p(z), \quad (3.136)$$

where we have included the subscript  $p$  to reinforce that, here, we are thinking of this as an arbitrary constant parametrizing the solution.

Consider (3.136) in the limit where  $p$  is very large. Doing so, it becomes clear that the leading-order behaviour in each term behaves as  $\mathcal{O}(p^2)$ . Thus, a consistent possibility is for the dominant  $p$ -dependence of  $\omega$  to be such that

$$\omega \sim \frac{\alpha}{\ell} p \quad (3.137)$$

at large  $p$ .

We can extract the equation that governs this behaviour and determines  $\alpha$ . Rescale

$\omega = \alpha p$  and peel off the terms in the differential equation that behave as  $\mathcal{O}(p^2)$  at large  $p$ . For consistency of notation, let us call  $R_p(z)$  in this limit  $h_0(z)$ . Carrying this out, we find the following differential equation:

$$0 = (-1 + z^4)h_0''(z) + \frac{(-1 + 5z^4)}{z}h_0'(z) + 4\left(\frac{n^2 z^4}{1 - z^4} + \alpha^2\right)h_0(z). \quad (3.138)$$

By determining the values of  $\alpha$  for which regular solutions to the above equation exist, we can determine the large  $p$  slope of the eigenvalues  $\omega$ . Note that it is only the quantum number  $n$  ( $= m/p$ ) that enters into the equation, as  $k$  has no fixed dependence on  $p$ . Thus, the eigenvalues  $\alpha = \alpha_{N,n}$  are characterized by two numbers: the overtone  $N$  and the quantum number  $n$ . In other words, there is an ‘emergent degeneracy’ at large  $p$ : The eigenvalues for all choices of  $k$  are effectively the same, provided that  $p > k$  is sufficiently large.

Unfortunately, we have not been able to solve this problem analytically (the equation is of Heun type). However, it is straight-forward to apply the same pseudospectral numerical techniques to this problem. We do not repeat the basic set up of this problem, and proceed directly to the results.

Some selected values of  $\alpha_{N,n}$  are presented in Table 3.2. These have been computed using the pseudospectral method to the accuracy shown in the table. While there is not a clear, discernible pattern for smaller values of  $n$ , it is clear that when  $n$  becomes large we have  $\alpha_{N,n} \approx n$ . Unfortunately, it becomes increasingly expensive to perform the computations when  $n$  becomes very large. Computing  $\alpha_{N,n}$  to five decimal places requires a Chebychev discretization of more than 1000 points when  $n$  exceeds about 1000.

### 3.10.1 Subleading Terms in a Large $p$ Expansion

In the previous subsection, we have extracted a differential equation whose solution leads to the leading-order slopes of the eigenvalues  $\omega$  at large values of  $p$ . It is possible to do somewhat better than this, without encountering additional obstructions. To this end, we approach the problem as one in perturbation theory, expanding in the small parameter  $\rho = 1/p$ .

We begin by expanding the eigenvalue and the eigenfunction as a perturbative series

Values of $\alpha_{N,n}$			
$n$	$N$		
	0	1	2
0	1.70203	2.93798	4.15256
1	2.42243	3.61436	4.80816
2	3.25439	4.38480	5.54238
3	4.14123	5.21301	6.33085
4	5.05869	6.07883	7.15802
5	5.99504	6.97048	8.01368
6	6.94397	7.88064	8.89089
7	7.90176	8.80456	9.78483
8	8.86607	9.73904	10.69202
9	9.83533	10.68180	11.60991
10	10.80848	11.63122	12.53658
50	50.47989	50.98209	51.54973
100	100.38136	100.78145	101.23488
500	500.22318	500.45767	500.72385
1000	1000.17715	1000.36329	1000.57462

Table 3.2: A selection of numerically obtained  $\alpha_{N,n}$  values.

in  $\rho$ :

$$\rho^2 R_p(z) = h_0(z) + \rho h_1(z) + \rho^2 h_2(z) + \cdots, \quad (3.139)$$

$$\rho^2 \omega^2 = \alpha_{N,n}^2 + \rho \beta_1 + \rho^2 \beta_2 + \cdots. \quad (3.140)$$

These expansions are then inserted into the differential equation, and an expansion in powers of  $\rho$  is performed. In general, determining the corrections requires knowledge of both the eigenvalues and the eigenfunctions at previous orders. However, a happy accident at  $\mathcal{O}(\rho)$  allows for direct determination of  $\beta_1$ . The differential operator for  $h_1(z)$  is identical to that determining  $h_0(z)$ , allowing for all terms involving derivatives to be eliminated. The problem then reduces to an algebraic equation that determines  $\beta_1$ , with the result

$$\beta_1 = 2n(1 + 2k). \quad (3.141)$$

Unfortunately, at higher orders it does not appear to be possible to obtain analytic results for the corrections. While progress could be made numerically, the problem becomes more complicated. Therefore, it is not clear there is any benefit to pursuing this path further.

### 3.11 Appendix D: Eguchi-Hanson Solitons as $p \rightarrow 2$

Having fruitfully studied the large  $p$  limit of the Eguchi-Hanson soliton in the previous section, here we will consider the limit  $p \rightarrow 2$ . The limit should be taken at fixed cosmological scale  $\ell$ , so that the theory under consideration is not altered. To this end, we write  $a = \mathcal{A}\ell$  and consider the limit  $p \rightarrow 2$ . This is simple, and just results in  $\mathcal{A} \rightarrow 0$ . The resulting geometry is

$$ds^2 = -g(r)dt^2 + \frac{dr^2}{g(r)} + \frac{r^2}{4} [d\psi + \cos(\theta)d\phi]^2 + \frac{r^2}{4} d\Omega_2^2, \quad g(r) = 1 + \frac{r^2}{\ell^2}, \quad (3.142)$$

with  $\psi$  normalized to have period  $2\pi$ . The metric on the sections of constant  $(t, r)$  is that of the projective space  $\mathbb{S}^3/\mathbb{Z}_2$ . The analysis of the wave equation on this space is useful for understanding the normal modes of Eguchi-Hanson-AdS for smaller values of  $p$ .

### 3.11.1 Solution of the Radial Equation as $p \rightarrow 2$

While (regular) Eguchi-Hanson solitons exist only for integer  $p \geq 3$ , it is sensible from the mathematical point of view to study properties of the radial equation (3.90) without this restriction imposed on  $p$ . Within this line of thought, the case  $p = 2$  is special, since for  $p = 2$  the parameter  $a$  vanishes. That is, if we directly substitute  $p = 2$  into the radial equation, it reduces to the radial equation for a scalar field on AdS, but with a special choice  $m = 2n$  inherited from the fact that the limiting geometry is not globally  $\text{AdS}_5$ , but instead the quotient space  $\text{AdS}_5/\mathbb{Z}_2$ . In this special case, the equation can be solved directly.

Substituting  $p = 2$  into the radial equation we obtain,

$$0 = r^2(r^2 + L^2)R''(r) + r(3L^2 + 5r^2)R'(r) + L^2 \left( -4(k+n)(1+k+n) + \frac{L^2 r^2 \omega^2}{L^2 + r^2} \right) R(r). \quad (3.143)$$

After setting  $L = 1$ , the above equation has the following solution in terms of hypergeometric functions

$$R(r) = (1 + r^2)^{\omega/2} \left[ C_1 r^{2(-1-k-n)} {}_2F_1 \left( -1 - k - n + \frac{\omega}{2}, 1 - k - n + \frac{\omega}{2}, -2k - 2n, -r^2 \right) + C_2 r^{2(k+n)} {}_2F_1 \left( k + n + \frac{\omega}{2}, 2 + k + n + \frac{\omega}{2}, 2(1 + k + n), -r^2 \right) \right]. \quad (3.144)$$

Enforcing the boundary conditions proceeds in exactly the same manner as when studying the wave equation on AdS. To ensure regularity as  $r \rightarrow 0$  we must set  $C_2 = 0$ . Then expanding near  $r \rightarrow \infty$ , the behaviour is

$$R(r) \sim \frac{C_1 \Gamma[2(1+k+n)]}{\Gamma[2+k+n-\omega/2] \Gamma[2+k+n+\omega/2]} + \frac{C_1 [2(k+n) + \omega] \Gamma[2(1+k+n)]}{2r^2 \Gamma[1+k+n-\omega/2] \Gamma[2+k+n+\omega/2]} + \mathcal{O}(r^{-4}). \quad (3.145)$$

To obtain the proper fall off, we must have the first two terms vanish, so that the radial solution decays at  $\mathcal{O}(r^{-4})$ . Obviously, we cannot set  $C_1 = 0$ , since this results in the trivial solution. Therefore, we use the property of the gamma function that  $\Gamma[-N] = \infty$ . Then, taking  $\omega$  to be a positive quantity, we obtain the solution:

$$\omega_{N,k,n}^{(p=2)} = 2(2 + k + n + N). \quad (3.146)$$

Remarkably, this analytic result matches with numerical results, despite the fact that the limit  $p \rightarrow 2$  is in a sense singular<sup>13</sup>. Numerical indications suggest that the eigenvalues  $\omega$  of the radial equation have a well-defined limit as  $p \rightarrow 2$  with result the same as that given just above:

$$\omega_{N,k,n}^{p \rightarrow 2^+} = \omega_{N,k,n}^{(p=2)} = 2(2 + k + n + N) , \quad (3.149)$$

where  $N$  is the overtone. We initially deduced this form by inspection, computing numerically values of  $\omega$  as a function of  $p$  in the close vicinity of  $p = 2$  for several values of  $n$  and  $k$ .<sup>14</sup>

To highlight the convergence of the numerical scheme in the limit  $p \rightarrow 2$ , we include in Figure 3.10 relevant plots. The top row depicts the case  $n = 0, k = 0$  with  $p = 2 + 10^{-3}$ , while in the bottom row the case  $n = 1, k = 0$  is shown — the results for different parameters are qualitatively similar. The top left plot shows the numerically computed value for the fundamental frequency as a function of the number of points used in the Chebychev discretization. The result converges to (3.149) from above/below depending on whether the number of points is odd/even. In the top right plot, we show the difference between the numerical results computed with  $\mathcal{N}$  and  $\mathcal{N} + 1$  points. The plot shows clearly the convergence. The plots included in the bottom row illustrate how, for  $n \neq 0$ , convergence is much more rapid (this has been a general feature of all our analysis here; it is not particular to the  $p \rightarrow 2$  limit.)

Finally, in Figure 3.11, we illustrate the dependence of the eigenvalues on  $n$  and  $k$  as a function of  $p$  in the case when  $p \rightarrow 2$ . The left plot shows  $n = 1$  with the three curves corresponding to  $k = 0, 1, 2$  (bottom to top), while the right plot shows the same values of  $k$  now for  $n = 2$ . The structure of the curve is rather close to a linear dependence on  $p$ , but this is not as accurate as in the large  $p$  limit.

---

<sup>13</sup>Consider the behaviour in the vicinity of  $r = a$ . For  $p > 2$ , we have the behaviour

$$R(r) \sim (r - a)^{|n|/2} \quad (3.147)$$

while for  $p = 2$ , the behaviour is

$$R(r) \sim r^{2(k+|n|)} . \quad (3.148)$$

Obviously, there is a singular change in behaviour as  $p \rightarrow 2$  (i.e.  $a \rightarrow 0$ ), provided  $n, k \neq 0$ .

<sup>14</sup>For example, it is possible to obtain convergent results with the pseudospectral method for  $p = 2 + 10^{-5}$  with a Chebychev discretization of about 500 points.

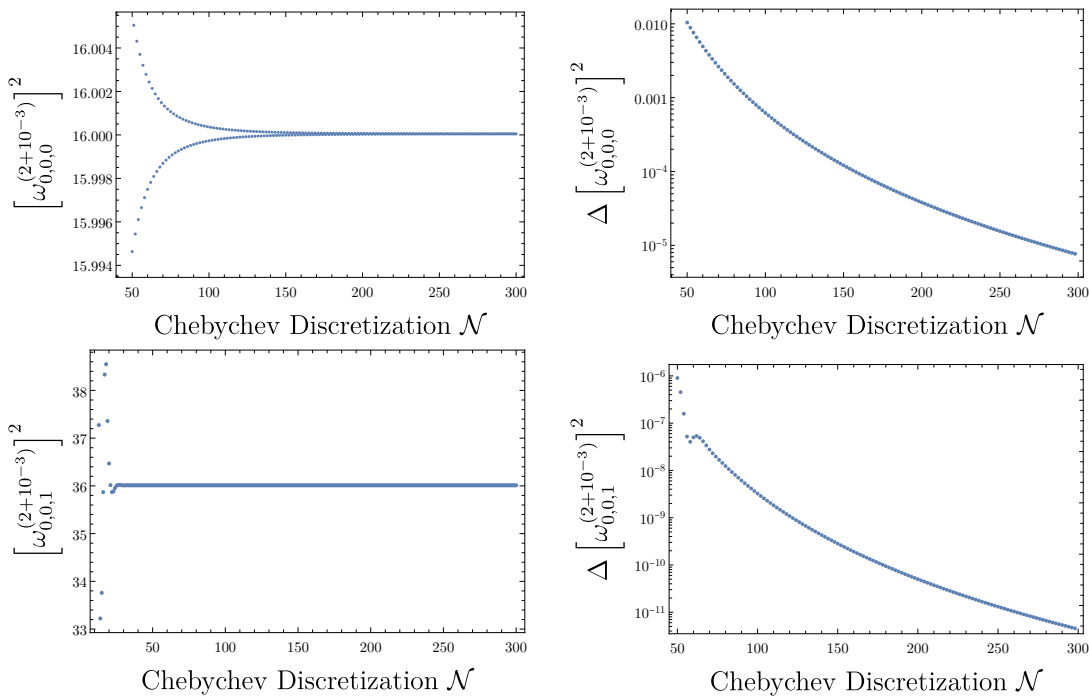


Figure 3.10: Top left: A plot of the lowest eigenvalue for  $n = 0$ ,  $k = 0$  and  $p = 2 + 10^{-3}$  as a function of the number of points  $\mathcal{N}$  used in the Chebychev discretization. The even and odd values of  $\mathcal{N}$  converge to the final result from opposite directions. Top right: A plot of the difference between the values of  $\omega$  determined for even and odd  $\mathcal{N}$  — it is clear that the difference is quite rapidly approaching zero as the number of points used in the discretization is increased, indicating convergence. At  $\mathcal{N} = 300$ , the value is  $\omega^2 = 16.000044$ , with even and odd discretizations differing at order  $10^{-6}$ . The bottom row shows the same information, but now for the  $n = 1$  mode. In this case, convergence is more rapid.

### 3.12 Appendix E: Tabulated Normal Mode Frequencies

Here we list the numerical values of the normal mode frequencies and the first eight overtones for  $p = 3, 4$  and  $5$  for  $0 \leq n \leq 5$  and  $0 \leq k \leq 5$ .

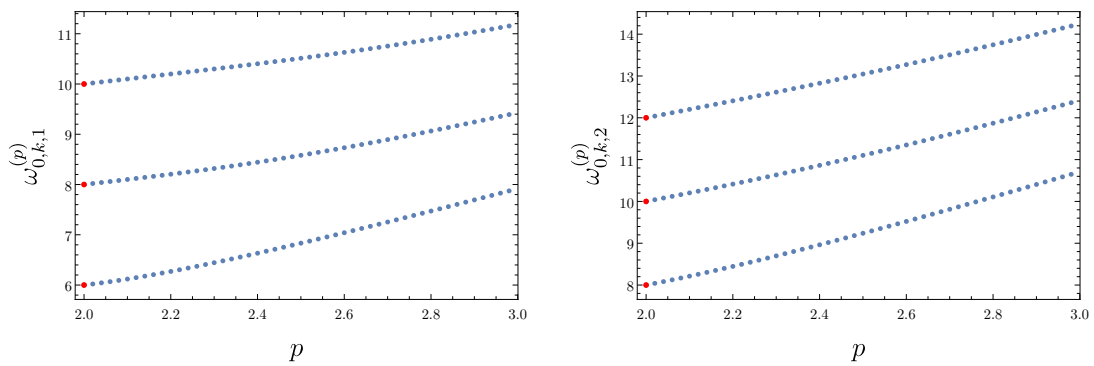


Figure 3.11: Left: a plot of  $\omega$  as a function of  $p$  near  $p = 2$  for  $n = 1$  and  $k = 0, 1, 2$ . The value of  $k$  increases vertically between the different curves. Right: a plot of  $\omega$  as a function of  $p$  near  $p = 2$  for  $n = 2$  and  $k = 0, 1, 2$ . The value of  $k$  increases vertically between the different curves. In all cases, the red dots at the far left indicate the value of  $\omega$  at  $p = 2$  determined via analytic calculations.

Selected Normal Modes for Eguchi-Hanson Solitons with $p = 3$									
$n$	$k$	$\ell\omega_{N,n,k}$							
0	0	5.29860	8.76887	12.26738	15.77064	19.27494	22.77952	26.28420	29.78891
0	1	6.30468	9.36992	12.69502	16.10285	19.54661	23.00934	26.48335	29.96461
0	2	7.92469	10.47381	13.51160	16.74837	20.07941	23.46252	26.87741	30.31310
0	3	9.82910	11.95092	14.65595	17.67462	20.85428	24.12706	27.45838	30.82877
0	4	11.84344	13.69088	16.06398	18.84279	21.84686	24.98695	28.21527	31.50380
0	5	13.88455	15.60829	17.68099	20.21454	23.03088	26.02396	29.13512	32.32874
1	0	7.91778	11.14589	14.49899	17.90981	21.35104	24.81006	28.28034	31.75819
1	1	9.42922	12.27359	15.38076	18.62934	21.95728	25.33320	28.74012	32.16812
1	2	11.18450	13.69814	16.53884	19.59402	22.78002	26.04869	29.37222	32.73377
1	3	13.06839	15.33579	17.92177	20.77130	23.79787	26.94192	30.16632	33.44760
1	4	15.01696	17.12117	19.48357	22.12918	24.98833	27.99678	31.11066	34.30082
1	5	16.99615	19.00469	21.18562	23.63863	26.32954	29.19684	32.19277	35.28387
2	0	10.70812	13.74673	16.95599	20.26005	23.62075	27.01752	30.43849	33.87643
2	1	12.41615	15.15809	18.13273	21.25980	24.48596	27.77830	31.11641	34.48725
2	2	14.24590	16.75210	19.50481	22.44836	25.52750	28.70191	31.94433	35.23645
2	3	16.14687	18.47772	21.03384	23.79816	26.72551	29.77380	32.91141	36.11579
2	4	18.08915	20.29630	22.68719	25.28394	28.06072	30.97927	34.00632	37.11648
2	5	20.05521	22.17902	24.43771	26.88344	29.51531	32.30412	35.21778	38.22946
3	0	13.57626	16.47128	19.55515	22.75613	26.03311	29.36154	32.72616	36.11706
3	1	15.38154	18.04874	20.92806	23.95921	27.09791	30.31357	33.58533	36.89890
3	2	17.25647	19.74496	22.44133	25.30787	28.30562	31.40240	34.57400	37.80273
3	3	19.17545	21.52829	24.06727	26.78005	29.63908	32.61474	35.68177	38.82033
3	4	21.12238	23.37482	25.78276	28.35616	31.08231	33.93772	36.89830	39.94336
3	5	23.08710	25.26671	27.56875	30.01910	32.62084	35.35928	38.21360	41.16357
4	0	16.48583	19.27040	22.24843	25.35576	28.55222	31.81198	35.11796	38.45854
4	1	18.34645	20.95265	23.75643	26.70864	29.77172	32.91802	36.12749	39.38560
4	2	20.25075	22.71605	25.36763	28.17479	31.10726	34.13883	37.24843	40.41971
4	3	22.18434	24.54022	27.06206	29.73690	32.54451	35.46273	38.47128	41.55312
4	4	24.13770	26.40968	28.82319	31.37983	34.07039	36.87869	39.78682	42.77817
4	5	26.10450	28.31272	30.63743	33.09049	35.67318	38.37654	41.18636	44.08744
5	0	19.41999	22.11767	25.00675	28.03092	31.15262	34.34625	37.59409	40.88356
5	1	21.31516	23.87006	26.61105	29.49631	32.49325	35.57697	38.72861	41.93395
5	2	23.23959	25.68024	28.29302	31.05090	33.92866	36.90416	39.95895	43.07815
5	3	25.18453	27.53459	30.03810	32.68119	35.44702	38.31775	41.27663	44.30901
5	4	27.14397	29.42265	31.83427	34.37546	37.03769	39.80841	42.67359	45.61964
5	5	29.11376	31.33639	33.67164	36.12358	38.69119	41.36761	44.14231	47.00348

Table 3.3: A selection of normal modes and their overtones for  $p = 3$ .

Selected Normal Modes for Eguchi-Hanson Solitons with $p = 4$									
$n$	$k$	$\ell\omega_{N,n,k}$							
0	0	6.93332	11.72096	16.48465	21.23594	25.98100	30.72257	35.46202	40.20008
0	1	7.60124	12.11154	16.76178	21.45093	26.15667	30.87111	35.59069	40.31358
0	2	8.78461	12.85744	17.30284	21.87462	26.50456	31.16608	35.84667	40.53964
0	3	10.30489	13.90214	18.08440	22.49536	27.01807	31.60343	36.22728	40.87641
0	4	12.03169	15.18497	19.07726	23.29755	27.68810	32.17741	36.72868	41.32121
0	5	13.88412	16.65214	20.25081	24.26344	28.50374	32.88095	37.34608	41.87064
1	0	10.24051	14.73250	19.33705	23.99139	28.67155	33.36672	38.07137	42.78236
1	1	11.51463	15.63997	20.03509	24.55669	29.14584	33.77494	38.42953	43.10133
1	2	13.01805	16.77399	20.92989	25.29093	29.76658	34.31176	38.90201	43.52302
1	3	14.67832	18.09221	21.99768	26.18007	30.52492	34.97130	39.48473	44.04451
1	4	16.44563	19.55760	23.21485	27.20908	31.41103	35.74686	40.17295	44.66234
1	5	18.28645	21.13971	24.55950	28.36294	32.41454	36.63116	40.96143	45.37263
2	0	13.83063	18.05755	22.48254	27.01100	31.59912	36.22446	40.87447	45.54163
2	1	15.36757	19.27010	23.47076	27.84021	32.31142	36.84779	41.42809	46.03928
2	2	17.02663	20.63114	24.60448	28.80398	33.14613	37.58225	42.08290	46.62951
2	3	18.77399	22.11310	25.86469	29.88939	34.09436	38.42154	42.83431	47.30889
2	4	20.58567	23.69313	27.23391	31.08382	35.14699	39.35901	43.67739	48.07369
2	5	22.44462	25.35262	28.69663	32.37531	36.29506	40.38791	44.60699	48.91994
3	0	17.55790	21.56648	25.82210	30.22019	34.70659	39.25103	43.83548	48.44859
3	1	19.23356	22.97093	27.01462	31.24942	35.60858	40.05209	44.55499	49.10106
3	2	20.98243	24.47698	28.31610	32.38580	36.61238	40.94854	45.36342	49.83637
3	3	22.78667	26.06675	29.71220	33.61852	37.70992	41.93430	46.25615	50.65094
3	4	24.63314	27.72554	31.19021	34.93744	38.89332	43.00329	47.22844	51.54105
3	5	26.51208	29.44134	32.73898	36.33320	40.15505	44.14953	48.27554	52.50291
4	0	21.36191	25.19187	29.29583	33.56898	37.95281	42.41246	46.92611	51.47943
4	1	23.12032	26.72433	30.63627	34.75182	39.00691	43.36073	47.78648	52.26597
4	2	24.92639	28.32918	32.05982	36.02062	40.14580	44.39074	48.72473	53.12633
4	3	26.76978	29.99453	33.55583	37.36661	41.36251	45.49695	49.73651	54.05703
4	4	28.64264	31.71054	35.11495	38.78177	42.65040	46.67401	50.81744	55.05453
4	5	30.53890	33.46910	36.72904	40.25880	44.00325	47.91671	51.96326	56.11529
5	0	25.21339	28.89566	32.86589	37.02311	41.30781	45.68286	50.12401	54.61483
5	1	27.02548	30.51774	34.31643	38.32580	42.48500	46.75368	51.10430	55.51758
5	2	28.87050	32.19326	35.83160	39.69815	43.73313	47.89463	52.15280	56.48605
5	3	30.74204	33.91404	37.40346	41.13315	45.04632	49.10086	53.26550	57.51693
5	4	32.63507	35.67325	39.02504	42.62444	46.41905	50.36769	54.43849	58.60695
5	5	34.54561	37.46519	40.69025	44.16628	47.84620	51.69068	55.66798	59.75290

Table 3.4: A selection of normal modes and their overtones for  $p = 4$ .

Selected Normal Modes for Eguchi-Hanson Solitons with $p = 5$									
$n$	$k$	$\ell\omega_{N,n,k}$							
0	0	8.60470	14.66629	20.66753	26.64481	32.61081	38.57065	44.52678	50.48049
0	1	9.11324	14.96233	20.87733	26.80748	32.74369	38.68298	44.62408	50.56631
0	2	10.05321	15.53752	21.29074	27.12989	33.00784	38.90668	44.81805	50.73752
0	3	11.31716	16.36255	21.89628	27.60647	33.40018	39.23985	45.10745	50.99326
0	4	12.80896	17.40204	22.67861	28.22944	33.91625	39.67973	45.49046	51.33228
0	5	14.45752	18.62026	23.62024	28.98940	34.55055	40.22285	45.96475	51.75293
1	0	12.62102	18.34009	24.16444	30.03559	35.93107	41.84070	47.75927	53.68385
1	1	13.78099	19.15265	24.78554	30.53704	36.35106	42.20180	48.07588	53.96567
1	2	15.14170	20.14934	25.56199	31.16994	36.88404	42.66161	48.47991	54.32587
1	3	16.65357	21.30438	26.48018	31.92650	37.52523	43.21697	48.96923	54.76291
1	4	18.27861	22.59355	27.52596	32.79821	38.26919	43.86428	49.54130	55.27497
1	5	19.98870	23.99529	28.68546	33.77618	39.11009	44.59954	50.19332	55.86000
2	0	17.02736	22.41656	28.02660	33.75054	39.53958	45.36902	51.22514	57.09976
2	1	18.48045	23.54323	28.93701	34.51085	40.19082	45.93785	51.72970	57.55290
2	2	20.04220	24.79302	29.96427	35.37729	40.93753	46.59272	52.31222	58.07710
2	3	21.68881	26.14828	31.09683	36.34228	41.77463	47.33009	52.97014	58.67048
2	4	23.40202	27.59345	32.32364	37.39823	42.69681	48.14618	53.70070	59.33097
2	5	25.16787	29.11511	33.63442	38.53767	43.69872	49.03708	54.50100	60.05635
3	0	21.62601	26.73381	32.13452	37.70106	43.36904	49.10308	54.88238	60.69395
3	1	23.23681	28.06247	33.25231	38.66034	44.20662	49.84506	55.54763	61.29643
3	2	24.91336	29.47653	34.45875	39.70509	45.12438	50.66151	56.28186	61.96287
3	3	26.64301	30.96426	35.74486	40.82877	46.11756	51.54890	57.08243	62.69125
3	4	28.41581	32.51548	37.10236	42.02508	47.18140	52.50364	57.94659	63.47945
3	5	30.22393	34.12150	38.52371	43.28799	48.31124	53.52215	58.87156	64.32526
4	0	26.33349	31.20580	36.41467	41.82709	47.37057	53.00282	58.69778	64.43856
4	1	28.03963	32.67149	37.68495	42.94117	48.35921	53.88953	59.50052	65.17118
4	2	29.78887	34.19866	39.02355	44.12449	49.41520	54.84053	60.36408	65.96115
4	3	31.57388	35.77939	40.42368	45.37162	50.53434	55.85255	61.28592	66.80645
4	4	33.38873	37.40685	41.87916	46.67746	51.71253	56.92233	62.26344	67.70499
4	5	35.22865	39.07512	43.38440	48.03724	52.94584	58.04671	63.29407	68.65470
5	0	31.10896	35.78320	40.81996	46.08697	51.50826	57.03751	62.64499	68.31085
5	1	32.87760	37.34615	42.20524	47.32327	52.62040	58.04577	63.56568	69.15707
5	2	34.67621	38.95485	43.64412	48.61614	53.78933	59.10958	64.53997	70.05460
5	3	36.50024	40.60382	45.13146	49.96119	55.01143	60.22602	65.56548	71.00152
5	4	38.34592	42.28828	46.66260	51.35432	56.28326	61.39222	66.63984	71.99588
5	5	40.21015	44.00411	48.23336	52.79171	57.60152	62.60539	67.76074	73.03575

Table 3.5: A selection of normal modes and their overtones for  $p = 5$ .

# Chapter 4

## Supersymmetric Asymptotically Locally $\text{AdS}_5$ Gravitational Solitons

This chapter is based on “Supersymmetric asymptotically locally  $\text{AdS}_5$  gravitational solitons” by Turkuler Durgut and Hari K. Kunduri, which is accepted in *Annals of Physics* 457, 169435 in July 2023.

### 4.1 Abstract

We construct supersymmetric gravitational soliton solutions of five-dimensional gauged supergravity coupled to arbitrarily many vector multiplets. The solutions are complete, globally stationary, 1/4-BPS and are asymptotically locally  $\text{AdS}_5$  with conformal boundary  $\mathbb{R} \times L(p, 1)$ . The construction uses an  $SU(2) \times U(1)$ -invariant ansatz originally used by Gutowski and Reall to construct supersymmetric asymptotically  $\text{AdS}_5$  black holes. A subset of these solutions have previously been obtained as supersymmetric limits of a class of local solutions of  $U(1)^3$  gauged supergravity found by Chong-Cvetič-Lu-Pope, and by Lucietti-Ovchinnikov in their classification of  $SU(2)$ -invariant solutions of minimal gauged supergravity.

## 4.2 Introduction

The Eguchi-Hanson-AdS<sub>5</sub>/Z<sub>p</sub> solution constructed by Clarkson and Mann is a globally static,  $U(1) \times SU(2)$ -invariant, geodesically complete vacuum solution of the Einstein equations with negative cosmological constant  $R_{ab} = -4\ell^{-2}g_{ab}$  [60, 61]. The geometry is not asymptotically globally AdS but rather to a freely acting discrete quotient of AdS<sub>5</sub>. It has a timelike conformal boundary  $\mathcal{I} = \mathbb{R} \times L(p, 1)$  where the lens space  $L(p, 1) \cong S^3/\mathbb{Z}_p$  with  $p \geq 3$ . The solution is therefore best interpreted as an asymptotically *locally* AdS<sub>5</sub> gravitational soliton. The underlying space is characterized by the presence of an  $S^2$  ‘bolt’ in the interior region. The solution has negative mass and is conjectured [62] to have the least mass amongst the space of metrics with the same conformal boundary, in much the same way that the classic AdS soliton, another vacuum solution of the Einstein equations with negative cosmological constant, is expected to have the least mass amongst all metrics with flat toroidal spatial sections on their conformal boundaries [58, 59].

Global AdS<sub>5</sub>, in addition to being the maximally symmetric vacuum solution (and the unique static spacetime with spherical spatial conformal boundary [?]) is also the unique maximally supersymmetric solution of five-dimensional gauged supergravity [102, 32]. In contrast the Eguchi-Hanson-AdS<sub>5</sub>/Z<sub>p</sub> soliton does not preserve any (local) supersymmetry. It is natural to expect, however, that it belongs to a larger family of solitons which carry charge and angular momenta, which could possibly contain supersymmetric members. Indeed, there are static, charged supersymmetric asymptotically locally AdS solitons with toroidal spatial conformal boundary [103]. As we discuss below, there are also supersymmetric solutions that are asymptotically locally AdS<sub>5</sub> in the sense that the spatial conformal boundary has topology  $S^1 \times S^2$  [104].

As a byproduct of their recent classification of supersymmetric solutions to five-dimensional minimal gauged supergravity with  $SU(2)$  symmetry, Lucietti and Ovchinnikov [40] constructed a family of  $U(1) \times SU(2)$ -invariant supersymmetric solitons asymptotic to AdS<sub>5</sub>/Z<sub>p</sub> for  $p \geq 3$  (the local solutions had been found earlier in the more general  $U(1)^3$  supergravity theory, but a global analysis was not carried out [41]). The main result of [40] was to establish a uniqueness theorem for  $SU(2)$ -invariant BPS AdS<sub>5</sub> black holes, namely, that the Gutowski-Reall family of solutions [31] exhaust the moduli space of this class of asymptotically globally AdS<sub>5</sub> BPS black holes.

This is a remarkable result, given the lack of uniqueness statements for AdS black holes in any dimension beyond the simple spherically symmetric setting. An analogous result for more general families of toric ( $U(1) \times U(1)$ -invariant) BPS AdS<sub>5</sub> black holes [38, 33] remains an open problem, although significant progress has been made in the direction [105]. A complete classification of classical BPS AdS<sub>5</sub> black hole solutions is motivated by the long standing problem to quantitatively reproduce the Bekenstein-Hawking entropy using the AdS/CFT correspondence (see the review [37] for details on the substantial progress made in recent years).

Analogous classification results for supersymmetric, horizonless soliton spacetimes remain to be addressed, although in minimal gauged supergravity, the situation for  $SU(2)$  symmetry is severely constrained [40]. The aim of the present work is to construct new  $SU(2) \times U(1)$ -invariant, supersymmetric and asymptotically locally AdS<sub>5</sub> soliton spacetimes of five-dimensional gauged supergravity coupled to an arbitrary number of vector multiplets (see (4.1) below). We will show how these solutions contain the regular solutions found in [40] (i.e. in a particular truncation of the theory when the scalar fields are constants and the Maxwell fields are set equal). In addition, we compute the conserved charges of these solutions and show that they have strictly negative mass, despite being supersymmetric and have equal and non-zero angular momenta in two independent planes of rotation. There is also a BPS relation that appears to depend on  $p$ .

Imposing the full set of regularity conditions on our general family of solutions is more difficult than in the minimal theory, for which there is only a single (zero-parameter) regular solution for fixed  $p$ . However, in the special case of  $U(1)^3$  gauged supergravity, we exhibit new explicit solutions which are indeed globally regular (local solutions of this type were constructed in [41] by taking supersymmetric limits of a family of local metrics, although a global analysis was not performed). The problem of whether there are asymptotically globally AdS<sub>5</sub> solitons within our class of solutions (that is, with  $p = 1$ ) remains open but we expect that there is enough freedom in the space of solutions to allow for this possibility.

Our local construction of these solutions is based upon a mild generalization of an  $SU(2) \times U(1)$ -invariant ansatz originally employed by Gutowski and Reall in their

novel construction of the first asymptotically AdS<sub>5</sub> BPS black holes of gauged supergravity coupled to an arbitrary number of vector multiplets [32]. Supersymmetric solutions of gauged supergravity (in regions where the supersymmetric Killing vector field is timelike) can be constructed in a systematic manner by choosing a four-dimensional Kähler ‘base space’ and then solving a set of coupled PDEs defined on this base space for various fields that are subsequently used to reconstruct the full spacetime metric, scalars, and Maxwell fields. In particular, for the class of solutions constructed in the present work, guided by the solutions of the minimal theory [40], we start from a natural  $SU(2) \times U(1)$ -invariant family of Kähler metrics and then, assuming the various geometric fields are themselves invariant under this symmetry, we can proceed in a systematic manner to construct a local family of cohomogeneity-one solutions parameterized by various integration constants. We then examine the regularity conditions required to extend the local metrics to globally regular, asymptotically locally AdS<sub>5</sub> solitons. Note that these solitons, like the Eguchi-Hanson soliton described above, are characterized by an  $S^2$  ‘bolt’. This is in contrast to the novel BPS solutions numerically constructed in [104], which have conformal boundary  $S^1 \times S^2$  and are of ‘NUT’ type (i.e. the spatial hypersurfaces have  $\mathbb{R}^4$  topology).

The gravitational solitons we construct are 1/4 BPS, as are all known asymptotically AdS<sub>5</sub> BPS black holes [33]. This should be contrasted with the asymptotically globally AdS<sub>5</sub> multi charged gravitational solitons we previously constructed [2] (special cases of these solutions were previously constructed in the minimal theory [39] and in  $U(1)^3$  supergravity [41]) which are 1/2-BPS and satisfy a simpler BPS relation which does not include an angular momentum term (see [41] for a discussion of BPS bounds in  $U(1)^3$  gauged supergravity). Those solutions are also cohomogeneity-one and  $SU(2) \times U(1)$ -invariant. However, in the standard decomposition for solutions admitting Killing spinors described above, the Kähler base is merely orthotoric and does not inherit the isometry group of the spacetime (this is related to the fact that the Killing spinor fields are not invariant under the symmetry [39]). As we demonstrated [2], this second class of solutions must possess an evanescent ergosurface [43], which strongly suggests that they are non-linearly unstable due to the stable trapping of null geodesics [45, 44]. For the class of solutions constructed in the present work, however, we find no evidence of such ergosurfaces.

The remainder of this note is organized as follows. Section 4.3 provides a concise review of the construction of supersymmetric solutions of  $U(1)^N$  gauged supergravity

and gives details on the derivation of the local solutions. We then impose regularity conditions to produce smooth soliton spacetimes and investigate the asymptotic behaviour of the solutions and compute the conserved charges. Finally we investigate some special subsets of solutions (in particular  $U(1)^3$  ‘STU’ gauged supergravity and minimal gauged supergravity) for which the regularity conditions can be solved explicitly. Section 4.4 concludes with a brief discussion.

## 4.3 Asymptotically locally $\text{AdS}_5$ supersymmetric solitons

### 4.3.1 Supersymmetric solutions to gauged supergravity

Here we briefly review the local construction of supersymmetric solutions to five-dimensional gauged supergravity coupled to  $N$  vector multiplets with scalars taking values in a symmetric space. The analysis was originally performed in [32] (see also [33] which uses the same mostly plus signature as used here). The bosonic sector of the theory is governed by the action

$$S = \frac{1}{16\pi} \int \left( R \star_5 1 - Q_{IJ} F^I \wedge \star_5 F^J - Q_{IJ} dX^I \wedge \star_5 dX^J - \frac{1}{6} C_{IJK} F^I \wedge F^J \wedge A^K + 2g^2 V \star_5 1 \right) \quad (4.1)$$

where the field content  $(g, F^I, X^I)$  consists of the spacetime metric,  $N$  Maxwell fields  $F^I = dA^I$  ( $I = 1 \dots N$ ) and the  $A^I$  are locally defined  $U(1)$  gauge fields, and  $N - 1$  real scalar fields which are conveniently parameterized by  $N$  real scalar fields  $X^I$  satisfying the constraint

$$\frac{1}{6} C_{IJK} X^I X^J X^K = 1. \quad (4.2)$$

The  $C_{IJK}$  are constants and as a tensor it is totally symmetric, i.e.  $C_{IJK} = C_{(IJK)}$  with  $I = 1 \dots N$  (their indices may be raised and lowered with a flat metric). The constant  $g$  appearing (4.1) is a constant which we will identify below with the inverse AdS length scale. A particular quadratic combination of scalar fields  $X^I$  that arises naturally is

$$X_I = \frac{1}{6} C_{IJK} X^J X^K. \quad (4.3)$$

In terms of these, the matrix of couplings  $Q_{IJ}$  appearing in the action is given by

$$Q_{IJ} = \frac{9}{2}X_I X_J - \frac{1}{2}C_{IJK}X^K. \quad (4.4)$$

The  $C_{IJK}$  are assumed to satisfy the following symmetric space condition

$$C_{IJK}C_{J'(LM}C_{PQ)K'}\delta^{JJ'}\delta^{KK'} = \frac{4}{3}\delta_{I(L}C_{MPQ)}. \quad (4.5)$$

We note that this condition is satisfied by the  $U(1)^3$  gauged supergravity theory that arises from compactification of Type IIB on  $S^5$ . More generally, in reductions of eleven-dimensional supergravity on a Calabi-Yau space  $Y$ , one obtains a five-dimensional ungauged supergravity theory in which the potential  $V$  above is the intersection form,  $X^I$  and  $X_I$  as defined above correspond to moduli parameterizing the size of two- and four-cycles, and  $C_{IJK}$  are the intersection numbers of  $Y$ . Gauging this theory leads to the theory (4.1). We refer the reader to [?] for further discussion.

For later use, we note that this can be rewritten explicitly as

$$C_{IJK}(C^{JLM}C^{KPQ} + C^{JLP}C^{KMQ} + C^{JLQ}C^{KMP}) = \delta_{IL}C_{MPQ} + \delta_{IM}C_{PQL} \\ + \delta_{IP}C_{QLM} + \delta_{IQ}C_{LMP}. \quad (4.6)$$

This condition ensures that  $Q_{IJ}$  has an inverse

$$Q^{IJ} = 2X^I X^J - 6C^{IJK}X_K, \quad (4.7)$$

where, as mentioned above, we make the identification  $C^{IJK} := C_{IJK}$ . This also allows us to invert for  $X^I$  in terms of the  $X_J$ :

$$X^I = \frac{9}{2}C^{IJK}X_J X_K, \quad (4.8)$$

which then implies

$$C^{IJK}X_I X_J X_K = \frac{2}{9}. \quad (4.9)$$

Finally the scalar potential is given by

$$V = 27C^{IJK}\bar{X}_I\bar{X}_J X_K, \quad (4.10)$$

where the  $\bar{X}_I$  are a set of constants (in the original work on constructing supersymmetric solutions of this theory, the  $V$  is expressed in terms of scalars  $V_I$  [32] which are proportional to  $\bar{X}_I$ ). As shown in [32], the vacuum AdS<sub>5</sub> background with radius  $\ell = 1/g$  corresponds to  $A^I \equiv 0$  and constant scalars  $X^I = \bar{X}^I$ , and

$$\bar{X}^I \equiv \frac{9}{2} C^{IJK} \bar{X}_J \bar{X}_K. \quad (4.11)$$

The special  $U(1)^3$  ‘STU’ supergravity theory which arises from the dimensional reduction of Type IIB on  $S^5$  corresponds to  $N = 3$ ,  $C_{IJK} = 1$  if  $(IJK)$  is a permutation of  $(123)$  and  $C_{IJK} = 0$  otherwise and  $\bar{X}^I = 1$ , or equivalently  $\bar{X}_I = 1/3$ . The symmetric space condition (4.5) holds automatically. For an explicit embedding of this theory into Type IIB supergravity, see [42].

Given a Killing spinor, one can show that there is a Killing vector field  $V$ , which is non-spacelike. In an open spacetime region where  $V^2 = -f^2 < 0$  so that  $f > 0$  for some function  $f$  one can introduce a local chart in which the metric can be decomposed as

$$ds^2 = -f^2(dt + \omega)^2 + f^{-1}h_{ab}dx^a dx^b, \quad (4.12)$$

where  $V = \partial/\partial t$ . Supersymmetry implies that the 4d metric  $h$  is Kähler with Kähler form  $J$ , and the orientation of the base space  $B$  is chosen so that  $J$  is anti self dual  $\star_4 J = -J$ . We choose the 5-form  $(dt + \omega) \wedge \text{dvol}(h)$  to be positively oriented in the full spacetime. In the following we summarize the necessary and sufficient conditions on the metric, Maxwell fields, and scalar fields to be a supersymmetric solution of the supergravity field equations [32]. We emphasize that apart from these two requirements, no further conditions have yet been made. In Section 2.2 below we will restrict attention to solutions that are invariant under  $SU(2) \times U(1)$  symmetry.

The Maxwell field can be expressed in the form

$$F^I = d[X^I f(dt + \omega)] + \Theta^I - 9gf^{-1}C^{IJK}\bar{X}_J X_K J, \quad (4.13)$$

where the  $\Theta^I$  are self-dual two-forms on  $B$ , and we must have

$$X_I \Theta^I = -\frac{2}{3}G^+, \quad (4.14)$$

and  $G^\pm$  is the (anti-)self dual two-form with  $\star_4 G^\pm = \pm G^\pm$ , defined as

$$G^\pm = \frac{1}{2}f(d\omega \pm \star_4 d\omega). \quad (4.15)$$

and  $\star_4$  refers to the Hodge dual with respect to  $(B, h)$ . This can be inverted so that

$$d\omega = f^{-1}(G^+ + G^-). \quad (4.16)$$

Since  $(B, h, J)$  is Kähler, we can define the Ricci two-form

$$\mathcal{R}_{ab} = \frac{1}{2}R_{abcd}J^{cd}. \quad (4.17)$$

Supersymmetry implies that  $\mathcal{R} = dP$  where  $P$  is the one-form

$$P = 3g\bar{X}_I(A^I - fX^I\omega). \quad (4.18)$$

This determines completely the function  $f$  as

$$f = -\frac{108g^2}{R}C^{IJK}\bar{X}_I\bar{X}_JX_K, \quad (4.19)$$

and the following condition holds

$$\mathcal{R} - \frac{R}{4}J = 3g\bar{X}_I\Theta^I. \quad (4.20)$$

All these conditions are necessary and turn out to be sufficient to guarantee and the existence of a supercovariantly constant spinor [32]. All the field equations are satisfied provided  $dF^I = 0$  (which is automatically true if we specify potentials), and the Maxwell equations

$$d(Q_{IJ}\star F^J) = -\frac{1}{4}C_{IJK}F^J \wedge F^K \quad (4.21)$$

are satisfied. The Bianchi identity and the Maxwell equation respectively reduce to the following equations on the base space

$$d\Theta^I = 9gC^{IJK}\bar{X}_Jd(f^{-1}X_K) \wedge J, \quad (4.22)$$

and

$$\begin{aligned} d \star_4 d(f^{-1} X_I) = & -\frac{1}{6} C_{IJK} \Theta^I \wedge \Theta^J + 2g \bar{X}_I f^{-1} G^- \wedge J \\ & + 6g^2 f^{-2} (Q_{IJ} C^{JM N} \bar{X}_M \bar{X}_N + \bar{X}_I X^J \bar{X}_J) d\text{vol}(h). \end{aligned} \quad (4.23)$$

### 4.3.2 Derivation of the local solution

In their original construction of  $SU(2) \times U(1)$ -invariant BPS black holes, Gutowski and Reall considered a natural ansatz in which the Kähler base itself is assumed to admit an isometric action of  $SU(2) \times U(1)$ , which is then naturally inherited by the full spacetime [32]. This is in contrast to the soliton solutions considered in our previous work [2] for which the full spacetime admits the full  $SU(2) \times U(1)$  symmetry group, but when decomposed into the form (4.12), the associated Kähler base is merely (ortho)toric.

We take as Kähler metric  $(h, J)$  the following  $SU(2) \times U(1)$ -invariant metric

$$\begin{aligned} h &= \frac{dr^2}{V(r)} + \frac{r^2}{4} (d\theta^2 + \sin^2 \theta d\phi^2) + \frac{r^2 V(r)}{4} (d\psi + \cos \theta d\phi)^2, \\ J &= d \left( \frac{r^2}{4} (d\psi + \cos \theta d\phi) \right) \end{aligned} \quad (4.24)$$

where  $V(r)$  is an arbitrary smooth function. The full  $SU(2) \times U(1)$  case is achieved if we choose  $\theta \in (0, \pi)$ ,  $\psi \in (0, 4\pi/p)$ ,  $\phi \in (0, 2\pi)$  where  $p \in \mathbb{N}$ . It is natural to write the metric in terms of the right-invariant one-forms

$$\sigma_1 = \sin \psi d\theta - \cos \psi \sin \theta d\phi, \quad \sigma_2 = \cos \psi d\theta + \sin \psi \sin \theta d\phi, \quad \sigma_3 = d\psi + \cos \theta d\phi \quad (4.25)$$

In particular the Kähler form is simply

$$J = d \left[ \frac{r^2}{4} \sigma_3 \right]. \quad (4.26)$$

The right-invariant 1-forms  $\sigma_i$  obey

$$d\sigma_i = -\frac{1}{2} \epsilon_{ijk} \sigma_j \wedge \sigma_k. \quad (4.27)$$

They are invariant under the ‘left-invariant’ Killing fields  $R_i$

$$\begin{aligned} R_1 &= -\cos\theta \cos\phi \partial_\phi - \sin\phi \partial_\theta + \frac{\cos\phi}{\sin\theta} \partial_\psi, \\ R_2 &= -\cot\theta \sin\phi \partial_\phi + \cos\phi \partial_\theta + \frac{\sin\phi}{\sin\theta} \partial_\psi, \\ R_3 &= \partial_\phi \end{aligned} \tag{4.28}$$

and in addition the particular quadratic combination of the  $\sigma_i$  appearing in  $h$  is invariant under the  $U(1)$  generator  $L_3 = \partial_\psi$ . The simplest spacetime solution resulting from this class of Kähler bases is  $\text{AdS}_5$  itself, which has  $p = 1$ , vanishing Maxwell fields  $F^I = 0$ , constant scalars  $X^I = \bar{X}^I$ , and

$$f = 1, \quad \omega = \frac{r^2}{2\ell} \sigma_3, \quad V = 1 + \frac{r^2}{\ell^2}. \tag{4.29}$$

where  $\ell = g^{-1}$  is the  $\text{AdS}_5$  length scale normalized so that  $R_{ab} = -4\ell^{-2}g_{ab}$ . For  $p > 1$ , one obtains an  $\text{AdS}_5$  orbifold, which is singular at the fixed point of the symmetry group at  $r = 0$ .

Returning to the general metric, the scalar curvature is determined by  $V(r)$  and its derivatives:

$$R_h = -\frac{8(V-1) + 7rV' + r^2V''}{r^2}, \tag{4.30}$$

and the Ricci form can be written

$$\mathcal{R} = d[P(r)\sigma_3], \tag{4.31}$$

with

$$P(r) = -\frac{1}{4}(rV' + 4(V-1)). \tag{4.32}$$

Choose now an orthonormal frame basis for  $(B, h)$

$$E^1 = \frac{dr}{\sqrt{V}}, \quad E^2 = \frac{rd\theta}{2}, \quad E^3 = \frac{r \sin\theta d\phi}{2}, \quad E^4 = \frac{r\sqrt{V}}{2}(d\psi + \cos\theta d\phi) \tag{4.33}$$

and an associated orthonormal frame for the spacetime:  $e^0 = f(dt + \omega)$ ,  $e^i = f^{-1/2}E^i$ . The Kähler form can be expressed as

$$J = E^1 \wedge E^4 - E^2 \wedge E^3 \tag{4.34}$$

which demonstrates that it is anti self dual, i.e.  $\star_4 J = -J$ . In order for the full spacetime to inherit the full  $SU(2) \times U(1)$  isometry, it is natural to search for solutions  $\omega$  of the form  $\omega = \omega_3(r)\sigma_3$ . We then have

$$d\omega = \frac{2\omega'_3}{r} E^1 \wedge E^4 - \frac{4\omega_3}{r^2} E^2 \wedge E^3, \quad \star_4 d\omega = \frac{2\omega'_3}{r} E^2 \wedge E^3 - \frac{4\omega_3}{r^2} E^1 \wedge E^4. \quad (4.35)$$

This gives

$$G^+ = rf [r^{-2}\omega_3]' (E^1 \wedge E^4 + E^2 \wedge E^3), \quad G^- = \frac{f}{r^3} [r^2\omega_3]' (E^1 \wedge E^4 - E^2 \wedge E^3) \quad (4.36)$$

which are manifestly self-dual and anti self-dual respectively. The Maxwell fields are also assumed to be invariant under  $SU(2) \times U(1)$ , which allows us to parameterize it in the form

$$A^I = X^I e^0 + U^I \sigma_3 \quad (4.37)$$

where the  $U^I = U^I(r)$  are smooth functions of  $r$  to be determined. The scalar fields are also assumed to be single-variable functions, namely  $X^I = X^I(r)$ . Now using (4.19) and (4.30) yields

$$f = \frac{108g^2 r^2 C^{IJK} \bar{X}_I \bar{X}_J X_K}{8(V-1) + 7rV' + r^2V''}. \quad (4.38)$$

The Maxwell fields are then

$$F^I = dA^i = d(X^I e^0) + \frac{dU^I}{dr} dr \wedge \sigma_3 - U^I \sigma^2 \wedge \sigma^3 \quad (4.39)$$

where  $\sigma^2 \wedge \sigma^3 = \sin\theta d\theta \wedge d\phi$ . Comparing this with the general formula for  $F^I$  (4.13) allows us to solve for the self-dual 2 forms  $\Theta^I$ . Taking the self dual and anti self dual parts of the resulting equation gives two conditions

$$\Theta^I = r \frac{d}{dr} \left( \frac{U^I}{r^2} \right) (E^1 \wedge E^4 + E^2 \wedge E^3), \quad (4.40)$$

$$\frac{f}{r^3} \frac{d}{dr} (r^2 U^I) = -9g C^{IJK} \bar{X}_J X_K. \quad (4.41)$$

These two equations are sufficient to guarantee that

$$d\Theta^I = 9g C^{IJK} \bar{X}_J d(f^{-1} X_K) \wedge J \quad (4.42)$$

which from (4.13) is equivalent to the Bianchi identity  $dF^I = 0$ . Now using (4.14) yields

$$f^{-1}X_I \frac{d}{dr} \left( \frac{U^I}{r^2} \right) = -\frac{2}{3} \frac{d}{dr} \left( \frac{w_3}{r^2} \right) \quad (4.43)$$

To make progress we will seek a solution for the scalars  $X_I$  of the same form as for the  $SU(2) \times U(1)$ -invariant BPS black holes [32]:

$$f^{-1}X_I = \bar{X}_I + \frac{q_I}{r^2}, \quad (4.44)$$

where the  $q_I$  are constants. This choice guarantees that in the asymptotic region  $r \rightarrow \infty$ ,  $X_I \rightarrow \bar{X}_I$  assuming that  $f \rightarrow 1$ , as expected for asymptotically locally  $\text{AdS}_5$  metrics. Using the constraints (4.2), (4.9) we find from (4.44) that

$$f = \frac{r^2}{[F(r)]^{1/3}}, \quad F(r) = r^6 + \alpha_2 r^4 + \alpha_1 r^2 + \alpha_0 \quad (4.45)$$

with

$$\alpha_0 = \frac{9}{2} C^{IJK} q_i q_J q_K, \quad \alpha_1 = \frac{27}{2} C^{IJK} \bar{X}_I q_J q_K, \quad \alpha_2 = \frac{27}{2} C^{IJK} \bar{X}_I \bar{X}_J q_K. \quad (4.46)$$

Using the assumption (4.44) we can integrate (4.41) to find

$$U^I = -\frac{9}{2} g C^{IJK} \bar{X}_J \left[ \frac{\bar{X}_K r^2}{2} + q_K \right] + \frac{U_0^I}{r^2} \quad (4.47)$$

where  $U_0^I$  are constants. We then integrate (4.43) to find

$$w_3 = \frac{g\alpha_2}{2} + \frac{g\alpha_1}{4r^2} + w_0 r^2 - \frac{3U_0^I \bar{X}_I}{2r^2} - \frac{U_0^I q_I}{r^4} \quad (4.48)$$

where  $w_0$  is another integration constant. Comparing this functional form to that of the minimal solution [40] suggests that generically  $U_0^I \neq 0$ . The integration constant  $w_0$  will be determined by imposing the Maxwell equation below. We now arrive at an explicit expression for  $\Theta^I$ :

$$\Theta^I = \left( \frac{9g C^{IJK} \bar{X}_J q_K}{r^2} - \frac{4U_0^I}{r^4} \right) (E^1 \wedge E^4 + E^2 \wedge E^4). \quad (4.49)$$

Substituting this into the condition (4.20) produces an ODE for  $V(r)$ :

$$-2r^2 + 2Vr^2 - \frac{3}{4}r^3V' - \frac{r^4V''}{4} = 2g^2\alpha_2r^2 - 12g\bar{X}_I U_0^I. \quad (4.50)$$

In the minimal theory, a general analysis of supersymmetric solutions was carried out in this symmetry class. It was shown that the soliton solutions (i.e. those with a ‘bolt’) must have a  $V(r)$  that has a simple zero at some  $r_0 > 0$  (the case of having an event horizon or a NUT solution corresponds allowing allowing  $r$  to reach zero with  $f$  vanishing or non vanishing respectively). We therefore assume  $V(r)$  takes the factorized form

$$V(r) = \frac{(r^2 - r_0^2)(a_0 + a_1r^2 + r^4g^2)}{r^4} \quad (4.51)$$

for some constants  $(r_0, a_0, a_1)$ . Inserting this form of  $V(r)$  into (4.50) imposes

$$a_1 = 1 + g^2r_0^2 + g^2\alpha_2 \quad (4.52)$$

$$a_0 = r_0^2(1 + g^2r_0^2 + g^2\alpha_2) - 6g\bar{X}_I U_0^I = r_0^2a_1 - 6g\bar{X}_I U_0^I. \quad (4.53)$$

The remaining necessary and sufficient requirement for a supersymmetric solution is the Maxwell equation (4.23). The left hand side is easily found to be

$$d \star_4 d(f^{-1}X_I) = \frac{2q_I V'}{r^3} = q_I \left( \frac{4g^2}{r^2} + \frac{4}{r^6}(-a_0 + a_1r^2) + \frac{8a_0r_0^2}{r^8} \right). \quad (4.54)$$

The right hand side is significantly more complicated, involving various products of the parameters  $U_0^I$  and  $q_I$ . We will not give it here, but simply note that it can be expressed as a sum of even powers of  $r$ . Satisfying the Maxwell equations then reduces to matching powers of  $r$  (from  $r^{-8}$  to  $r^0$ ). In particular, the left hand side has no constant term. This gives the condition

$$0 = \bar{X}_I(-16gw_0 + 8g^2) \quad (4.55)$$

which fixes the integration constant

$$w_0 = \frac{g}{2} = \frac{1}{2\ell}. \quad (4.56)$$

The  $r^{-2}$  coefficients agrees automatically and the  $r^{-4}$  condition is also automatically

satisfied, taking into account the identity

$$C_{IJK}C^{JLM}C^{KPQ}\bar{X}_Lq_M\bar{X}_Pq_Q = -\frac{1}{9}C_{IJK}\bar{X}^J C^{KMQ}q_Mq_Q + \frac{2\alpha_1}{27}\bar{X}_I + \frac{2\alpha_2}{27}q_I \quad (4.57)$$

which follows from the symmetric space condition. The  $r^{-6}$  and  $r^{-8}$  coefficients yield the following constraints:

$$(3\bar{X}_J U_0^J)q_I = 3C_{IJK}U_0^J C^{KMN}\bar{X}_Mq_N - (U_0^J q_J)\bar{X}_I, \quad (4.58)$$

$$a_0 r_0^2 q_I = -\frac{2}{3}C_{IJK}U_0^J U_0^K. \quad (4.59)$$

We will assume  $a_0, r_0 \neq 0$ . Define

$$u_0^3 := C_{IJK}U_0^I U_0^J U_0^K. \quad (4.60)$$

Then (4.59) imposes

$$u_0^3 = -\frac{3}{2}a_0 r_0^2 q_I U_0^I. \quad (4.61)$$

Finally (4.58) imposes

$$3(\bar{X}_L U_0^L)C_{IJK}U_0^J U_0^K = 3I - u_0^3 \bar{X}_I \quad (4.62)$$

where

$$I = C_{IJK}C^{KMN}C_{NPQ}U_0^J \bar{X}_M U_0^P U_0^Q. \quad (4.63)$$

Rewriting the symmetric space condition (4.5) as

$$C_{MKN} [C^{KIJ}C^{NPQ} + C^{KIP}C^{NJQ} + C^{KIQ}C^{NJP}] = \delta_{MI}C_{JPQ} + \delta_{MJ}C_{PQI} + \delta_{MP}C_{QIJ} + \delta_{MQ}C_{IJP}, \quad (4.64)$$

and contracting this with  $U_0^J \bar{X}_M U_0^P U_0^Q$  yields

$$3I = 3C_{MKN}C^{KIJ}C^{NPQ}U_0^P U_0^Q U_0^J \bar{X}_M = u_0^3 \bar{X}_I + 3(\bar{X}_L U_0^L)C_{IJK}U_0^J U_0^K. \quad (4.65)$$

This identity guarantees that the constraint (4.58) is satisfied. This exhausts the conditions imposed the Maxwell equation.

In summary, we have constructed a local supersymmetric solution that is parameterized by the integration constants  $U_0^I$  and the parameter  $r_0$ . These determine the

parameters  $q_I$  implicitly through (4.59), which reads

$$3 [r_0^2(1 + g^2 r_0^2 + g^2 \alpha_2) - 6g\bar{X}_K U_0^K] q_I = -2C_{IJK} U_0^J U_0^K \quad (4.66)$$

and recall  $\alpha_2$  depends linearly on the parameters  $q_I$ .

### 4.3.3 Global analysis and conserved charges

In the  $(t, r, \psi, \theta, \phi)$  coordinate system, the local metric is obviously analytic, and so any potential singularities will occur at the zero sets of  $f$  and  $V$  [40]. It turns out that in the minimal theory [105] the only regular case with  $f = 0$  corresponds to the BPS black hole solutions of [31] and we expect a similar conclusion will hold in the general gauged supergravity theory (4.1). From (4.45), we see  $f$  will vanish at  $r = 0$  provided  $\alpha_0 \neq 0$  (if we allow for  $f$  to vanish at  $r = 0$ , then one gets a ‘NUT’ type soliton provided  $V(0) = 1$  and  $V(r)$  is a smooth function of  $r^2$ , see e.g. the numerical solutions constructed in [104]). To obtain a soliton, we need that  $r \geq r_0$  with  $V(r_0) = 0$  and  $f(r_0) > 0$ . The geometries we have constructed are asymptotically locally AdS<sub>5</sub> in the sense that they are conformally compact with a timelike conformal boundary  $\mathcal{I} \cong \mathbb{R} \times S^3/\mathbb{Z}_p$ . This can be seen by introducing a new set of coordinates  $(T, R, \hat{\psi}, \theta, \phi)$  defined by

$$T = t, \quad \hat{\psi} = \psi - \frac{2}{\ell}t, \quad R = \sqrt{r^2 + \frac{\alpha_2}{3}}. \quad (4.67)$$

In the asymptotic region  $R \rightarrow \infty$ , the solutions take the manifestly static (locally) AdS<sub>5</sub> form

$$\begin{aligned} ds^2 = & - \left( 1 + \frac{R^2}{\ell^2} + O(R^{-4}) \right) dT^2 + O(R^{-2}) dt(d\hat{\psi} + \cos \theta d\phi) \\ & + \left( 1 + \frac{R^2}{\ell^2} + O(R^{-4}) \right)^{-1} dR^2 \\ & + \frac{R^2}{4} (1 + O(R^{-4})) \left( (d\hat{\psi} + \cos \theta d\phi)^2 + d\theta^2 + \sin^2 \theta d\phi^2 \right). \end{aligned} \quad (4.68)$$

The conformal boundary carries the metric

$$ds_4^2 = -dT^2 + \frac{\ell^2}{4} \left( (d\hat{\psi} + \cos \theta d\phi)^2 + d\theta^2 + \sin^2 \theta d\phi^2 \right) \quad (4.69)$$

Spatial sections are  $L(p, 1)$  with a round metric provided  $\theta \in (0, \pi)$  and the  $(\hat{\psi}, \phi)$  plane has the identifications  $(\hat{\psi}, \phi) \sim (\hat{\psi} + 4\pi/p, \phi)$  and  $(\hat{\psi}, \phi) \sim (\hat{\psi} + 2\pi, \phi + 2\pi)$ . Global  $\text{AdS}_5$  with conformal boundary  $\mathbb{R} \times S^3$  corresponds to  $p = 1$ . Regularity of the metric in the interior will impose restrictions on allowed values of  $p$ .

Possible singularities will occur at  $f = 0$  and  $V = 0$ . The former situation is characteristic of an event horizon (i.e. the non-spacelike supersymmetric Killing vector field  $\partial_t$  becomes null) which is necessarily degenerate. This will occur if the coordinate  $r$  ranges to  $r = 0$ . As our primary interest is in gravitational solitons, which are globally stationary, we will assume  $r_0 > 0$  and so  $V$  has one root and assume the parameters  $\alpha_i$  are chosen so that  $f > 0$  for all  $r \geq r_0$ . Thus the metric is defined on  $\mathbb{R} \times (r_0, \infty) \times L(p, 1)$ . At  $r = r_0$ , the Killing field  $\partial_\psi$  degenerates. In a neighbourhood of  $r = r_0$ , constant time slices have topology  $\mathbb{R}^2 \times S^2$  with  $r = r_0$  playing the role of the ‘origin of coordinates’ in the  $(r, \psi)$  plane. We may then compactify the interior region by adding an  $S^2$  at  $r = r_0$ , producing a smooth manifold without boundary. The region  $r \geq r_0$  is then geodesically complete (i.e. geodesics that reach  $r = r_0$  can be extended again to large values of  $r$ , as in the behaviour of geodesics near the origin in Euclidean space). Note that this is equivalent to requiring that the Kähler metric  $h$  has a smooth bolt at  $r = r_0$  where the Killing vector field  $\partial_\psi$  degenerates. Regularity of the spacetime metric (removal of Dirac-Misner strings) requires that  $\omega(\partial_\psi) = 0$  or equivalently  $\omega_3(r_0) = 0$ . This imposes the constraint

$$u_0^3 = 3a_0 r_0^6 \left[ -\frac{g\alpha_2}{4} - \frac{g\alpha_1}{8r_0^2} - \frac{gr_0^2}{4} + \frac{3\bar{X}_I U_0^I}{4r_0^2} \right]. \quad (4.70)$$

This guarantees that  $\omega$  vanishes as  $O(\rho^2)$  where  $\rho = \sqrt{r - r_0}$ . Assuming that  $\psi$  is identified with period  $4\pi/p$ , smoothness at the fixed point of  $\partial_\psi$  at  $r = r_0$  requires

$$p = \frac{r_0 V'(r_0)}{2} = a_1 + \frac{a_0}{r_0^2} + g^2 r_0^2 \quad (4.71)$$

To see this, note that the spatial geometry near the bolt ( $\rho^2 = r - r_0 \rightarrow 0$ ) is

$$\begin{aligned} h &= \frac{4d\rho^2}{V'(r_0)} + \frac{r_0^2 V'(r_0) \rho^2}{4} (d\psi + \cos\theta d\phi)^2 + \frac{r_0^2}{4} (d\theta^2 + \sin^2\theta d\phi^2) \\ &= \frac{4}{V'(r_0)} \left( d\rho^2 + \frac{r_0^2 V'(r_0)^2}{16} \rho^2 (d\psi + \cos\theta d\phi)^2 \right) + \frac{r_0^2}{4} (d\theta^2 + \sin^2\theta d\phi^2) \end{aligned} \quad (4.72)$$

Thus smoothness as  $\rho \rightarrow 0$  requires that  $\tilde{\psi} := r_0 V'(r_0)/4\psi$  be identified with period  $2\pi$ . However, since  $\psi \sim \psi + 4\pi/p$ , we arrive at (4.71). We then obtain

$$a_0 = r_0^2 p - a_1 r_0^2 - g^2 r_0^4 \quad (4.73)$$

and using (4.53) gives

$$a_1 = \frac{1}{2} [p - g^2 r_0^2] + \frac{3g \bar{X}_I U_0^I}{r_0^2} \quad (4.74)$$

and using the formula for  $a_1$  (4.52) we find

$$g^2 \alpha_2 = \frac{1}{2} \left[ p - 2 - 3g^2 r_0^2 + \frac{6g \bar{X}_I U_0^I}{r_0^2} \right] \quad (4.75)$$

which allows us to solve for  $a_0$ :

$$a_0 = \frac{r_0^2}{2} \left[ p - g^2 r_0^2 - \frac{6g \bar{X}_I U_0^I}{r_0^2} \right]. \quad (4.76)$$

This then determines  $q_I$  via (4.59) totally in terms of the integration constants  $U_0^I$ ,  $p \in \mathbb{N}$  and  $r_0$ . With the symmetric space condition we find

$$\alpha_1 = \frac{8(\bar{X}_I U_0^I) u_0^3}{a_0^2 r_0^4}. \quad (4.77)$$

Subbing this back into (4.70) gives, using (4.61)

$$-\frac{3}{2} a_0 r_0^2 q_I U_0^I = -3a_0 r_0^4 \left[ \frac{g r_0^4}{4} - \frac{3}{4} \bar{X}_I U_0^I + \frac{g(\bar{X}_I U_0^I) u_0^3}{a_0^2 r_0^4} + \frac{g}{4} r_0^2 \alpha_2 \right]. \quad (4.78)$$

This produces is a complicated constraint between  $(U_0^I, r_0, p)$  which should determine the allowed values of  $p$ . We therefore expect smooth soliton solutions with one discrete parameter  $p$  and  $N - 1$  continuous parameters. We have been unable to analyze all solutions to (4.78) in generality. We will proceed below by looking at the special case of the  $U(1)^3$  supergravity, and in particular, the special case of minimal supergravity which arises when the three gauge fields are set equal.

Before doing so, however, we may compute the asymptotic conserved charges associated to our general family of solutions. We emphasize that in general we have not addressed existence of an open set in the space of parameters that actually satisfy

the regularity conditions. To compute the mass, it is convenient to use the Ashtekar-Magnon prescription [?], which assigns a conserved charge to a spacetime with a Killing vector field. To compute the mass, we use the timelike Killing vector field  $\partial_T$  that is non-rotating at infinity. The asymptotic fall-off of the Weyl tensor in the coordinate chart (4.67) as  $R \rightarrow \infty$  is

$$C_{RTR}^T = \frac{1}{R^6} \left[ -4r_0^4 \left( 1 + \frac{r_0^2}{\ell^2} \right) + 2\ell^2 \alpha_2 \left( 1 - \frac{2r_0^4}{\ell^4} \right) + 3\alpha_1 + \frac{4\alpha_0}{\ell^2} + 6\ell U_0^I \bar{X}_I \left( 3 + \frac{4r_0^2}{\ell^2} \right) + \frac{16U_0^I q_I}{\ell} \right] + O(R^{-8}) \quad (4.79)$$

which yields the mass after a suitable rescaling by the conformal boundary defining function and an integration over  $L(p, 1)$  spatial boundary at infinity (see [2] for details of a similar computation)

$$\mathbf{M}_{\text{AD}} = \frac{\pi}{8p} \left[ -4x^2 \ell^2 (1 + x) + 2\alpha_2 (1 - 2x^2) + \frac{3\alpha_1}{\ell^2} + \frac{4\alpha_0}{\ell^4} + \frac{6U_0^I \bar{X}_I}{\ell} (3 + 4x) + \frac{16U_0^I q_I}{\ell^3} \right] \quad (4.80)$$

where we have defined the dimensionless parameter  $x := r_0^2/\ell^2$  which is a rough measure of the radius of the  $S^2$  bubble in AdS length units. The angular momentum, computed using a Komar integral with respect to  $-\partial_\psi$  gives<sup>1</sup>

$$\begin{aligned} \mathbf{J} &= \frac{1}{16\pi} \int_{L(p,1)} \star d[g(-\partial_\psi, \sim)] \\ &= \frac{\pi \ell^3}{p} \left[ \frac{1}{8\ell^6} (2\alpha_0 + \alpha_1 \ell^2) - \frac{x^2 \alpha_2}{4\ell^2} + \frac{U_0^I q_I}{\ell^5} + \frac{3U_0^I \bar{X}_I}{4\ell^3} (1 + 2x) - \frac{x^2}{4} (1 + x) \right]. \end{aligned} \quad (4.81)$$

The angular momentum associated to the spatial Killing field  $\partial_\phi$  vanishes identically. The soliton spacetime therefore has equal angular momenta with respect to two orthogonal planes of rotation at infinity. The soliton also carries electric charge defined by

$$\mathbf{Q}_I := \frac{1}{8\pi} \int_{L(p,1)} Q_{IJ} \star F^J, \quad (4.82)$$

where the integral is taken over the conformal boundary as  $R \rightarrow \infty$  on a spatial

---

<sup>1</sup>the sign in the prefactor follows the convention used in [32].

hypersurface defined by  $t = T = \text{constant}$ . A computation gives

$$\star F^I = -f^{-2} \star_4 d(X^I f) + e^0 \wedge (X^I f \star_4 d\omega + \Theta^I + 9f^{-1} g C^{IJK} \bar{X}_J X_K J). \quad (4.83)$$

As  $R \rightarrow \infty$ , we find that, pulled back to an  $R = \text{constant}$ ,  $T = \text{constant}$  surface, as  $R \rightarrow \infty$

$$\begin{aligned} \star F^I = & \left( -\frac{9}{8\ell^2} C^{IJK} q_J q_K - \frac{U_0^I}{2\ell} + \frac{3}{4\ell} U_0^J \bar{X}_J \bar{X}^I + \frac{\alpha_1 \bar{X}^I}{8\ell^2} + \frac{\alpha_2 \bar{X}^I}{4} \right. \\ & \left. - \frac{9}{4} C^{IJK} \bar{X}_J q_K - \frac{9\alpha_2}{2\ell^2} C^{IJK} \bar{X}_J q_K + O(R^{-2}) \right) \sin \theta d\psi \wedge d\theta \wedge d\phi \end{aligned} \quad (4.84)$$

and clearly as  $R \rightarrow \infty$ ,  $Q_{IJ} = \frac{9}{2} \bar{X}_I \bar{X}_J - \frac{1}{2} C_{IJK} \bar{X}^K + O(R^{-2})$ . This leads to global electric charges

$$\begin{aligned} \mathbf{Q}_I = & \frac{2\pi}{p} \left[ \frac{3}{2} \left( -\frac{\alpha_1}{8\ell^2} - \frac{3U_0^K \bar{X}_K}{4\ell} - \frac{3\alpha_2 \bar{X}^J q_J}{\ell^2} + \frac{\alpha_2^2}{2\ell^2} \right) \bar{X}_I + \frac{3}{8} \left( 1 + \frac{2\alpha_2}{\ell^2} \right) q_I \right. \\ & \left. + \frac{C_{IJK} \bar{X}^J U_0^K}{4\ell} + \frac{9}{16\ell^2} C_{IJK} \bar{X}^J C^{KMN} q_M q_N \right]. \end{aligned} \quad (4.85)$$

A considerable simplification arises if one considers the ‘total charge’

$$\bar{X}^I \mathbf{Q}_I = \frac{\pi}{p} \left[ \frac{\alpha_1}{8\ell^2} + \alpha_2 \left( \frac{1}{4} - \frac{\alpha_2}{\ell^2} \right) + \frac{3U_0^I \bar{X}_I}{4\ell} \right]. \quad (4.86)$$

We now turn to studying the existence of solutions which satisfy all the regularity conditions. The above regularity condition (4.78) is difficult to analyze in the general multicharge theory. We will focus on the standard  $U(1)^3$  supergravity theory obtained by dimensional reduction of a truncation of Type IIB supergravity on  $S^5$ . We take  $I = i = 1, 2, 3$  and  $\bar{X}_i = 1/3$ ,  $\bar{X}^i = 1$ . The constants  $C_{ijk} = |\epsilon_{ijk}| = 1$  if  $(i, j, k)$  are a permutation of 1, 2, 3 and zero otherwise. We set  $\mathbf{q}_i := 3q_i$ . Using these relations one finds  $\alpha_0 = \mathbf{q}_1 \mathbf{q}_2 \mathbf{q}_3$ ,  $\alpha_1 = \mathbf{q}_1 \mathbf{q}_2 + \mathbf{q}_2 \mathbf{q}_3 + \mathbf{q}_1 \mathbf{q}_3$ ,  $\alpha_2 = \mathbf{q}_1 + \mathbf{q}_2 + \mathbf{q}_3$  and hence

$$f^{-3} = \left( 1 + \frac{\mathbf{q}_1}{r^2} \right) \left( 1 + \frac{\mathbf{q}_2}{r^2} \right) \left( 1 + \frac{\mathbf{q}_3}{r^2} \right). \quad (4.87)$$

We have from (4.59) that

$$\mathbf{q}_1 = -\frac{4U_0^2 U_0^3}{a_0 r_0^2} \quad (4.88)$$

and similar expressions for  $\mathbf{q}_2, \mathbf{q}_3$ . The remainder of the solution is then explicitly given by

$$\omega_3 = \frac{g}{2} \sum_i \mathbf{q}_i + \frac{g}{4r^2} (\mathbf{q}_1 \mathbf{q}_2 + \mathbf{q}_1 \mathbf{q}_3 + \mathbf{q}_2 \mathbf{q}_3) + \frac{gr^2}{2} - \frac{1}{2r^2} \sum_i U_0^i + \frac{4U_0^1 U_0^2 U_0^3}{a_0 r_0^2 r^4} \quad (4.89)$$

$$A^1 = \left(1 + \frac{\mathbf{q}_1}{r^2}\right)^{-1} (dt + w_3(d\psi + \cos \theta d\phi)) - \left(\frac{g}{2} (r^2 + \mathbf{q}_2 + \mathbf{q}_3) + \frac{U_0^1}{r^2}\right) (d\psi + \cos \theta d\phi) \quad (4.90)$$

$$X^i = \left[f \left(1 + \frac{\mathbf{q}_i}{r^2}\right)\right]^{-1} \quad (4.91)$$

with similar expressions for  $A^2, A^3$  with the obvious permutations of the charge parameters  $\mathbf{q}_i$ .

We now examine the restrictions on the parameters in detail. It is convenient to introduce dimensionless parameters  $y_0^i := U_0^i/\ell^3 = U_0^i g^3$  and  $x := r_0^2/\ell^2$ . Firstly, (4.53) and (4.52) give respectively

$$\begin{aligned} \sum y_0^i &= \frac{g^2}{2} (r_0^2 a_1 - a_0), \\ y_0^1 y_0^2 + y_0^2 y_0^3 + y_0^1 y_0^3 &= \frac{g^4 a_0 r_0^2}{4} (1 + x - a_1). \end{aligned} \quad (4.92)$$

Squaring the first and subtracting twice the second gives

$$\sum_i (y_0^i)^2 = \frac{g^4}{4} (a_0^2 + a_1^2 r_0^4 - 2a_0 r_0^2 (1 + x)). \quad (4.93)$$

Now the condition that  $\omega_3(r_0) = 0$  becomes

$$1 = \frac{a_1}{2} + \frac{a_0}{2r_0^2} + \frac{8y_0^1 y_0^2 y_0^3}{g^2 a_0 x^3} + \frac{1}{4x} (1 + x - a_1)^2 - \frac{4}{g^4 a_0^2 x^3} ((y_0^1 y_0^2)^2 + (y_0^2 y_0^3)^2 + (y_0^1 y_0^3)^2). \quad (4.94)$$

The last term above can be written as

$$\begin{aligned} -\frac{4}{g^4 a_0^2 x^3} ((y_0^1 y_0^2)^2 + (y_0^2 y_0^3)^2 + (y_0^1 y_0^3)^2) &= \frac{2}{g^4 a_0^2 x^3} ((y_0^1)^4 + (y_0^2)^4 + (y_0^3)^4) \\ &\quad - \frac{g^4}{8a_0^2 x^3} [a_0^2 + a_1^2 r_0^4 - 2a_0 r_0^2 (1 + x)]^2. \end{aligned} \quad (4.95)$$

We also have the algebraic identity

$$3y_0^1 y_0^2 y_0^3 = (y_0^1)^3 + (y_0^2)^3 + (y_0^3)^3 + \sum_i y_0^i \cdot \left( y_0^1 y_0^2 + y_0^2 y_0^3 + y_0^1 y_0^3 - \sum_j (y_0^j)^2 \right). \quad (4.96)$$

One can replace the right hand sides of these identities with expressions for the charge parameters  $y_0^i$  in terms of  $(a_0, a_1, r_0)$  using (4.92) and (4.93). Then, we eliminate  $a_1$  in terms of  $(r_0, a_0)$  using the regularity condition (4.71). Next, one can eliminate any power of  $a_0$  higher than 1 by solving for  $a_0^2$  using (4.93). Finally one can get a linear equation for  $a_0$  by substituting this back into (4.94). This allows us to determine  $(a_0, a_1)$  in terms of the  $y_0^i$  and  $x$ . Carrying this out produces a complicated polynomial equation in  $(x, y_0^i)$  (8th-order in  $x$ ) which we will not display here. There does not seem to be a simple way to determine all allowed values of  $(p, x)$  from this in general unless additional simplifications are assumed. We will be able to show that the procedure described above can be carried out in two specific cases.

### Equal charges

In the case of equal charges  $\mathfrak{q}_i = \mathfrak{q}$ ,  $U(1)^3$  theory will simplify, upon suitable field redefinitions, to the minimal theory and our solutions should reduce to those found in [40]. Then we have immediately from (4.52) that

$$a_1 = 1 + x + 3g^2 \mathfrak{q}. \quad (4.97)$$

Since all the gauge fields  $A^i = A$ , we should have equal integration constants  $U_0^i$ . Fix the dimensionless parameter  $\mathcal{U}_0 = U_0^I / \ell^3$ . Then

$$\mathfrak{q} = -\frac{4\mathcal{U}_0^2}{a_0 r_0^2 g^6}. \quad (4.98)$$

We then have from (4.97)

$$\mathcal{U}_0^2 = \frac{1}{12} (1 + x - a_1) g^4 a_0 r_0^2. \quad (4.99)$$

On the other hand (4.53) gives

$$\mathcal{U}_0 = \frac{g^2}{6}(r_0^2 a_1 - a_0) \quad (4.100)$$

and combining these two expressions for  $\mathcal{U}_0^2$  gives

$$a_0^2 - 3a_0 r_0^2 + a_0 a_1 r_0^2 + a_1^2 r_0^4 - 3a_0 r_0^2 x = 0. \quad (4.101)$$

Note that this is precisely (4.93) when one sets all dimensionless charge parameters equal, i.e.  $y_0^i \equiv \mathcal{U}_0$ . The regularity conditions (4.71) inserted into (4.70) gives the condition

$$-\frac{6\mathcal{U}_0^2}{x} + \frac{12\mathcal{U}_0^4}{x^3 g^2 a_0} + \frac{g^2 a_0 x}{2} - \frac{3\mathcal{U}_0 a_0}{2r_0^2} + \frac{4\mathcal{U}_0^3}{x^3} = 0. \quad (4.102)$$

This gives an equation quadratic in  $a_0, a_1$  (keeping in mind to eliminate the  $\mathcal{U}_0^4, \mathcal{U}_0^3$  terms using (4.99)). Then use the regularity condition to get rid of  $a_1$  terms, the constraint (4.101) to eliminate the  $a_0^2$  terms, and one is left with the condition

$$a_0 = \frac{2p^2 - 4p + 3 + (p - 8)x}{g^2(p + 1)}. \quad (4.103)$$

Subbing back into (4.101) produces

$$27x^2 - (p - 2)(p^2 + 14p - 5)x + (p - 2)^3 p = 0. \quad (4.104)$$

This equation is identical to the regularity condition derived in [40]. For fixed  $p$  this yields a quadratic for  $x$ . The analysis of [40] demonstrates that the only possible smooth solutions have  $p \geq 3$  with the corresponding larger (positive) root  $x$  of (4.104). For this class of solutions of the minimal theory, there are no continuous parameters once the topology is fixed by the choice of  $p$ . Explicitly, the spacetime metric is (4.12)

is determined by

$$f = \left(1 - \frac{r_0^2 + 1 - a_1}{3r^2}\right)^{-1} \quad (4.105)$$

$$\omega_3 = \frac{r^2 - r_0^2}{2\ell} + \frac{(a_1 - 1)\ell}{2} + \frac{r_0^4 + r_0^2\ell^2(2 - 5a_1) + 3a_0\ell^2 + \ell^4(1 - a_1)^2}{12\ell r^2} \quad (4.106)$$

$$- \frac{(a_0 + a_1 r_0^2)(r_0^2 + (1 - a_1)\ell^2)\ell}{18r^2} - \frac{\ell(a_0^2\ell^2 + a_0(a_1 - 3)\ell^2 r_0^2 - 3a_0 r_0^4 + a_1\ell^2 r_0^4)}{18r^6}, \quad (4.107)$$

along with the relations

$$a_1 = p - x - \frac{a_0}{r_0^2}, \quad \frac{a_0}{r_0^2} = \frac{2p^2 - 4p + 3 + (p - 8)x}{x(p + 1)}, \quad (4.108)$$

$$x = \frac{p - 2}{54} \left( (p^2 + 14p - 5) + (1 + p)\sqrt{(1 + p)(25 + p)} \right), \quad (4.109)$$

and the Maxwell field by

$$F = d \left[ \frac{\sqrt{3}}{2} [f(dt + \omega)] + \frac{\ell}{2\sqrt{3}} P \right] \quad (4.110)$$

where  $P$  is given by (4.32).

For these globally smooth and stationary gravitational solitons with conformal boundary  $\mathbb{R} \times L(p, 1)$ , we may compute their conserved charges. The asymptotic integrals are computed in the limit  $R \rightarrow \infty$  in the asymptotically static  $(T, R, \bar{\psi}, \theta, \phi)$  coordinate chart (4.67). For the mass, it is natural to use the Ashtekar-Magnon mass, which yields the result

$$\mathbf{M}_{\text{AD}} = - \frac{(p - 2)^2(2p + 5)\ell^2\pi}{108p} \quad (4.111)$$

where we have used the asymptotically static Killing field  $\partial_T$  to define the mass. Note that since  $p \geq 3$ ,  $M_{\text{AD}}$  is strictly negative. This is not unexpected, as these solutions are not asymptotically globally  $\text{AdS}_5$  and a positive energy theorem does not apply. Indeed, the mass of the vacuum Eguchi-Hanson- $\text{AdS}_5/\mathbb{Z}_p$  soliton family of solutions (whose members are also asymptotically locally  $\text{AdS}_5/\mathbb{Z}_p$  for  $p \geq 3$ ) is strictly negative. The angular momentum computed using the Komar integral (4.81) is

$$\mathbf{J} = - \frac{\ell^3(p - 2)^3\pi}{108p}. \quad (4.112)$$

Finally, the electric charge can be computed from the integral

$$\mathbf{Q} = \frac{1}{4\pi} \int_{L(p,1)} \star F = -\frac{\ell^2(p-2)\pi}{6p\sqrt{3}} \quad (4.113)$$

where we have used the formula

$$\begin{aligned} \star F = & \frac{\sqrt{3}}{2} \left[ \frac{f'Vr^3}{8f^2} \sin\theta d\theta \wedge d\phi \wedge d\psi + \frac{rf^2\omega_3'}{2} (dt + \omega_3\sigma_3) \sin\theta \wedge d\theta \wedge d\phi - \frac{2f^2\omega_3}{r} dt \wedge dr \wedge \sigma_3 \right] \\ & + \frac{\ell}{2\sqrt{3}} \left[ \frac{rfP'}{2} (dt + \omega_3\sigma_3) \wedge \sin\theta d\theta \wedge d\phi - \frac{2Pf}{r} (dt + \omega_3\sigma_3) \wedge dr \wedge \sigma_3 \right]. \end{aligned} \quad (4.114)$$

Using these definitions, we arrive at the BPS-type relation ( $p \geq 3$ )

$$\mathbf{M}_{\text{AD}} = \frac{\sqrt{3}(p-2)\mathbf{Q}}{2} + \frac{2\mathbf{J}}{\ell}. \quad (4.115)$$

One can of course define the mass for a family of non-supersymmetric black hole solutions in terms of a ‘thermodynamic energy’ as in [41] and then take a supersymmetric limit, and then choose the local parameters in these metrics so that a soliton geometry, rather than a black hole, is obtained. However, the Ashtekar-Magnon definition appears more natural here, particularly since solitons have no horizon and hence no associated temperature<sup>2</sup>. As further evidence in support of identifying  $\mathbf{M}_{\text{AD}}$  with the mass of the soliton spacetimes, consider the holographic stress tensor approach [77, 106]. Adapted to the present setting, one considers a dual CFT on  $\mathbb{R} \times L(p, 1)$  in a spacetime with conformal metric (4.69) and computes the expectation value of the stress tensor given by (in units where the gravitational constant  $G = 1$ )

$$\langle T_{\mu\nu} \rangle = \lim_{R \rightarrow \infty} \frac{R^2}{8\pi\ell^2} \left[ -(K_{\mu\nu} - \text{Tr}_{\bar{h}} K \bar{h}_{\mu\nu}) - \frac{3}{\ell} \bar{h}_{\mu\nu} + \frac{\ell}{2} \bar{G}_{\mu\nu} \right] \quad (4.116)$$

where  $(\bar{h}, K)$  are the (Lorentzian) metric and extrinsic curvature associated to the surfaces  $R = \text{constant}$  in the asymptotically static chart (4.67), and  $\bar{G}_{\mu\nu}$  is the Einstein tensor of  $\bar{h}$ . In particular, we choose the outward pointing normal so that  $K_{\mu\nu} = \dot{\bar{h}}_{\mu\nu}/(2g_{RR})$  where the overdot  $\dot{\phantom{x}}$  denotes a derivative with respect to  $R$ . The

---

<sup>2</sup>Nonetheless, solitons are still thermodynamically relevant. One can derive a ‘soliton mechanics’, i.e. a Smarr-type relation and variation formulae for both globally and locally Anti-de Sitter solitons [70, 25, 3]. Moreover, solitons arise in Hawking-Page type phase transitions between black holes and solitons with the same conformal boundary [80, 3].

holographic energy is then obtained by integrating the function  $T_{TT}$  over the conformal boundary with metric (4.69). One obtains

$$\mathbf{E} = \int_{L(p,1)} T_{TT} \, \text{dvol}(\bar{h}) = \frac{\ell^2 \pi (-79 + 96p + 24p^2 - 16p^3)}{864p} \quad (4.117)$$

which is strictly negative for  $p \geq 3$ . This energy can be expressed in terms of the Ashtekar-Magnon mass as

$$\mathbf{E} = \mathbf{M}_{\text{AD}} + \frac{3\ell^2 \pi}{32p}. \quad (4.118)$$

The second term is recognized to be the Casimir energy of the CFT on  $\mathbb{R} \times L(p, 1)$ ; this is the energy of the  $\text{AdS}_5/\mathbb{Z}_p$  orbifold (it has an orbifold singularity at the fixed point of the  $SO(4)$  action). Note that  $\mathbf{M}_{\text{AD}} < 0$ , so the presence of the (globally smooth) soliton *lowers* the energy with respect to the orbifold vacuum geometry.

Finally, we note that the non-contractible  $S^2$  at  $r = r_0$  carries a ‘dipole charge’  $\mathcal{D}$  which is physically interpreted as a flux of  $F$  that prevents its collapse. In particular note that  $F$  is not globally exact, and the dipole charge is

$$\mathcal{D} = \frac{1}{4\pi} \int_{S^2} F = \frac{\ell(p-2)}{4\sqrt{3}}. \quad (4.119)$$

The charge is not conserved in the sense that it is only non-zero if the 2 surface on which it is defined encloses the bubble.

### Solutions with non-equal charges

A second set of smooth solutions can be obtained by choosing the dimensionless integration constant vector to take the form  $y_0^i = (y_0, y_0, \beta y_0)$  for  $\beta \in \mathbb{R}$ . We then have for the charge parameters

$$\mathfrak{q}_1 = \mathfrak{q}_2 = -\frac{4\beta y_0^2}{g^4 a_0 x}, \quad \mathfrak{q}_3 = -\frac{4y_0^2}{g^4 a_0 x} \quad (4.120)$$

where, as above,  $x = r_0^2 g^2$  is dimensionless. The constraints (4.92) immediately can be used to find

$$y_0 = \frac{g^2 (a_1 r_0^2 - a_0)}{2(2 + \beta)} \quad (4.121)$$

and using the regularity condition (4.71) to eliminate  $a_1$  as well as (4.94) one can follow the procedure described above to eliminate  $a_0$  and obtain a polynomial equation for  $x$  with coefficients depending on the parameter  $\beta$  and the natural number  $p$ :

$$4(\beta - 1)^3 x^3 - ((\beta - 1)^2 p(p + 2) - 7\beta^2 + 22\beta + 4)\beta + 8) x^2 + (p - 2)(4p + \beta(\beta^2(p - 1)^2 - 4 + 2p(p + 2) - 2\beta(1 + p(p - 4))))x - p\beta(p - 2)^3 = 0. \quad (4.122)$$

For  $\beta = 1$  this reduces to the quadratic that determines  $x$  in the minimal theory (4.108). We also note that the case  $\beta = 0$  leads to a solution for which  $p \geq 3$  and  $\mathbf{Q}_1 = \mathbf{Q}_2 \neq 0, \mathbf{Q}_3 = 0$ . Although this special case appears pathology-free, we find that it has  $\mathbf{M}_{\text{AD}} = 0$  so we will not pursue it further.

Rather than attempting an exhaustive analysis of the full space of solutions of (4.122), we will confine ourselves to some simple illustrative example. An obvious question is whether one can obtain asymptotically globally AdS<sub>5</sub> solitons ( $p = 1$ ) which, as we explained above, cannot exist for  $\beta = 1$ . We have not yet been able to find any smooth examples with simple values for  $\beta$  (one finds the function  $f$  has zeroes for  $r > r_0$ ). However, a systematic investigation may lead to examples. Consider the case  $\beta = 2, p = 3$ . Then the cubic (4.122) factors as  $2(2x - 3)(1 - 18x + x^2)$  producing solutions  $x_1 = 3/2, x_2 = 9 + 4\sqrt{5}, x_3 = 1/x_2$ . Consider  $x = x_1$ . Then we have  $a_0 = 3/(8g^2), a_1 = 5/4$ , and  $y_0 = 3/16$ . This leads to

$$\mathfrak{q}_1 = \mathfrak{q}_2 = -\frac{1}{2g^2}, \quad \mathfrak{q}_3 = -\frac{1}{4g^2}. \quad (4.123)$$

Then we may write

$$f^3 = \frac{r^6}{(r^2 - r_0^2 + 2\ell^2)^2(r^2 - r_0^2 + \frac{5\ell^2}{4})} \quad (4.124)$$

which is obviously positive for  $r > r_0 = \sqrt{3/2}\ell$ . The solution has a mass  $\mathbf{M}_{\text{AD}} = -\pi\ell^2/48$  and  $\mathbf{Q}_1 = \mathbf{Q}_2 = -3\mathbf{Q}_3/2 = 3\pi\ell^2/32$ . Repeating this procedure for the case  $\beta = 4, p = 3$  leads to a well behaved solution of (4.122) with  $x_{\pm} = 2/3 \pm \sqrt{11/27} > 0$ . The resulting solutions for either root leads to regular solitons with non vanishing mass  $\mathbf{M}_{\text{AD}}$ , angular momentum  $\mathbf{J}$  and charges  $\mathbf{Q}_i$ .

## 4.4 Discussion

We have constructed asymptotically  $\text{AdS}_5/\mathbb{Z}_p$  supersymmetric gravitational soliton solutions of five-dimensional gauged supergravity coupled to an arbitrary number of vector multiplets. The solutions are globally stationary and admit an  $SU(2) \times U(1)$  isometry group. The local solutions are characterized by  $N + 1$  continuous parameters  $(r_0, U_0^I)$ . The local solutions extend to globally defined metrics provided these parameters satisfy an additional two constraints for a given  $p \in \mathbb{N}$  which determines the topology of the conformal boundary. We have investigated in detail a subset of these local solutions for which we can explicitly solve these constraints for  $p \geq 3$  and showed there are examples beyond the minimal theory. Given their similarity to the Eguchi-Hanson- $\text{AdS}_5/\mathbb{Z}_p$  vacuum solitons, we could identify these solutions as supersymmetric generalizations that carry, in addition to negative mass relative to the AdS orbifold background, non-vanishing angular momentum and charge.

We close with a brief discussion of some further problems which arise as a consequence of our work. A natural question to investigate is the question of stability. Famously, robust numerical investigation have provided strong evidence that global AdS is nonlinearly unstable [52, 54] to the formation of black holes as energy tends to get concentrated to shorter scales. One might expect supersymmetric solitons in AdS to suffer from a similar instability. Dold has rigorously established that the maximal development of  $SU(2) \times U(1)$ -invariant initial data sufficiently close to Eguchi-Hanson- $\text{AdS}_5/\mathbb{Z}_p$  do not form future horizons. This suggests that the endpoint of the evolution (assuming it settles to a static spacetime with the same conformal boundary) would be a spacetime containing a naked singularity.

More recently, mode solutions of the linear scalar wave equation on the Eguchi-Hanson- $\text{AdS}_5/\mathbb{Z}_p$  soliton were analyzed [3]. It was shown that, similar to AdS, the geometry admits a normal mode spectrum, so that scalar modes neither grow nor decay in time. These two stability results are consistent, as [3] is purely a linear result. It would be interesting to extend both of these analyses to the stationary, supersymmetric solitons constructed here to determine whether there are obstructions to horizon formation and/or a normal mode spectrum. A related challenging problem would be to study linearized gravitational perturbations of the background. Since the solutions have  $SU(2) \times U(1)$  symmetry, one could decompose metric and Maxwell field perturbations using the strategy developed in [107].

Our preliminary analysis at least reveals that there are no ergoregions (with respect to either the stationary Killing fields  $\partial_t$  or  $\partial_T$ ), which are known to be another channel for instabilities. As mentioned in the Introduction, this is in stark contrast to the 1/2-BPS supersymmetric solitons constructed in [2] which actually contain evanescent horizons (the supersymmetric Killing vector field becomes null on a co-dimension two timelike surface) which provide a geometric mechanism for instability. The absence of such tapping mechanisms suggests that the supersymmetric solitons constructed here could be nonlinearly stable.

**Acknowledgements** We are grateful to James Lucietti for useful comments. HKK acknowledges the support of the NSERC Grant RGPIN-2018-04887.

# Chapter 5

## Conclusion and Future Work

### 5.1 Conclusion

This thesis has presented several new results on the topic of asymptotically  $\text{AdS}_5$  gravitational solitons. Broadly, we have focussed on finding new explicit examples of such solutions, generalizing previous work, and studying their geometric properties. Secondly, we have performed a thorough stability analysis of a well-known family of solitons, by studying solutions of the linear wave equation on the fixed soliton background.

In more detail, the results for the projects presented above can be summarized as follows:

- Asymptotically globally  $\text{AdS}_5$  gravitational soliton solutions of five-dimensional gauged supergravity coupled to arbitrarily many vector multiplets were constructed. It is shown that they contain evanescent ergosurfaces and hence gives strong evidence that they exhibit nonlinear instability through the mechanism of stable trapping.
- The mode solutions of the scalar wave equation of the Eguchi-Hanson- $\text{AdS}_5$  gravitational solitons were investigated. In addition, geometric and thermodynamic properties of these solitons were analyzed.
- New supersymmetric gravitational soliton solutions of five-dimensional gauged supergravity coupled to arbitrarily many vector multiplets were constructed by a

systematic search of  $SU(2) \times U(1)$  solutions of the supergravity equations. These differ from the ones in the first chapter in that they preserve one-quarter of the supersymmetry as opposed to one-half. All the examples we have constructed explicitly are asymptotically locally  $\text{AdS}_5$ , that is they approach a quotient  $\text{AdS}_5/\mathbb{Z}_p$  for  $p \geq 3$ . These solutions can be thought of as BPS versions of the Eguchi-Hanson- $\text{AdS}_5$  solitons studied in the previous chapter.

## 5.2 Future Work

In this section, we will present our ongoing project about generalization of asymptotically globally  $\text{AdS}_5$  gravitational solitons that were first considered in [25] as introduced in Chapter 1. This work is in preparation. The work on the Klein-Gordon equation in 5.2.3 is my own and the material in 5.2.1 and 5.2.2 is work in collaboration with my supervisor, Dr. Robert Mann and Dr. Robie Hennigar and is a natural progression of our article.

In the following subsections, we will be referring to the asymptotically  $\text{AdS}_5$  non-supersymmetric gravitational soliton (1.26) and refer to the notation given there. The local solutions have only been studied in the asymptotically globally  $\text{AdS}$  case, when there is a spherical boundary. This means  $k = 1$  in the identifications of the angles (1.30). In our ongoing work we are studying what happens if constraint the parameters so that we allow  $k > 1$ . Note that in this case, these solitons are like charged, rotating generalizations of the vacuum Eguchi-Hanson- $\text{AdS}_5$  solution.

### 5.2.1 Asymptotically locally $\text{AdS}_5$ solutions

The action for minimal five-dimensional supergravity is

$$I = \frac{1}{16\pi} \int_M \left[ \left( R + \frac{12}{\ell^2} \right) d\text{vol}(g) - 2F \wedge \star F - \frac{8}{3\sqrt{3}} F \wedge F \wedge A \right]. \quad (5.1)$$

The equations of motion are

$$\begin{aligned} R_{ab} &= 2 \left( F_{ac} F_b{}^c - \frac{1}{6} |F|^2 g_{ab} \right) - \frac{4}{\ell^2} g_{ab}, \\ d \star F + \frac{2}{\sqrt{3}} F \wedge F &= 0. \end{aligned} \quad (5.2)$$

It can be verified directly that the soliton metric (1.26) along with the Maxwell field

$$F = \frac{3q}{2} d \left[ \left( \frac{1}{r^2} \right) \left( \frac{j}{2} \sigma_3 - dt \right) \right] \quad (5.3)$$

gives a solution to the field equations. Now we choose our parameters so that there is a simultaneous simple zero of  $b(r)^2$  and  $W(r)$  at  $r = r_0$ . This imposes the conditions on the parameters given by (1.32). In order that the vector field  $\partial_\psi$  degenerate smoothly at  $r = r_0$  (i.e. there are conical singularities) imposes

$$\psi \sim \psi + \frac{4\pi}{\sqrt{W'(r_0) (b^2(r_0))'}}. \quad (5.4)$$

By defining dimensionless parameters

$$x \equiv \frac{r_0^2}{j^2} \quad \text{and} \quad \alpha \equiv \frac{j^2}{\ell^2}, \quad (5.5)$$

the regularity condition is written as

$$(2+x)^2 [1+x(\alpha-1)] - k^2 = 0. \quad (5.6)$$

It can also be written as

$$(1-\alpha)x^3 + (3-4\alpha)x^2 - 4x\alpha + k^2 - 4 = 0 \quad (5.7)$$

The globally AdS<sub>5</sub> case corresponds to  $k = 1$  and has been analyzed before. The appearance of  $k > 1$  dramatically changes the space of solutions. For  $k = 1$  it was shown that there is a single solution provided that  $0 \leq \alpha \leq 1$ . We have checked that for  $k = 2$  there are two solutions, but only one has  $x > 0$  (the case  $x < 0$  implies  $r_0$  is imaginary, so must be discarded). If  $k \geq 3$ , some detailed analysis indicates that there is a real constant  $\alpha_*$  such that for  $0 < \alpha < \alpha_*$  there are no solutions, for  $\alpha_* < \alpha < 1$

there are two regular solutions for  $x$ , and for  $\alpha > 1$  there is a single regular solution. This implies that for fixed asymptotic boundary conditions (i.e. fixed  $k \geq 3$ ) one can have two possible solutions, a ‘large’ and ‘small’ soliton, corresponding to the two roots  $x_2 > x_1 > 0$ .

### 5.2.2 Conserved charges

Here we briefly study the computation of the mass and angular momentum of these solutions for general  $k$ . To calculate the Ashtekar–Magnon–Das mass, we first need to map the metric to its conformal boundary by

$$\bar{g}_{\mu\nu} = \Omega^2 g_{\mu\nu} \quad (5.8)$$

where the conformal scale is

$$\Omega = \frac{\ell}{r}. \quad (5.9)$$

The conformal boundary is the asymptotic region as  $r \rightarrow \infty$ . The conformal boundary metric is the metric induced by pulling back  $\bar{g}_{\mu\nu}$  to a surface  $r = \text{constant}$  with  $r \rightarrow \infty$ :

$$\bar{g}_4 = -dt^2 + \ell^2 g_3 \quad (5.10)$$

where  $g_3$  is the round metric on  $L(k, 1)$ . This is the metric at timelike infinity  $\mathcal{I}$ .

The electric part of the Weyl tensor, which is calculated by projecting the Weyl tensor to the boundary, is given by

$$\bar{\mathcal{E}}_\nu^\mu = \frac{\ell^2}{\Omega^2} \bar{g}^{\alpha\gamma} \bar{g}^{\beta\sigma} n_\gamma n_\sigma C_{\alpha\nu\beta}^\mu \quad (5.11)$$

where  $n = d\Omega$  is the unit normal for constant- $r$  surfaces. The conserved quantity associated with the Killing vector  $K$  is given by

$$Q[K] = \frac{\ell}{16\pi} \int_\Sigma \bar{\mathcal{E}}_\nu^\mu K^\nu d\Sigma_\mu. \quad (5.12)$$

The integral will be taken at infinity with the timelike normal  $dt$  and the timelike Killing vector is  $\partial/\partial t$  and  $\Sigma$  is spatial geometry  $L(k, 1)$  equipped with the round metric as described above. It has a volume  $2\pi^2/k$ . Therefore,  $\nu$  and  $\mu$  in the above equation should be taken as  $t$ . This shows us that the only relevant Weyl tensor

component would be  $C_{rtr}^t$ , which is

$$C_{rtr}^t = \frac{6\ell^2 p - 6\ell^2 q + 4pj^2}{r^6} + \mathcal{O}\left(\frac{1}{r^8}\right). \quad (5.13)$$

Hence, the Ashtekar-Magnon-Das mass is

$$M = \frac{\pi}{4k} \left( 3p - 3q + \frac{pj^2}{\ell^2} \right). \quad (5.14)$$

To calculate the angular momentum in the  $\psi$ -direction, consider the Killing vector  $\frac{2\partial}{\partial\psi}$ , i.e.,  $2\pi$ -periodic orbits. In this case, the only relevant component of the Weyl tensor is  $C_{r\psi r}^t$ . Then, the angular momentum is

$$J \left[ \frac{2\partial}{\partial\psi} \right] = -\frac{(2p - q)j\pi}{2k}. \quad (5.15)$$

It should be noted of course that the parameters  $(p, q)$  appearing here are actually fixed by (1.32) and then these parameters must satisfy the regularity conditions for the given  $k$ .

### 5.2.3 Euclidean Action

We have argued above that for general  $k \geq 3$ , there are regions in the parameter space where there are *two* solitons, one large, and one small. Thus for a fixed conformal boundary (say  $L(k, 1)$ ) there are multiple solutions: a black hole with these asymptotics (this can be easily found by taking quotients of known globally AdS<sub>5</sub> black hole metrics) and also additional solitons. Typically, when this happens, we expect ‘phase transitions’ between solutions as we vary some parameter (such as the charge or angular momentum, or temperature if we have a black hole). The most famous example of this is the Hawking-Page phase transition, which describes a transition from empty AdS to a Schwarzschild-AdS black hole (see Chapter 3 for a discussion in the Eguchi-Hanson-AdS case).

To get a positive-definite metric, the obvious choice is to define an imaginary time by  $t = i\tau$ . To get a real metric we then set  $j = i\hat{j}$ . However the parameter  $q$  appears linearly in the metric functions, which means  $q = i\hat{q}$  cannot be set. The

positive-signature metric is

$$ds_E^2 = \frac{r^2 \hat{W}(r)}{4\hat{b}(r)^2} d\tau^2 + \frac{dr^2}{\hat{W}(r)} + \frac{r^2}{4} (\sigma_1^2 + \sigma_2^2) + \hat{b}(r)^2 (\sigma_3 + \hat{f}(r)d\tau)^2, \quad (5.16)$$

with the metric functions

$$\begin{aligned} \hat{W}(r) &= 1 + \frac{4b(r)^2}{\ell^2} - \frac{2}{r^2} (p - q) + \frac{q^2 - 2p\hat{j}^2}{r^4}, \\ \hat{b}(r)^2 &= \frac{r^2}{4} \left( 1 + \frac{\hat{j}^2 q^2}{r^6} - \frac{2\hat{j}^2 p}{r^4} \right), \\ \hat{f}(r) &= \frac{\hat{j}}{2b(r)^2} \left( \frac{2p - q}{r^2} - \frac{q^2}{r^4} \right), \end{aligned} \quad (5.17)$$

and the Maxwell field is

$$F = \frac{\sqrt{3}q}{2} d \left[ \left( \frac{1}{r^2} \right) \left( \frac{j\sigma_3}{2} - dt \right) \right] = \frac{\sqrt{3}iq}{2} d \left[ \left( \frac{1}{r^2} \right) \left( \frac{\hat{j}\sigma_3}{2} - d\tau \right) \right] \quad (5.18)$$

would be imaginary, which does not cause a problem. The equations of motion for  $(g, F)$  are

$$R_{ab} = 2 \left( F_{ac} F_b{}^c - \frac{1}{6} |F|^2 g_{ab} \right) - \frac{4}{\ell^2} g_{ab}, \quad d \star F + \frac{2}{\sqrt{3}} F \wedge F = 0. \quad (5.19)$$

This means on-shell

$$R = \frac{1}{3} |F|^2 - \frac{20}{\ell^2}, \quad -\frac{8}{3\sqrt{3}} F \wedge F \wedge A = \frac{4}{3} d(\star F \wedge A) + \frac{4}{3} F \wedge \star F. \quad (5.20)$$

but  $A$  is not globally defined. Using the identity

$$F \wedge \star F = \frac{|F|^2}{2} d\text{Vol}(g), \quad (5.21)$$

we find the on-shell supergravity Lagrangian

$$\left( R + \frac{12}{\ell^2} \right) d\text{vol}(g) - 2F \wedge \star F - \frac{8}{3\sqrt{3}} F \wedge F \wedge A \quad (5.22)$$

$$= -\frac{8}{\ell^2} d\text{vol}(g) + \frac{4}{3} d(\star F \wedge A). \quad (5.23)$$

The Euclidean action is then given by

$$\hat{I} = -\frac{1}{16\pi G} \left[ \int_M \left( -\frac{8}{\ell^2} \right) d\text{Vol}(g) \right. \quad (5.24)$$

$$\left. + 2 \int_{\partial M} \left[ \frac{2}{3} \star F \wedge A + \left( \text{Tr}K - \frac{3}{\ell} - \frac{\ell R_h}{4} \right) d\text{Vol}(h) \right] \right]. \quad (5.25)$$

At  $r = r_0$  provided we fix

$$q = \frac{r_0^4}{\hat{j}^2}, \quad p = \frac{r_0^4(r_0^2 + \hat{j}^2)}{2\hat{j}^4}, \quad (5.26)$$

and using similar definitions as in the Lorentzian case

$$\hat{x} := -\frac{r_0^2}{\hat{j}^2}, \quad \hat{\alpha} := -\frac{\hat{j}^2}{\ell^2}, \quad (5.27)$$

the regularity condition becomes

$$(2 + \hat{x})^2(1 - \hat{x}(1 - \hat{\alpha})) = k^2. \quad (5.28)$$

A computation gives

$$\star F = \frac{\sqrt{3iq}}{2} \left[ -\frac{\hat{f}\hat{W}}{8\hat{b}^2} d\tau \wedge \sin\theta d\theta \wedge d\phi \right. \quad (5.29)$$

$$\left. -\frac{\hat{b}^2}{r^2} \left( 1 + \frac{\hat{f}\hat{j}}{2} \right) (\sigma_3 + \hat{f}d\tau) \wedge \sin\theta d\theta \wedge d\phi - \frac{\hat{j}}{r^3} d\tau \wedge dr \wedge \sigma_3 \right].$$

We see that the gauge field  $A$  appears within the boundary integral for the Euclidean action. We can choose it to be (up to additional gauge freedoms)

$$A = \frac{\sqrt{3iq}}{2} \left( \frac{1}{r^2} \right) \left( \frac{\hat{j}\sigma_3}{2} - d\tau \right). \quad (5.30)$$

At  $r = r_0$  the vector field  $\partial_\psi$  degenerates, so to be in a regular gauge we need  $A(\partial_\psi) = 0$  at  $r = r_0$ . This requires choosing

$$A = \frac{\sqrt{3iq}}{2} \left[ \left( \frac{1}{r^2} \right) \left( \frac{\hat{j}\sigma_3}{2} - d\tau \right) - \frac{\hat{j}d\psi}{2r_0^2} \right]. \quad (5.31)$$

The last term in  $\star F$  above vanishes when pulling back to a surface of constant  $r$ . Thus,

$$\begin{aligned} \star F \wedge A \Big|_{r=R} &= \frac{3q^2}{4} d\tau \wedge d\psi \wedge \sin\theta d\theta \wedge d\phi \left[ \left( \frac{1}{R^2} - \frac{1}{r_0^2} \right) \left[ \frac{\hat{b}^2 \hat{j} \hat{f}}{2R^2} \left( 1 + \frac{\hat{f} \hat{j}}{2} \right) + \frac{\hat{j} \hat{f} \hat{W}}{16\hat{b}^2} \right] \right. \\ &\quad \left. + \frac{\hat{b}^2}{R^4} \left( 1 + \frac{\hat{f} \hat{j}}{2} \right) - c_1 \frac{\hat{b}^2}{r^2} \left( 1 + \frac{\hat{f} \hat{j}}{2} \right) \right]. \end{aligned} \quad (5.32)$$

While this looks complicated, as one takes  $R \rightarrow \infty$  the terms in square brackets vanish as  $O(1/R^2)$ . Thus we do not expect these to contribute to the action. In the (Euclidean) black hole case, the Maxwell boundary term does contribute.

The Euclidean action reduces to the calculation if the  $\star F \wedge A$  term is not present and gives

$$\begin{aligned} \hat{I} &= \frac{\pi\beta}{32\ell^2 k} [(3\ell^4 + 8j^2 p + 8\ell^2(p - q)) - 8r_0^4] \\ &= \frac{\pi\beta}{32\ell^2 k} \left[ 3\ell^4 + 4r_0^4 \left( 1 + \frac{\ell^2}{j^2} \right) \left[ \frac{r_0^2}{j^2} - 1 \right] \right] \\ &= \frac{\pi\beta\ell^2}{32k} [3 + 4\hat{x}^2(1 + \hat{x})(1 - \hat{\alpha})\hat{\alpha}]. \end{aligned} \quad (5.33)$$

It remains to evaluate the action for the two possible solitons for fixed  $k$  and  $\alpha_* < \alpha < 1$ . The soliton with least action is ‘favoured’ (i.e. it has less free energy). A phase transition occurs when we move into a region where the other soliton becomes preferred.

## 5.2.4 Klein-Gordon Equation

Finally we note that even for  $k = 1$ , there has been no attempt at a stability analysis for the class of gravitational solitons given by (1.26). We have already performed an analysis for the simpler static Eguchi-Hanson-AdS solution (Chapter 3). The present case is somewhat more difficult as the metric is more complicated, and in particular, stationary but non-static. Here we describe some preliminary work by showing that the equation admits separable solutions, and the analysis can be reduced to a single radial Schödinger type equation. To begin, recall that the Klein-Gordon equation for

a scalar field  $\Phi$  with a mass  $M$  is given by

$$\nabla^\mu \nabla_\mu \Phi = M^2 \Phi, \quad (5.34)$$

or

$$\frac{1}{\sqrt{-g}} \frac{\partial}{\partial x^\mu} \left( g^{\mu\nu} \sqrt{-g} \frac{\partial \Phi}{\partial x^\nu} \right) = M^2 \Phi. \quad (5.35)$$

Explicitly

$$\frac{1}{\sqrt{-g}} \frac{\partial}{\partial r} \left( g^{rr} \sqrt{-g} \frac{\partial \Phi}{\partial r} \right) + \frac{1}{\sqrt{-g}} \frac{\partial}{\partial \theta} \left( g^{\theta\theta} \sqrt{-g} \frac{\partial \Phi}{\partial \theta} \right) + \frac{1}{\sqrt{-g}} \frac{\partial}{\partial x^A} \left( g^{AB} \sqrt{-g} \frac{\partial \Phi}{\partial x^B} \right) = M^2 \Phi$$

where  $A, B = t, \phi, \tilde{\psi}$ . Then the Klein-Gordon equation becomes

$$\begin{aligned} \frac{1}{r^3} \frac{\partial}{\partial r} \left( r^3 W(r) \frac{\partial \Phi}{\partial r} \right) &+ \frac{4}{r^2 \sin \theta} \frac{\partial}{\partial \theta} \left( \sin \theta \frac{\partial \Phi}{\partial \theta} \right) - \frac{\tilde{b}(r)^2}{r^2 W(r)} \left( \frac{\partial}{\partial t} - \frac{f(r)}{2} \frac{\partial}{\partial \tilde{\psi}} \right)^2 \Phi \\ &+ \frac{4}{r^2} \left( \frac{\cot \theta}{2} \frac{\partial}{\partial \tilde{\psi}} - \frac{1}{\sin \theta} \frac{\partial}{\partial \phi} \right)^2 \Phi + \frac{1}{\tilde{b}(r)^2} \frac{\partial^2 \Phi}{\partial \tilde{\psi}^2} = M^2 \Phi. \end{aligned} \quad (5.36)$$

By using the separation ansatz

$$\Phi = e^{-i\omega t} e^{im\tilde{\psi}} R(r) Y(\theta, \phi), \quad (5.37)$$

we get

$$\begin{aligned} \frac{1}{r^3} \frac{\partial}{\partial r} \left( r^3 W(r) \frac{\partial \Phi}{\partial r} \right) &+ \frac{4}{r^2 \sin \theta} \frac{\partial}{\partial \theta} \left( \sin \theta \frac{\partial \Phi}{\partial \theta} \right) + \frac{\tilde{b}(r)^2}{r^2 W(r)} \left( \omega + \frac{mf(r)}{2} \right)^2 \Phi \\ &- \frac{m^2 \cot^2 \theta}{r^2} \Phi + \frac{4}{r^2 \sin^2 \theta} \frac{\partial^2 \Phi}{\partial \phi^2} - \frac{4im \cos \theta}{r^2 \sin^2 \theta} \frac{\partial \Phi}{\partial \phi} - \frac{m^2}{\tilde{b}(r)^2} \Phi = M^2 \Phi. \end{aligned} \quad (5.38)$$

Defining a one-form on  $S^2$

$$A_\mu = \frac{\cos \theta}{2} d\phi, \quad (5.39)$$

and letting

$$D_\mu = \nabla_{S_\mu^2} - imA_\mu, \quad (5.40)$$

the Klein - Gordon equation can be rewritten as

$$\frac{1}{r^3} \frac{\partial}{\partial r} \left( r^3 W(r) \frac{\partial \Phi}{\partial r} \right) + \frac{D^2 \Phi}{r^2} + \frac{\tilde{b}(r)^2}{r^2 W(r)} \left( \omega + \frac{mf(r)}{2} \right)^2 \Phi - \frac{m^2}{\tilde{b}(r)^2} \Phi = M^2 \Phi. \quad (5.41)$$

Or, explicitly

$$\begin{aligned}
& \frac{1}{r^3} e^{-i\omega t} e^{im\bar{\psi}} Y(\theta, \phi) \frac{d}{dr} \left( r^3 W(r) \frac{dR(r)}{dr} \right) + e^{-i\omega t} e^{im\bar{\psi}} R(r) \frac{D^2 Y(\theta, \phi)}{r^2} \\
+ & \frac{\tilde{b}(r)^2}{r^2 W(r)} \left( \omega + \frac{mf(r)}{2} \right)^2 e^{-i\omega t} e^{im\bar{\psi}} R(r) Y(\theta, \phi) - \frac{m^2}{\tilde{b}(r)^2} e^{-i\omega t} e^{im\bar{\psi}} R(r) Y(\theta, \phi) \\
= & M^2 e^{-i\omega t} e^{im\bar{\psi}} R(r) Y(\theta, \phi). \tag{5.42}
\end{aligned}$$

Here,  $Y(\theta, \phi)$  is an eigenfunction of the charged scalar Laplacian on  $CP^1$ , satisfying

$$D^2 Y(\theta, \phi) = -\mu Y(\theta, \phi) \tag{5.43}$$

where

$$\begin{aligned}
\mu &= l(l+2) - m^2, \\
l &= 2k + |m|, \\
k &= 0, 1, 2, \dots
\end{aligned} \tag{5.44}$$

Therefore, the Klein-Gordon equation is reduced to a one-variable equation as follows

$$\begin{aligned}
\frac{1}{r^3} \frac{d}{dr} \left( r^3 W(r) \frac{dR(r)}{dr} \right) + \left[ -\frac{\mu}{r^2} + \frac{\tilde{b}(r)^2}{r^2 W(r)} \left( \omega + \frac{mf(r)}{2} \right)^2 \right. \\
\left. - \frac{m^2}{\tilde{b}(r)^2} - M^2 \right] R(r) = 0. \tag{5.45}
\end{aligned}$$

In future work we intend to determine the spectrum of allowed frequencies  $\omega$  satisfying the boundary conditions (i.e. reflective at conformal infinity, and regular at the ‘origin’  $r = r_0$ ). In particular, it is open question as to whether, like the Eguchi-Hanson-AdS soliton, these more complicated solitons also have normal modes (i.e. there are no decaying or growing ‘quasi’-normal modes).

# Bibliography

- [1] André Lichnerowicz. *Théories relativistes de la gravitation et de l'électromagnétisme: relativité générale et théories unitaires*. Paris: Masson, 1955.
- [2] Turkuler Durgut and Hari K. Kunduri. Supersymmetric multi-charge solitons in AdS<sub>5</sub>. *Phys. Rev. D*, 105:064068, 2022.
- [3] Turkuler Durgut, Robie A. Hennigar, Hari K. Kunduri, and Robert B. Mann. Phase transitions and stability of Eguchi-Hanson-AdS solitons. *JHEP*, 03:114, 2023.
- [4] B. P. Abbott et al. Observation of Gravitational Waves from a Binary Black Hole Merger. *Phys. Rev. Lett.*, 116(6):061102, 2016.
- [5] B. P. Abbott et al. Multi-messenger Observations of a Binary Neutron Star Merger. *Astrophys. J. Lett.*, 848(2):L12, 2017.
- [6] Charles W. Misner, Kip S. Thorne, and John A. Wheeler. *Gravitation*. W. H. Freeman, San Francisco, 1973.
- [7] Arthur Komar. Covariant conservation laws in general relativity. *Phys. Rev.*, 113:934–936, 1959.
- [8] Richard Schon and Shing-Tung Yau. On the Proof of the positive mass conjecture in general relativity. *Commun. Math. Phys.*, 65:45–76, 1979.
- [9] Richard Schon and Shing-Tung Yau. Proof of the positive mass theorem. 2. *Commun. Math. Phys.*, 79:231–260, 1981.
- [10] Edward Witten. A Simple Proof of the Positive Energy Theorem. *Commun. Math. Phys.*, 80:381, 1981.
- [11] Stephen W. Hawking. Black holes in general relativity. *Commun. Math. Phys.*, 25:152–166, 1972.

- [12] John L. Friedman, Kristin Schleich, and Donald M. Witt. Topological censorship. *Phys. Rev. Lett.*, 71:1486–1489, 1993. [Erratum: *Phys.Rev.Lett.* 75, 1872 (1995)].
- [13] Gary W. Gibbons. Supergravity vacua and solitons. In *A Newton Institute Euroconference on Duality and Supersymmetric Theories*, pages 267–296, 10 2011.
- [14] Tetsuya Shiromizu, Seiju Ohashi, and Ryotaku Suzuki. A no-go on strictly stationary spacetimes in four/higher dimensions. *Phys. Rev. D*, 86:064041, 2012.
- [15] Hari K. Kunduri and James Lucietti. No static bubbling spacetimes in higher dimensional Einstein–Maxwell theory. *Class. Quant. Grav.*, 35(5):054003, 2018.
- [16] Iosif Bena and Nicholas P. Warner. Black holes, black rings and their microstates. *Lect. Notes Phys.*, 755:1–92, 2008.
- [17] Stefano Giusto and Samir D. Mathur. Geometry of D1-D5-P bound states. *Nucl. Phys. B*, 729:203–220, 2005.
- [18] Iosif Bena and Nicholas P. Warner. Bubbling supertubes and foaming black holes. *Phys. Rev. D*, 74:066001, 2006.
- [19] Per Berglund, Eric G. Gimon, and Thomas S. Levi. Supergravity microstates for BPS black holes and black rings. *JHEP*, 06:007, 2006.
- [20] Iosif Bena, Stefano Giusto, Clement Ruef, and Nicholas P. Warner. A (Running) Bolt for New Reasons. *JHEP*, 11:089, 2009.
- [21] Geoffrey Compere, Keith Copsey, Sophie de Buyl, and Robert B. Mann. Solitons in Five Dimensional Minimal Supergravity: Local Charge, Exotic Ergoregions, and Violations of the BPS Bound. *JHEP*, 12:047, 2009.
- [22] Nikolay Bobev and Clement Ruef. The Nuts and Bolts of Einstein-Maxwell Solutions. *JHEP*, 01:124, 2010.
- [23] Samir D. Mathur. The Fuzzball proposal for black holes: An Elementary review. *Fortsch. Phys.*, 53:793–827, 2005.
- [24] Hari K. Kunduri and James Lucietti. The first law of soliton and black hole mechanics in five dimensions. *Class. Quant. Grav.*, 31(3):032001, 2014.
- [25] Shane Andrews, Robie A. Hennigar, and Hari K. Kunduri. Chemistry and complexity for solitons in  $\text{AdS}_5$ . *Class. Quant. Grav.*, 37(20):204002, 2020.
- [26] Juan Martin Maldacena. The Large N limit of superconformal field theories and supergravity. *Adv. Theor. Math. Phys.*, 2:231–252, 1998.

- [27] Abhay Ashtekar and Saurya Das. Asymptotically Anti-de Sitter space-times: Conserved quantities. *Class. Quant. Grav.*, 17:L17–L30, 2000.
- [28] Jerome P. Gauntlett, Jan B. Gutowski, Christopher M. Hull, Stathis Pakis, and Harvey S. Reall. All supersymmetric solutions of minimal supergravity in five-dimensions. *Class. Quant. Grav.*, 20:4587–4634, 2003.
- [29] Veronika Breunhölder and James Lucietti. Moduli space of supersymmetric solitons and black holes in five dimensions. *Commun. Math. Phys.*, 365(2):471–513, 2019.
- [30] Simon F. Ross. Non-supersymmetric asymptotically AdS(5) x S\*\*5 smooth geometries. *JHEP*, 01:130, 2006.
- [31] Jan B. Gutowski and Harvey S. Reall. Supersymmetric AdS(5) black holes. *JHEP*, 02:006, 2004.
- [32] Jan B. Gutowski and Harvey S. Reall. General supersymmetric AdS(5) black holes. *JHEP*, 04:048, 2004.
- [33] Hari K. Kunduri, James Lucietti, and Harvey S. Reall. Supersymmetric multi-charge AdS(5) black holes. *JHEP*, 04:036, 2006.
- [34] Alejandro Cabo-Bizet, Davide Cassani, Dario Martelli, and Sameer Murthy. Microscopic origin of the Bekenstein-Hawking entropy of supersymmetric AdS<sub>5</sub> black holes. *JHEP*, 10:062, 2019.
- [35] Sunjin Choi, Joonho Kim, Seok Kim, and June Nahmgoong. Large AdS black holes from QFT. 10 2018.
- [36] Francesco Benini and Elisa Milan. Black Holes in 4D  $\mathcal{N}=4$  Super-Yang-Mills Field Theory. *Phys. Rev. X*, 10(2):021037, 2020.
- [37] Alberto Zaffaroni. AdS black holes, holography and localization. *Living Rev. Rel.*, 23(1):2, 2020.
- [38] Z. W. Chong, Mirjam Cvetič, Hong Lu, and Christopher N. Pope. General non-extremal rotating black holes in minimal five-dimensional gauged supergravity. *Phys. Rev. Lett.*, 95:161301, 2005.
- [39] Davide Cassani, Jakob Lorenzen, and Dario Martelli. Comments on supersymmetric solutions of minimal gauged supergravity in five dimensions. *Class. Quant. Grav.*, 33(11):115013, 2016.
- [40] James Lucietti and Sergei G. Ovchinnikov. Uniqueness of supersymmetric AdS<sub>5</sub> black holes with SU(2) symmetry. *Class. Quant. Grav.*, 38(19):195019, 2021.

- [41] Mirjam Cvetič, Gary W. Gibbons, Hong Lu, and Christopher N. Pope. Rotating black holes in gauged supergravities: Thermodynamics, supersymmetric limits, topological solitons and time machines. 4 2005.
- [42] Mirjam Cvetič, M. J. Duff, P. Hoxha, James T. Liu, Hong Lu, J. X. Lu, R. Martínez-Acosta, Christopher N. Pope, H. Sati, and Tuan A. Tran. Embedding AdS black holes in ten-dimensions and eleven-dimensions. *Nucl. Phys. B*, 558:96–126, 1999.
- [43] Gary W. Gibbons and Nicholas P. Warner. Global structure of five-dimensional fuzzballs. *Class. Quant. Grav.*, 31:025016, 2014.
- [44] Felicity C. Eperon, Harvey S. Reall, and Jorge E. Santos. Instability of supersymmetric microstate geometries. *JHEP*, 10:031, 2016.
- [45] Joseph Keir. Evanescent ergosurface instability. *Anal. Part. Diff. Eq.*, 13(6):1833–1896, 2020.
- [46] Joe Keir. Slowly decaying waves on spherically symmetric spacetimes and ultracompact neutron stars. *Class. Quant. Grav.*, 33(13):135009, 2016.
- [47] Georgios Moschidis. Logarithmic local energy decay for scalar waves on a general class of asymptotically flat spacetimes. 9 2015.
- [48] Joseph Keir. Wave propagation on microstate geometries. *Annales Henri Poincaré*, 21(3):705–760, 2019.
- [49] Sharmila Gunasekaran and Hari K. Kunduri. Slow decay of waves in gravitational solitons. *Annales Henri Poincaré*, 22(3):821–872, 2021.
- [50] Gustav Holzegel and Jacques Smulevici. Decay properties of Klein-Gordon fields on Kerr-AdS spacetimes. *Commun. Pure Appl. Math.*, 66:1751–1802, 2013.
- [51] Gustav Holzegel and Jacques Smulevici. Quasimodes and a lower bound on the uniform energy decay rate for Kerr-AdS spacetimes. *Anal. Part. Diff. Eq.*, 7(5):1057–1090, 2014.
- [52] Piotr Bizon and Andrzej Rostworowski. On weakly turbulent instability of anti-de Sitter space. *Phys. Rev. Lett.*, 107:031102, 2011.
- [53] Piotr Bizoń, Maciej Maliborski, and Andrzej Rostworowski. Resonant Dynamics and the Instability of Anti-de Sitter Spacetime. *Phys. Rev. Lett.*, 115(8):081103, 2015.
- [54] Oscar J. C. Dias, Gary T. Horowitz, and Jorge E. Santos. Gravitational Turbulent Instability of Anti-de Sitter Space. *Class. Quant. Grav.*, 29:194002, 2012.

- [55] Xiao Dong Wang. On the uniqueness of the AdS spacetime. *Acta Math. Sin. (Engl. Ser.)*, 21(4):917–922, 2005.
- [56] W. Boucher, Gary W. Gibbons, and Gary T. Horowitz. Uniqueness theorem for anti-de Sitter spacetime. *Phys. Rev. D (3)*, 30(12):2447–2451, 1984.
- [57] Jie Qing. On the uniqueness of AdS space-time in higher dimensions. *Annales Henri Poincaré*, 5(2):245–260, apr 2004.
- [58] G. J. Galloway, S. Surya, and E. Woolgar. A Uniqueness theorem for the AdS soliton. *Phys. Rev. Lett.*, 88:101102, 2002.
- [59] G. J. Galloway, S. Surya, and E. Woolgar. On the geometry and mass of static, asymptotically AdS space-times, and the uniqueness of the AdS soliton. *Commun. Math. Phys.*, 241:1–25, 2003.
- [60] R. Clarkson and Robert B. Mann. Soliton solutions to the Einstein equations in five dimensions. *Phys. Rev. Lett.*, 96:051104, 2006.
- [61] R. Clarkson and Robert B. Mann. Eguchi-Hanson solitons in odd dimensions. *Class. Quant. Grav.*, 23:1507–1524, 2006.
- [62] Dominic Dold. Global dynamics of asymptotically locally AdS spacetimes with negative mass. *Class. Quant. Grav.*, 35(9):095012, 2018.
- [63] David Kastor, Sourya Ray, and Jennie Traschen. Enthalpy and the Mechanics of AdS Black Holes. *Class. Quant. Grav.*, 26:195011, 2009.
- [64] S. W. Hawking and Don N. Page. Thermodynamics of Black Holes in anti-De Sitter Space. *Commun. Math. Phys.*, 87:577, 1983.
- [65] Gabriele Benomio. The stable trapping phenomenon for black strings and black rings and its obstructions on the decay of linear waves. *Anal. Part. Diff. Eq.*, 14(8):2427–2496, 2021.
- [66] Tohru Eguchi and Andrew J. Hanson. Asymptotically Flat Selfdual Solutions to Euclidean Gravity. *Phys. Lett. B*, 74:249–251, 1978.
- [67] Gary T. Horowitz and Robert C. Myers. The AdS / CFT correspondence and a new positive energy conjecture for general relativity. *Phys. Rev. D*, 59:026005, 1998.
- [68] Don N. Page. Phase transitions for gauge theories on tori from the AdS / CFT correspondence. *JHEP*, 09:037, 2008.
- [69] Edgar Shaghoulian. Modular Invariance of Conformal Field Theory on  $S^1S^3$  and Circle Fibrations. *Phys. Rev. Lett.*, 119(13):131601, 2017.

- [70] Saoussen Mbarek and Robert B. Mann. Thermodynamic Volume of Cosmological Solitons. *Phys. Lett. B*, 765:352–358, 2017.
- [71] A. Ashtekar and A. Magnon. Asymptotically anti-de Sitter space-times. *Class. Quant. Grav.*, 1:L39–L44, 1984.
- [72] David Kubiznak, Robert B. Mann, and Mae Teo. Black hole chemistry: thermodynamics with Lambda. *Class. Quant. Grav.*, 34(6):063001, 2017.
- [73] Sharmila Gunasekaran, Uzair Hussain, and Hari K. Kunduri. Soliton mechanics. *Phys. Rev. D*, 94(12):124029, 2016.
- [74] Michael Appels, Ruth Gregory, and David Kubiznak. Thermodynamics of Accelerating Black Holes. *Phys. Rev. Lett.*, 117(13):131303, 2016.
- [75] Alvaro Ballon Bordo, Finnian Gray, Robie A. Hennigar, and David Kubizňák. Misner Gravitational Charges and Variable String Strengths. *Class. Quant. Grav.*, 36(19):194001, 2019.
- [76] Roberto Emparan, Clifford V. Johnson, and Robert C. Myers. Surface terms as counterterms in the AdS / CFT correspondence. *Phys. Rev. D*, 60:104001, 1999.
- [77] Vijay Balasubramanian and Per Kraus. A Stress tensor for Anti-de Sitter gravity. *Commun. Math. Phys.*, 208:413–428, 1999.
- [78] Yasuaki Hikida. Phase Transitions of Large N Orbifold Gauge Theories. *JHEP*, 12:042, 2006.
- [79] Edgar Shaghoulian. Emergent gravity from Eguchi-Kawai reduction. *JHEP*, 03:011, 2017.
- [80] Sumati Surya, Kristin Schleich, and Donald M. Witt. Phase transitions for flat AdS black holes. *Phys. Rev. Lett.*, 86:5231–5234, 2001.
- [81] Hari K. Kunduri and James Lucietti. Notes on non-extremal, charged, rotating black holes in minimal D=5 gauged supergravity. *Nucl. Phys. B*, 724:343–356, 2005.
- [82] Robert C. Myers, Moshe Rozali, and Benson Way. Holographic Quenches in a Confined Phase. *J. Phys. A*, 50(49):494002, 2017.
- [83] Tai Tsun Wu and Chen Ning Yang. Dirac Monopole Without Strings: Monopole Harmonics. *Nucl. Phys. B*, 107:365, 1976.
- [84] Nicholas P. Warner. The Spectra of Operators on  $CP^N$ . *Proc. Roy. Soc. Lond. A*, 383:217–230, 1982.

- [85] P. Hoxha, R. R. Martinez-Acosta, and C. N. Pope. Kaluza-Klein consistency, Killing vectors, and Kahler spaces. *Class. Quant. Grav.*, 17:4207–4240, 2000.
- [86] C. M. Bender and S. A. Orszag. *Advanced Mathematical Methods for Scientists and Engineers*. McGraw-Hill, 1978.
- [87] Peter Breitenlohner and Daniel Z. Freedman. Stability in Gauged Extended Supergravity. *Annals Phys.*, 144:249, 1982.
- [88] John P. Boyd. *Chebyshev and Fourier Spectral Methods*. Dover Publications, 2001.
- [89] C. Canuto, M.Y. Hussaini, A. Quarteroni, and T.A. Zang. *Spectral Methods: Fundamentals in Single Domains*. Scientific Computation. Springer Berlin Heidelberg, 2007.
- [90] Óscar J. C. Dias, Jorge E. Santos, and Benson Way. Numerical Methods for Finding Stationary Gravitational Solutions. *Class. Quant. Grav.*, 33(13):133001, 2016.
- [91] Keiju Murata and Jiro Soda. Stability of Five-dimensional Myers-Perry Black Holes with Equal Angular Momenta. *Prog. Theor. Phys.*, 120:561–579, 2008.
- [92] Takaaki Ishii, Keiju Murata, Jorge E. Santos, and Benson Way. Superradiant instability of black resonators and geons. *JHEP*, 07:206, 2020.
- [93] Markus Garbiso, Takaaki Ishii, and Keiju Murata. Resonating AdS soliton. *JHEP*, 08:136, 2020.
- [94] Neil R. Constable and Robert C. Myers. Spin two glueballs, positive energy theorems and the AdS / CFT correspondence. *JHEP*, 10:037, 1999.
- [95] Robert C. Myers. Stress tensors and Casimir energies in the AdS / CFT correspondence. *Phys. Rev. D*, 60:046002, 1999.
- [96] Anson W. C. Wong and Robert B. Mann. Five-Dimensional Eguchi-Hanson Solitons in Einstein-Gauss-Bonnet Gravity. *Phys. Rev. D*, 85:046010, 2012.
- [97] Cristóbal Corral, Gastón Giribet, and Rodrigo Olea. Self-dual gravitational instantons in conformal gravity: Conserved charges and thermodynamics. *Phys. Rev. D*, 104(6):064026, 2021.
- [98] Cristóbal Corral, Daniel Flores-Alfonso, Gastón Giribet, and Julio Oliva. Higher-curvature generalization of Eguchi-Hanson spaces. *Phys. Rev. D*, 106(8):084055, 2022.

- [99] M. Cvetič, Gary W. Gibbons, D. Kubiznak, and C. N. Pope. Black Hole Entropy and an Entropy Inequality for the Thermodynamic Volume. *Phys. Rev. D*, 84:024037, 2011.
- [100] Gary W. Gibbons, M. J. Perry, and C. N. Pope. The First law of thermodynamics for Kerr-anti-de Sitter black holes. *Class. Quant. Grav.*, 22:1503–1526, 2005.
- [101] Stefan Hollands, Akihiro Ishibashi, and Donald Marolf. Comparison between various notions of conserved charges in asymptotically AdS-spacetimes. *Class. Quant. Grav.*, 22:2881–2920, 2005.
- [102] Jerome P. Gauntlett and Jan B. Gutowski. All supersymmetric solutions of minimal gauged supergravity in five-dimensions. *Phys. Rev. D*, 68:105009, 2003. [Erratum: *Phys.Rev.D* 70, 089901 (2004)].
- [103] Andrés Anabalón, Antonio Gallerati, Simon Ross, and Mario Trigiante. Supersymmetric solitons in gauged  $\mathcal{N} = 8$  supergravity. *JHEP*, 02:055, 2023.
- [104] Davide Cassani and Dario Martelli. The gravity dual of supersymmetric gauge theories on a squashed  $S^1 \times S^3$ . *JHEP*, 08:044, 2014.
- [105] James Lucietti, Praxitelis Ntokos, and Sergei G. Ovchinnikov. On the uniqueness of supersymmetric AdS(5) black holes with toric symmetry. *Class. Quant. Grav.*, 39(24):245006, 2022.
- [106] Sebastian de Haro, Sergey N. Solodukhin, and Kostas Skenderis. Holographic reconstruction of space-time and renormalization in the AdS / CFT correspondence. *Commun. Math. Phys.*, 217:595–622, 2001.
- [107] Keiju Murata. Instabilities of Kerr-AdS(5)  $\times S^{*5}$  Spacetime. *Prog. Theor. Phys.*, 121:1099–1124, 2009.